論文 / 著書情報
Article / Book Information

題目(和文)	チタン種を担持したメソポーラスシリカの水中ルイス酸触媒作用に関する研究
Title(English)	Studies on Lewis Acid Catalysis of Titanium Deposited Mesoporous Silica in Water
著者(和文)	新宅泰
Author(English)	Hiroshi Shintaku
出典(和文)	学位:博士（工学）, 学位授与機関:東京工業大学, 報告番号:甲第9819号, 授与年月日:2015年3月26日, 学位の種別:課程博士, 審査員:原　亨和,彌田　智一,鎌田　慶吾,神谷　利夫,北野　政明,馬場　俊秀
Citation(English)	Degree:, Conferring organization: Tokyo Institute of Technology, Report number:甲第9819号, Conferred date:2015/3/26, Degree Type:Course doctor, Examiner:,,,,,
学位種別(和文)	博士論文
Type(English)	Doctoral Thesis

Studies on Lewis Acid Catalysis of Titanium Deposited Mesoporous Silica in Water

(和訳：チタン種を担持したメソポーラスシリカの水中ルイス酸触媒作用に関する研究)

Department of Innovative and Engineered Materials

Interdisciplinary Graduate School of Science and Engineering

Tokyo Institute of Technology

Hiroshi Shintaku

This thesis was submitted to Tokyo Institute of Technology
for the degree of Doctor of Engineering

2015 Doctor Thesis

Contents

Chapter 1

General Introduction

1.1 Background

Catalyst plays the key role for the development of chemical industry, and largely contributes to our modern society for the production of extremely large amounts of fuels and chemicals [1]. Early in the 20th century, the discovery of osmium catalyst for ammonia synthesis by Haber enabled us to utilize atmospheric nitrogen as nearly inexhaustible nitrogen source for NH_3 production. Bosch and Mittasch subsequently developed iron based catalyst that can be applicable to industrial production of NH_3 from N_2 and H_2. We feed the enormous population worldwide using chemical nitrogen fertilizer. Catalytic refinery of fossil resources is also an essential process in chemical industry. Due to catalytic reforming and cracking of petroleum, we can obtain large amounts of high-quality gasoline as an energy source. Propylene, one of most important hydrocarbons in recent years, can be converted into acrylonitrile, an important building block monomer for fiber or resin by ammoxidation with Mo-Bi-Fe oxide catalyst. Ziegler-Natta catalyst containing titanium trichloride or tetrachloride promotes a polymerization of α-olefins. Catalyst is also indispensable for environmental protection, represented by three-way catalytic converter for exhaust gas of gasoline powered vehicles. It promotes the oxidation of hydrocarbon and carbon monoxide to carbon dioxide, and reduction of nitric oxide (NO_x) to nitrogen, resulting in the significant decrease of atmospheric pollution. As such, it is no exaggeration to say that our modern society has relied largely on the catalytic chemistry.

Continuous efforts have being made nowadays to develop a new catalysis, especially from the point of view of Green Sustainable Chemistry (GSC). The word “GSC” is defined as the design, development and implementation of chemical processes and products to reduce or eliminate substances hazardous to human health and the environment [2]. As shown in 12 Principles of Green Chemistry (Table 1-1), various efforts are needed to construct environmentally benign chemical process. Replacement of homogeneous catalyst to easily separable and reusable heterogeneous solid catalyst is one of the significant schemes for bulk chemical production. Many shortcomings of homogeneous catalysts such as un-reusability or difficulties of separation can be solved by the development of solid catalysts.

Acid catalyst has been widely applied to many kinds of reactions such as isomerization, hydration, dehydration, alkylation, and esterification, for the production of petrochemicals, pharmaceuticals, agrochemicals, polymers and fragrances [3-6]. For example, sulfuric acid, an important homogeneous acid catalyst, is adopted for the Beckmann rearrangement of cyclohexanone

oxime to produce ε-caprolactam which is used as a starting material for nylon production [3]. Replacement of homogeneous catalysts by heterogeneous counterparts is meaningful challenge in the field of acid catalysts, due to the severe corrosion of reactor and to avoid large amounts of by-product, such as gypsum, from waste acids.

Table 1-1. Green chemistry principles. From [2]. Reprinted with permission from AAAS.

1.	It is better to prevent waste than to treat or clean up waste after it is formed.
2.	Synthetic methods should be designed to maximize the incorporation of all materials used in the process into the final product.
3.	Wherever practicable, synthetic methodologies should be designed to use and generate substances that possess little or no toxicity to human health and the environment.
4.	Chemical products should be designed to preserve efficacy of function while reducing toxicity.
5.	The use of auxiliary substances (e.g., solvents, separation agents, and so forth) should be made unnecessary wherever possible and innocuous when used.
6.	Energy requirements should be recognized for their environmental and economic impacts and should be minimized. Synthetic methods should be conducted at ambient temperature and pressure.
7.	A raw material or feedstock should be renewable rather than depleting wherever technically and economically practicable.
8.	Unnecessary derivatization (blocking group, protection/deprotection, temporary modification of physical/chemical processes) should be avoided whenever possible.
9.	Catalytic reagents (as selective as possible) are superior to stoichiometric reagents.
10.	Chemical products should be designed so that at the end of their function they do not persist in the environment and break down into innocuous degradation products.
11.	Analytical methodologies need to be developed further to allow for real-time in-process monitoring and control before the formation of hazardous substances.
12.	Substances and the form of a substance used in a chemical process should be chosen so as to minimize the potential for chemical accidents, including releases, explosions, and fires.

One excellent example of the heterogeneous acid catalysis for GSC is development of a mesoporous Zr-Si mixed oxide for the production of polytetramethylene ether glycol (PTMEG) [7,8]. PTMEG is a polymer of tetrahydrofuran and used for producing functional elastic fiber (Scheme 1-1). However, harmful fluorosulfuric acid is used for conventional processes as the non-recyclable catalyst, resulting in the formation of 0.13 kg of fluorine-containing acid waste per 1 kg of PTMEG production, in addition to severe corrosion of reactor. In order to reduce environmental loads in this process, heterogeneous system using a mesoporous Zr-Si mixed oxide was developed by Setoyama et al. from Mitsubishi Chemical Co. Ltd. Moderate Lewis acidity and mesoporous structure are key technological components for the catalysis.

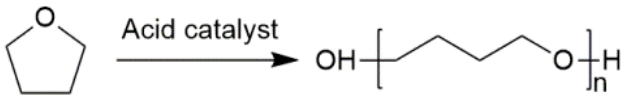

Scheme 1-1. Acid catalyzed PTMEG synthesis.

A shift from diminishing fossil resources to renewable biomass, represented by lignocellulose and oil from plants, is also one of the principal efforts in GSC, to reduce the usage of finite fossil resources and the emission of CO_2 (Figure 1-1) [2,9-14]. Catalytic conversion of biomass to fundamental platform chemicals by hydrolysis, hydrogenation, pyrolysis or dehydration reaction has been attracting great attention [9]. Acid catalysts also play a crucial role for the hydrolysis of cellulose or isomerization and dehydration, for example.

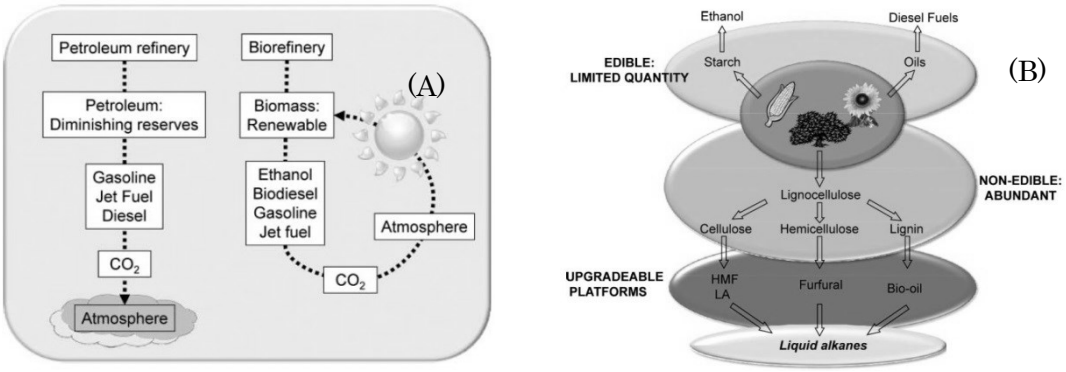

Figure 1-1. (A) CO_2 cycles for petroleum-and biomass-derived fuels. (B) Biomass-derived feedstock and platforms. Reproduced from [11] with permission of The Royal Society of Chemistry.

In recent years, replacing the organic solvents by water is also a trend of the times in the field of GSC [15-20]. Water is a widely available, non-toxic and non-flammable solvent. Due to the protic polar property, water shows high solubility for polar solute including biomass-derived sugars, and sometimes shows unique reactivity and selectivity for organic reactions. Furthermore, adoption

of aqueous reaction system makes dehydration of substrates and solvents unnecessary, resulting in the decrease of total energy consumption of the chemical process. Despite such many advantageous, the usage of aqueous medium is limited due to the low resistance of conventional acid catalysts. Thus, development of heterogeneous and water compatible acid catalysts is essential to realize environmental friendly chemical production.

In this chapter, fundamental background of acid catalysts has been summarized first. Then, some of acid catalysts, including water tolerant Lewis acid catalysts and Lewis acid catalysis for biomass conversion or organic synthesis, are reviewed.

1.2 Acid catalyst

1.2.1 Fundamental aspect

1.2.1.1 Type of Acid Catalyst

According to the definition of acid by Brönsted and Lewis, acid catalysts can be classified into two groups. One is Brönsted acid catalyst, which donates a proton to a basic molecule, and the other is Lewis acid catalyst, which accepts electron pair from a nucleophilic molecule. Though the concept of Lewis acid includes Brönsted acid, these two groups of catalysts are usually distinguished due to the large difference in catalytic property.

1.2.1.2 Theory of Brönsted Acid Catalyst

Brönsted acid interacts with Brönsted base through proton transfer as shown in the following equation.

$$HA + B \rightarrow BH^+ + A^-$$

Here, proton transfers from Brönsted acid, HA, to Brönsted base, B, resulting in a generation of the conjugated base, A^-, and the conjugated acid, HB^+. In the case of metal oxides, Brönsted acid site generally exists as hydroxyl groups on oxide surface.

The property of Brönsted acid site depends on the acid strength, density, location (environment) and so on. Various methods have been established to evaluate Brönsted acidity. Acid strength of solid acid is expressed by H_0, Hammet acidity function, measured by titration method using basic color indicator.

$$H_o = pKa + \log\frac{[B]}{[BH^+]}$$

where [B] is the concentration of basic indicator and $[BH^+]$ is concentration of its conjugated acid.

A great deal of efforts has been devoted to estimate the amount and property of Brönsted acid site on solid surface by using various basic probe molecules (Table 1-2) [21-24]. Amine titration method using indicator is a conventional, well established method. Ammonia temperature programed desorption (Ammonia TPD) is a conventional method to evaluate the acid density and acid strength.

Fourier transform infra-red (FT-IR) spectroscopy using basic probe molecule is also a frequently adopted method. As shown in Table 1-2, useful information for acid site such as type, amount and location can be obtained by selecting the probe molecule discreetly. Nuclear magnetic resonance (NMR) spectroscopy using probe molecule is also a powerful method to measure acid strength and location [25,26].

Table 1-2. Methods for acidity characterization. Adopted from [25] with permission of The Royal Society of Chemistry.

Method	Acid type		Acid	Acid	Acid
	Brönsted	Lewis	location	amount	strength
Amine titration	++	++	-	++	++
NH_3 TPD	++	++	-	++	-
IR (hydroxyls)	++	-	-	-	++
IR (pyridine adsorption)	++	++	++	+	+
IR (CO adsorption)	++	++	-	+	++
^{1}H NMR (hydroxyls)	++	-	-	+	-
^{1}H NMR (pyridine)	++	-	-	+	++
^{1}H NMR (acetonitrile)	++	-	-	+	++
^{13}C NMR (acetone)	-	-	-	-	++
^{31}P NMR (trimethylphosphine)	++	++	-	++	++
^{31}P NMR (trimethylphosphine oxide)	++	++	++	++	++

1.2.1.3 Theory of Lewis Acid Catalyst

Lewis acid interacts with Lewis base through electron interaction.

$$A + :B \rightarrow A^{\delta-} - B^{\delta+}$$

Here, lowest unoccupied molecular orbital (LUMO) of Lewis acid (A) accepts electron pair of highest occupied molecular orbital (HOMO) of Lewis base (B), resulting in the generation of acid-base adduct. Lewis acid site also exists in a form of unsaturated metal species on oxide surface.

In contrast to the Brönsted acid catalyst, it is not easy to describe the acid strength of Lewis acid catalyst. Electron negativity of the Lewis acid metal center is effective for predicting acid catalysis to some extent. In order to explain the affinities of Lewis acid and base, R.G. Pearson came up with the concept of “Hard and soft acids and bases” (HSAB) theory [27-29]. He classified Lewis acids and bases into two groups; one is hard acids and bases with small size, high charge and low polarizability, the other is soft acids and bases with large size, low charge, and high polarizability.

Based on his theory, hard acids prefer to associate with hard bases under charge-controlled manner, and soft acids prefer to associate with soft bases under orbital-controlled manner. From the point of view of frontier orbital theory, hard acid-base interaction is dominated by larger energy difference in HOMO of acids and LUMO of bases resulting in charge controlled manner, while soft acid-base interaction is dominated by orbital interaction of HOMO and LUMO with small energy difference.

1.2.2 Examples of homogeneous and heterogeneous acid catalysts

As acid catalysts have served as important functional materials for the chemical industry including petroleum chemistry, a number of authors have already reported many acid catalysts, and representative acid catalysts are summarized in Table 1-3. Many kinds of acid catalysts have been utilized for various reactions depending on its characters such as state of matter (solid or acid), acid type (Lewis or Brönsted), acid strength, acid density, porous structure, surface area, hydrophobicity/hydrophilicity and so on. In this section, fundamental structure and property of popular acid catalysts is reviewed, especially focusing on the Lewis acid catalysts workable in water.

Table 1-3. Acid catalysts and properties.

Catalyst classification	Example	Acid type	State	Porous strucure	Reaction example
Liquid acid	H_2SO_4, HNO_3	Brönsted	Liquid	-	alkylation, esterfication, hydration, acylation
Metal halide	$AlCl_3$, $TiCl_4$	Lewis	Soluble Solid	-	alkylation, cracking
Zeolite	ZSM-5, USY	Brönsted/Lewis	Solid	Micro	alkylation, isomerization, cracking
Metal oxide	alumina, Silica-alumina, Nb_2O_5	Brönsted/Lewis	Solid	- / Micro/ Meso	cracking alkylation ethylene hydration
Sulfated zirconia	Sulfated zirconia	Brönsted	Solid	-	paraffin isomerization
Ion exchanged resin	Nafion	Brönsted	Solid	-	dehydration, oligomerization
Heteropolyacid	$Cs_xH_{3-x}PW_{12}O_{40}$	Brönsted	Solid	-	ethylacetate synthesis

1.2.2.1 Metal halides

Metal halides, such as $AlCl_3$, $TiCl_4$, $SnCl_4$ and $FeCl_3$, can function as Lewis acid catalysts due to its capacity of accepting lone pair of nucleophilic substrates into metal empty orbital. These catalysts have been applied to many kinds of important Lewis acid catalyzed reaction, the Friedel-Crafts alkylation (Scheme 1-2 (a)) and acylation (Scheme 1-2 (b)), the Mukaiyama aldol reaction (Scheme 1-2 (c)), and the Diels-Alder reaction (Scheme 1-2 (d)) [30]. However, these salts readily undergo the hydrolysis in the presence of small amount of water, thus requiring strictly anhydrous conditions.

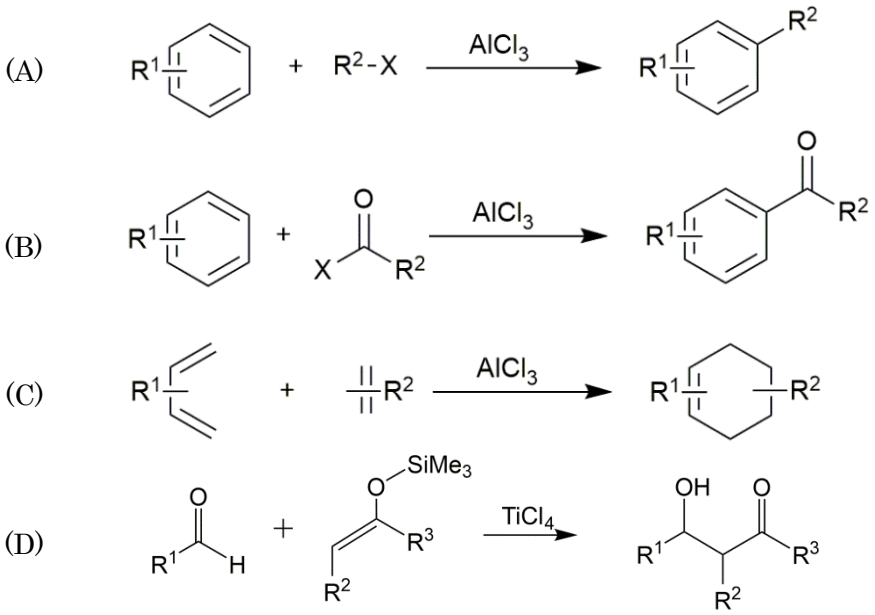

Scheme 1-2. Lewis acid catalyzed reactions. (A) Friedel-Crafts alkylation, (B)Friedel-Crafts acylation, (C) Diels-Alder reaction and (D) Mukaiyama aldol reaction.

However, recently some of these metal halides are reported to work in water medium. Fringuelli et al. reported the usage of $AlCl_3$, $TiCl_4$, $InCl_3$ and $SnCl_4$ as the Lewis acids catalysts for azidolysis of α,β-epoxyhexanoic acid in water (Scheme 1-3) [31]. Though they agree with the fast hydrolysis of these metal salts in water, they also insist that in the suitable pH aqueous medium (pH 1.5), stable metal aqua ions can exist and promote the reaction.

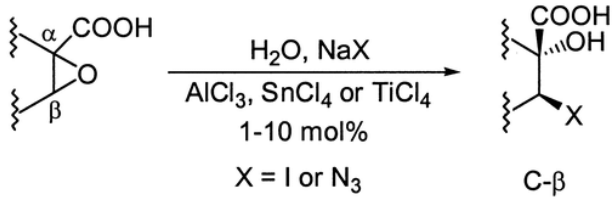

Scheme 1-3. Azidolysis or indolysis of α,β-epoxyhexanoic acid in water [31].

$SnCl_4 \cdot 5H_2O$-catalyzed alkyl lactate synthesis from dihydroxyacetone (DHA) has been reported by Hayashi et al. [32], and lactic acid synthesis by series of metal halides such as $AlCl_3$, $CrCl_2$ and $CrCl_3$ has been achieved by Rasrendra et al. (Scheme 1-4) [32]. Although there is no discussion on the hydrolysis or reusability of metal halides in these papers, these reactions proceed catalytically (TON above 10). As shown in these examples above, some metal halides have possibilities to work as water tolerant Lewis acid catalysts in specific conditions.

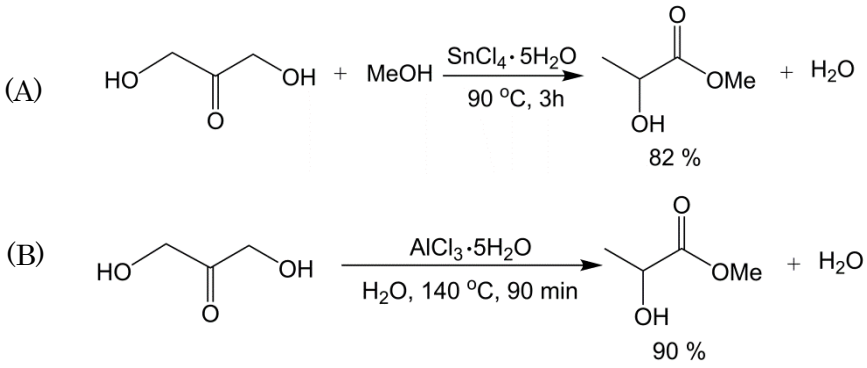

Scheme 1-4. Metal chloride catalyzed 1,3-dihydroxyacetone conversion [32]. (A) Hydrated tin chloride catalyzed methyl lactate synthesis and (B) aluminum chloride catalyzed lactic acid synthesis in water.

1.2.2.2 Metal trifluoromethanesulfonates (triflates)

Kobayashi and co-workers developed a series of Lewis acid catalyzed organic synthesis reactions in water with Lanthanide triflates such as $Sc(OTf)_3$, $Yb(OTf)_3$ and $Ln(OTf)_3$ [34-37]. For example, they reported the Mukaiyama-aldol reaction of benzaldehyde with cyclohexanone-derived silicone enolate in water-tetrahydrofuran (THF) medium in 1994 (Scheme 1-5) [35]. They found that in the presence of small amount of proton (pH 4 solution), silicone enolate, a reactant of the reaction, easily undergo hydrolysis, results in the extremely low product yield. They examined the hydrolysis of the lanthanide triflates carefully and revealed that lanthanide triflates can be recovered and reused for subsequent reactions. Based on these insights, metal triflates are considered as water tolerant Lewis acid catalyst.

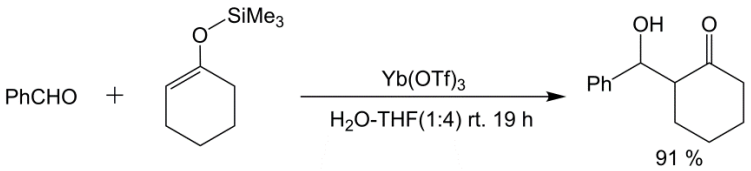

Scheme 1-5. Mukaiyama-aldol reaction in water containing medium [35].

Kobayashi et al. also attempted to evaluate the catalytic activity of metal salt Lewis acids in water, on the basis of the hydrolysis constants (pKh) and exchange rate constants for the substitution of inner-sphere water ligands (water exchange rate constants (WERC)) of the metal cations [17,38]. Hydrolysis constants are influenced by stability of metal cations in water. Metal cations with small pKh values are easily converted into metal hydroxide and proton by hydrolysis, leading to the deactivation of the catalyst or decomposition of substrates. On the other hand, metal cations with too large pKh value do not have enough Lewis acidity to promote the reaction. WERC value reflects the efficiency of the exchange between water molecules coordinated to the metal

cations and substrates. According to their report, active metal compounds have pKh value from 4 to 10 and WERC value greater than 3.2×10^{6} $m^{-1}s^{-1}$.

The coordination number (CN) of water molecules around lanthanide cations during the aqueous Mukaiyama-Aldol reaction was investigated by Allen et al. using luminescence decay measurement [39,40]. They used $Eu(OTf)_3$ as a model salt and reported that CN of water around lanthanide metal center was estimated to be 8.3 in pure aqueous medium. This CN value means that all of OTf ligands have dissociated during the reaction, and stable lanthanide aqua complexes have been formed in water. The importance of the dissociative capability of ligands was also confirmed by control experiment using $Eu(NO_3)_3$. NO_3 ligand is less dissociative than OTf ligand, resulting in the lower water CN and slower reaction rate. These insights strongly support the stability of lanthanide cations in water reported by Kobayashi and co-workers.

1.2.2.3 Zeolites

Zeolites can be defined as crystalline (metallo)silicates with periodic porous structure, and consist of TO_4 tetrahedron as primary building blocks (T atom is Si^{4+}, Al^{3+} or other metal species) [3-5,41,42]. TO_4 tetrahedra are connected with each other by sharing the oxygen atoms, resulting in the formation of characteristic three dimensional network with channels and cavities in molecular dimensions (0.2 to 1.4 nm). The representative structures of zeolite with different channel size and geometry are shown in figure 1-2. Owing to its wide usability for catalysis, absorbent, drying agent etc., originated from high surface area, adsorption capacity, ion exchangeability, stability and acidity, more than 200 types of natural and artificial zeolites has been reported so far.

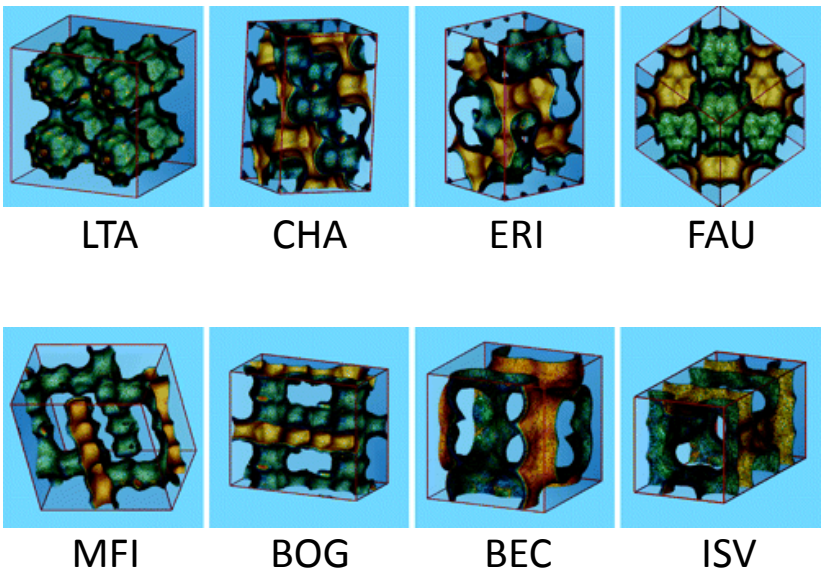

Figure 1-2. Structures of representative zeolites. Reprinted with permission from [43]. Copyright (2006) American Chemical Society.

The Brönsted acid sites of zeolite are originated from the substitution of Si^{4+} to trivalent heteroatom (M^{3+} species, Al^{3+}, Ga^{3+} or B^{3+}) [3-5,41,42]. For example, the introduction of AlO_4 tetrahedra leads to the formations of a negative charge on the oxygen atoms surrounding Al ion, and this negative charge on the framework is compensated by cations such as Na^+, K^+, NH_4^+ or proton, resulting in the origin of Brönsted acidity (Scheme 1-6). The strength of Brönsted acid sites is dependent on several factors such as Si/Al ratio and zeolite topology (bond angle and length of Si-O-Al). It has been reported that for zeolites with similar Si/Al ratio, the strength of acid sites in medium pore size zeolites is higher than those in large pore size zeolites [3, 44].

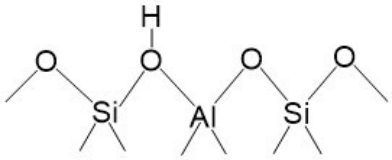

Scheme 1-6. Schematic structure of acid sites on zeolite.

One of the important properties of zeolites as catalyst is molecular shape selectivity including reactant selectivity, product selectivity and restricted transition state selectivity. Sharp selective synthesis of *p*-xylene was achieved on the basis of these properties [1]. Thus, enormous amounts of zeolites are used in commercial catalytic processes for cracking, hydrocracking, isomerization, alkylation, and dewaxing.

Heteroatom substituted microporous zeolites are attracting much attention as Lewis acidic zeolites in recent years. Among them, particular attention has been paid to titanium silicate-1(TS-1), an isolated Lewis acid sites containing zeolite with MFI structure [45-47]. The important structural features of TS-1 as Lewis acid catalyst are as follows. (i) Substituted Ti^{4+} species have tetrahedral coordination and function as Lewis acid sites using their empty d orbital to accept lone pair of substrates, even in the protic polar solvents, water. (ii) Hydrophobic reaction cavity originated from high crystallinity of zeolite framework, enables hydrophobic reactant molecules to enter zeolite pores efficiently. An excellent example of TS-1 catalyzed reaction is epoxidation of propylene using hydrogen peroxide as an oxidant (Scheme1-7). Direct observation of catalytic active sites for TS-1 using UV-Raman measurement has been reported by Li and coworkers [48,49]. Raman band associated with TiO_4 unit in TS-1 zeolite was observed with UV laser line at 244 nm, which is close to the energy of ligand to metal charge transfer of titanium tetrahedra. Combining UV-Raman, UV-Vis and DFT calculation, bare and water-coordinated TiO_4 ($TiO_4(H_2O)_2$) have been considered as catalytic active sites for the propylene oxidation with H_2O_2 (Scheme 1-6). TS-1 has been applied to some commercial chemical processes, such as phenol hydroxylation, cyclohexanone ammoximation or propylene epoxidation [47]. To overcome the diffusion restrictions of 10

membered-ring medium pores of TS-1 (openings close to 0.55 nm), effort have been devoted to synthesize Ti zeolite with larger 12-membered ring, such as Ti-Beta, Ti-ZSM-12 and Ti-MWW.

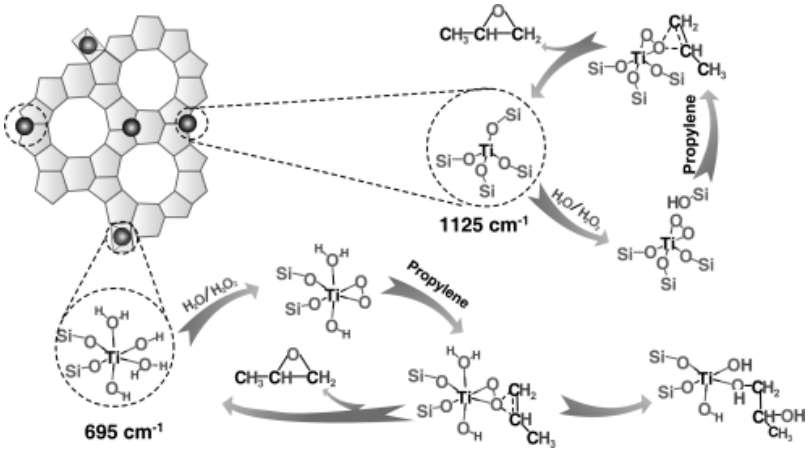

Scheme 1-7. Reaction mechanism of propylene oxidation catalyzed by TS-1. Reproduced from [49] with permission of John Wiley & Sons.

Not only the titanium substituted zeolites, but also many kinds of other heteroatom substituted zeolites have been reported. Tin, zirconium, niobium and tantalum have been successfully incorporated into Beta zeolite or MCM-41 framework, and found to be active for oxidation reaction with aqueous hydrogen peroxide or Meerwein−Ponndorf−Verley (MPV) reduction [50-53]. For example, Corma et al. reported that Sn-beta zeolite shows high catalytic performance for the MPV reduction of cyclohexanone with 2-butanol, which gives cyclohexanol with quantitative yield (Scheme 1-8) [51]. Isolated metal sites are considered as catalytic active sites that can activate carbonyl group in reactant molecule. Due to shape selective catalysis associated with restricted zeolite micropores, Sn-beta zeolite promotes MPV reduction of alkylcyclohexanones with high *cis* selectivity [51]. Recently, Sn- or Ti-Beta catalyzed glucose isomerization has been reported by Davis and coworkers (Scheme 1-9) [54-57]. Large-sized micropores in the framework of Beta zeolites contribute to glucose diffusion in water, and hydrophobic environments in micropores are important factor for effective catalysis. ^{119}Sn solid state NMR revealed that framework Sn species in close and/or open form would be regarded as active sites for the isomerization in water (Figure 1-3). The details of the glucose isomerization are discussed in section 1.3.1.1..

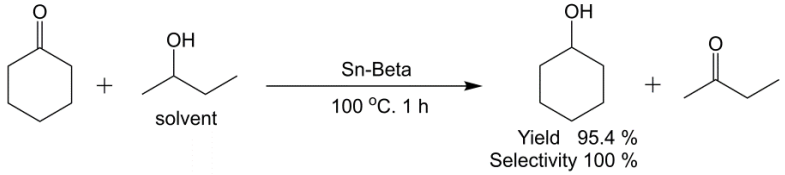

Scheme 1-8. MPV reduction of cyclohexanone [51].

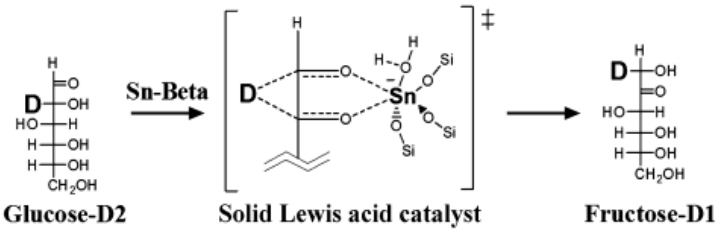

Scheme 1-9. Glucose isomerization into fructose via intramolecular hydride transfer. Reproduced from [55] with permission of John Wiley & Sons.

1.2.2.4 Metal oxides

Although most of metal oxides show acidity and basicity that depend on the electron negativity of metal atom, it is generally considered that Lewis acidity of metal oxides is decomposed or deactivated by the presence of water. This is due to the irreversibly coordinative adsorption of water molecule on acidic metal sites or dissociative water adsorption to produce hydroxide and a proton. However, some recent results show that some simple metal oxides have water tolerant Lewis acid sites on the surface.

Nb_2O_5 is well-known as Brönsted acid catalyst with high acid strength (H_0= –5.6), and has been applied to some acid catalyzed reactions such as hydration, dehydration and esterification, so far [58,59]. Niobic acid also has Lewis acidity even in the aqueous medium, in addition to Brönsted acidity. In 2011, Nakajima et al. reported Nb_2O_5 catalyzed allylation of benzaldehyde with tetraallyl tin, a typical Lewis acid catalyzed reaction in water [60]. According to FT-IR and Raman measurements, coordinately unsaturated NbO_4 tetrahedra act as Lewis acid sites for the reaction (Figure 1-3). Although most of NbO_4 tetrahedra (ca. 80%) are deactivated in water, but the remaining 20% of NbO_4 still maintains Lewis acidity and promote acid-catalyzed reactions even in the presence of water. Conversion of glucose into 5-(hydroxymethyl) furfural (HMF), a consecutive reaction consisting of acid catalyzed isomerization and dehydration, is also successfully promoted by bare and phosphate-immobilized Nb_2O_5.

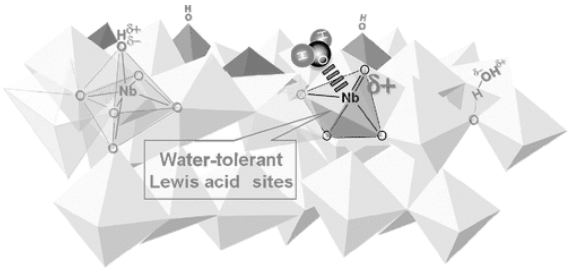

Figure 1-3. Schematic structure of acid sites on Nb_2O_5. Reprinted with permission from [60]. Copyright (2011) American Chemical Society.

Nakajima and co-workers also reported the group 4 metal oxide, anatase TiO_2, as a Lewis acid catalyst workable in water [61]. Anatase TiO_2 with low crystallinity promotes hydride transfer of pyruvaldehyde into lactic acid and the allylation of benzaldehyde with tetraallyltin in water. Similar to the NbO_4, coordinately unsaturated metal species, unsaturated TiO_4 tetrahedra are proposed as presumable Lewis acid sites. TiO_2 has a higher density of effective Lewis acid sites in water in comparison with Nb_2O_5, because Lewis acid sites on TiO_2 are weaker than those of Nb_2O_5 and thus maintain their acidity even in the presence of water.

Wang and co-workers found that CeO_2 is also a water-tolerant Lewis acid catalyst for hydrolysis of 4-methyl-1,3-dioxane to 1,3-butanediol or one-pot synthesis of 1,3-butanediol from propylene and formaldehyde (Scheme 1-10) [62]. Combining FT-IR, Raman, ^{31}P NMR, ion exchange of acid site, and isotope labeling experiments, they confirmed that CeO_2 (111) can be assigned as the catalytically active crystalline facet, and no water dissociation on oxygen vacancy of ceria prevent decomposition/deactivation of original Lewis acid sites even in water. They concluded that such phenomena can explain why the ceria catalyst is water-tolerant.

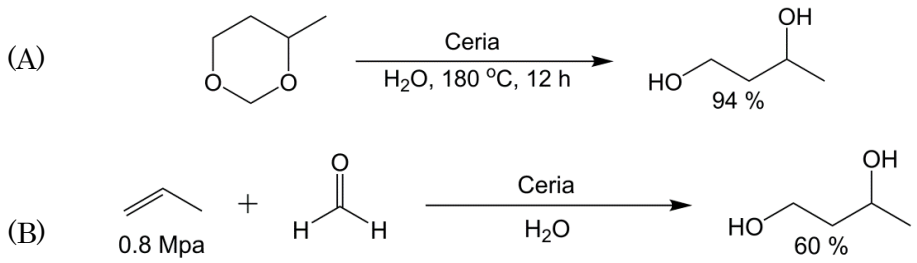

Scheme1-10. Ceria catalyzed 1,3-butanediol synthesis [62]. (A) Hydrolysis of 4-methyl-1,3-dioxane and (B) one-pot synthesis 1,3-butanediol from propylene and formaldehyde via prins condensation and hydrolysis of 4-methyl-1,3-dioxane.

1.2.4.5 Supported Lewis acid catalyst

To develop reusable and easily separable solid acid catalyst, Kobayashi et al. successfully synthesized two types of polymer supported Lewis acid catalysts, microencapsulated scandium triflates and polymer-supported scandium [63-65]. The former is synthesized by using microencapsulation technique: a high density of scandium triflate complex was encapsulated within polystyrene network (Figure 1-4 (A)) [63,64]. Physically enveloped metal triflates by polymer is also chemically stabilized by the interaction between π electrons of benzene rings of the polystyrene and vacant orbitals of scandium metal. It promotes aldol reaction, Michael reaction, Diels-Alder reaction, and Friedel-Crafts acylation in organic solvents. The latter is synthesized by treating the sulfonated polystyrene based polymer with scandium salts (Figure 1-4 (B)) [65]. Because of the strong coordination of scandium species with sulfonic acid group bounded to benzene ring in

polystyrene-based polymer, high reusability and stability of the scandium species was observed for several consecutive reactions. Some Lewis acid catalyzed reaction such as aldol reaction, allylation reaction and Diels-Alder reaction, has also been promoted in water by the latter catalyst.

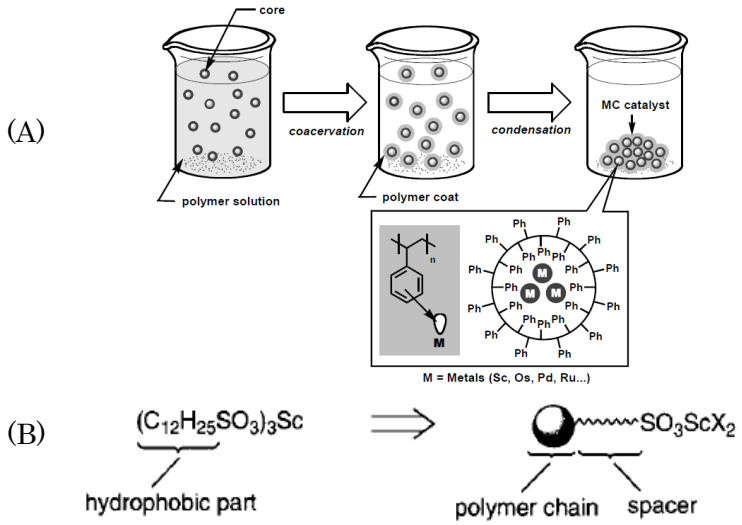

Figure 1-4. Schematic synthetic procedures of solid lanthanide catalysts. (A) Microencapsulated scandium. Reprinted with permission from [64]. Copyright (1996) American Chemical Society. (B) Polymer supported scandium. Reproduced from [65] with permission of John Wiley & Sons.

Kaneda and co-workers studied Montmorillonite enwrapped scandium aqua complexes (Sc-mont), prepared by a simple ion-exchange treatment of the Na^+-mont with aqueous $Sc(OTf)_3$ solution, as a water tolerant Lewis acid catalyst [66,67]. Monomeric Sc^{3+} aqua complex with 6 water molecules ($[Sc(H_2O)_6]^{3+}$) is stabilized in anionic interlayer of the montmorillonite, and responsible as effective Lewis acid sites for Michael reaction in water (Scheme 1-10). Due to the hydrophilicity and layered structure of montmorillonite, basal spacing is expanded in water medium, which results in the efficient diffusion of substrates to Lewis acid sites in each internal layer. Furthermore, Sc ion has relatively large pKh value and is stable in water, it can therefore remain monomeric.

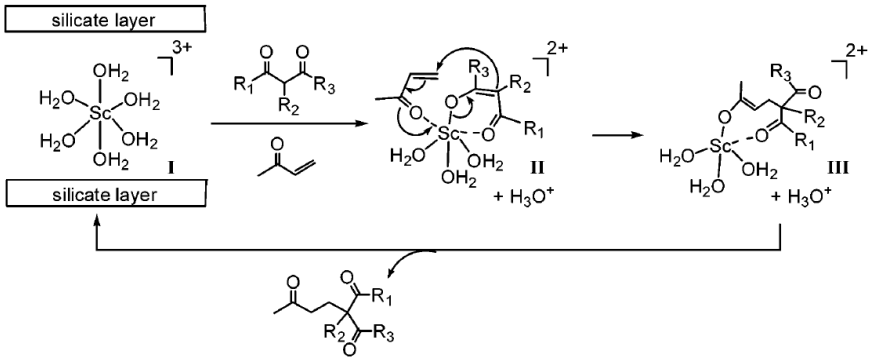

Scheme 1-11. Sc-mont catalyzed Michael reaction in water. Reprinted with permission from [66]. Copyright (2006) American Chemical Society.

1.3 Lewis acid catalyzed reaction in water

1.3.1 Biomass conversion

Lignocellulosic biomass is a natural abundant carbon neutral feedstock, and candidate as renewable resource to be replace with finite fossil carbon resources such as coal, petroleum and natural gas (Figure 1-2) [2,9-14]. In the light of inedibility, lignocellulosic biomass takes great advantage over first-generated biomass, represented by corn starch. Bozell and Petersen summarized and compiled the list of top chemical opportunities from bio refinery carbohydrates (Table 1-4) [68]. The list includes ethanol, furans, Lactic acid and sugar alcohol, and gives a guideline for the development of carbon neutral chemical industry by using biomass-derived carbohydrates as renewable resources.

Table 1-4. New top chemical opportunities from biorefinery carbohydrates. Adopted from [68] with permission of The Royal Society of Chemistry.

Compound	1. Extensive recent literature	2. Multiple product applicability	3. Direct substitute	4. High volume product	5. Platform potential	6. Industrial scaleup	7. Existing commercial product	8. Primary building block	9. Commercial biobased product
Ethanol	+++	+++	+++	+++	+++	+++	+++	+++	+++
Furfural	+++	++	+	++	+	+	+++	++	+++
Hydroxymethyl furfural (HMF)	+++	++	+	+	++	+	+	++	+
Furan-2,5-dicarboxylic acid (FDCA)	+++	+	+	+++	++	+	+	+	+
Glycerol /derivatives	+++	+++	+++	+++	+++	+++	+++	+++	+++
Isoprene	+++	++	+++	+++	+	+++	+++	+	+
Biohydrocarbons	+++	++	+++	+	+	+	+	++	+
Lactic acid	+++	+++	+	+++	++	+	++	+	+
Succinic acid	+++	+++	+	+	+++	+++	+	+	+
Hydroxypropionic acid(HPA)	+++	+	+++	+++	++	+	+	+	+
Levulinic acid	+++	++	+++	++	+++	+++	+	+++	+
Sorbitol	+++	+++	+++	+++	+++	+++	+++	+++	+++
Xylitol	+++	+++	+	+	+++	+	++	+++	++

+++ = Good performance against criterion; ++ = emerging performance against criterion; + = lower performance against criterion.

As shown in Figure 1-5, main constituents of lignocellulosic biomass are cellulose, hemicellulose, and lignin [10]. Cellulose is a polymer of D-glucose units connected via β-1,4 glycoside linkage, and abundant in lignocellulosic biomass. It is generally essential for the efficient

hydrolysis of cellulose to adopt severe and hazardous reaction system, due to its crystal structure and extensive hydrogen bonding network. However, such severe condition leads to the formation of undesirable by-products, anhydrous sugars. Hemicellulose is a polymer of some kinds of carbohydrates including xylose, glucose, galactose, mannose, arabinose, and glucuronic acid. Different from crystalline cellulose, hemicellulose is an amorphous with a low degree of polymerization and branch. Thus, hydrolysis of hemicellulose is easier than cellulose. Lignin is amorphous polymer consisted with highly cross-linked phenolic building blocks (*p*-coumaryl, cofineryl- and sinayl alcohol unit). Although lignin is a candidate for the source of aromatic compounds, owing to the robustness of aromatic C-O-C bonds and cross-linking network, its depolymerization is extremely difficult.

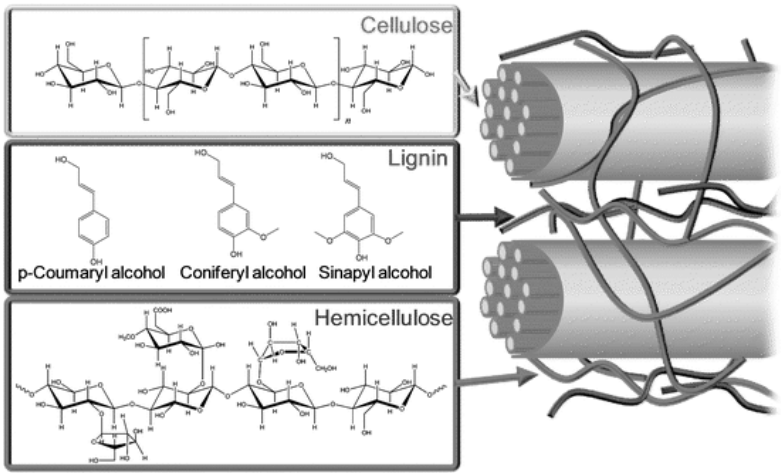

Figure 1-5. Structure of lignocellulosic biomass with cellulose, hemicellulose, and lignin. Reproduced from [10] with permission of The Royal Society of Chemistry.

Lignocellulosic materials can be converted to chemicals or fuels via three routes, (i) gasification, (ii) pyrolysis and (iii) liquid-phase reforming, as shown in Figure 1-6 [9-14]. Syngas, a mixture of hydrogen and carbon monoxide, is obtained by gasification of lignocellulosic biomass, and subsequently converted to chemicals by using well-established Fischer–Tropsch process. Pyrolysis and liquefaction of lignocellulosic biomass gives bio-oil. However, usage of bio-oil as chemical feedstock is not easy because it consists of more them 300 chemicals. Furthermore, high water content (up to 50%) and high oxygen-containing functional groups make bio-oil much more difficult to use as a fuel. High energy consumption of the gasification or pyrolysis process is also undesirable.

On the other hands, liquid phase reforming of lignocellulosic biomass has a possibility to give chemicals in high yield. In the following section, representative liquid phase biomass reforming reactions, the conversions of glucose to fructose and lactic acid synthesis are summarized.

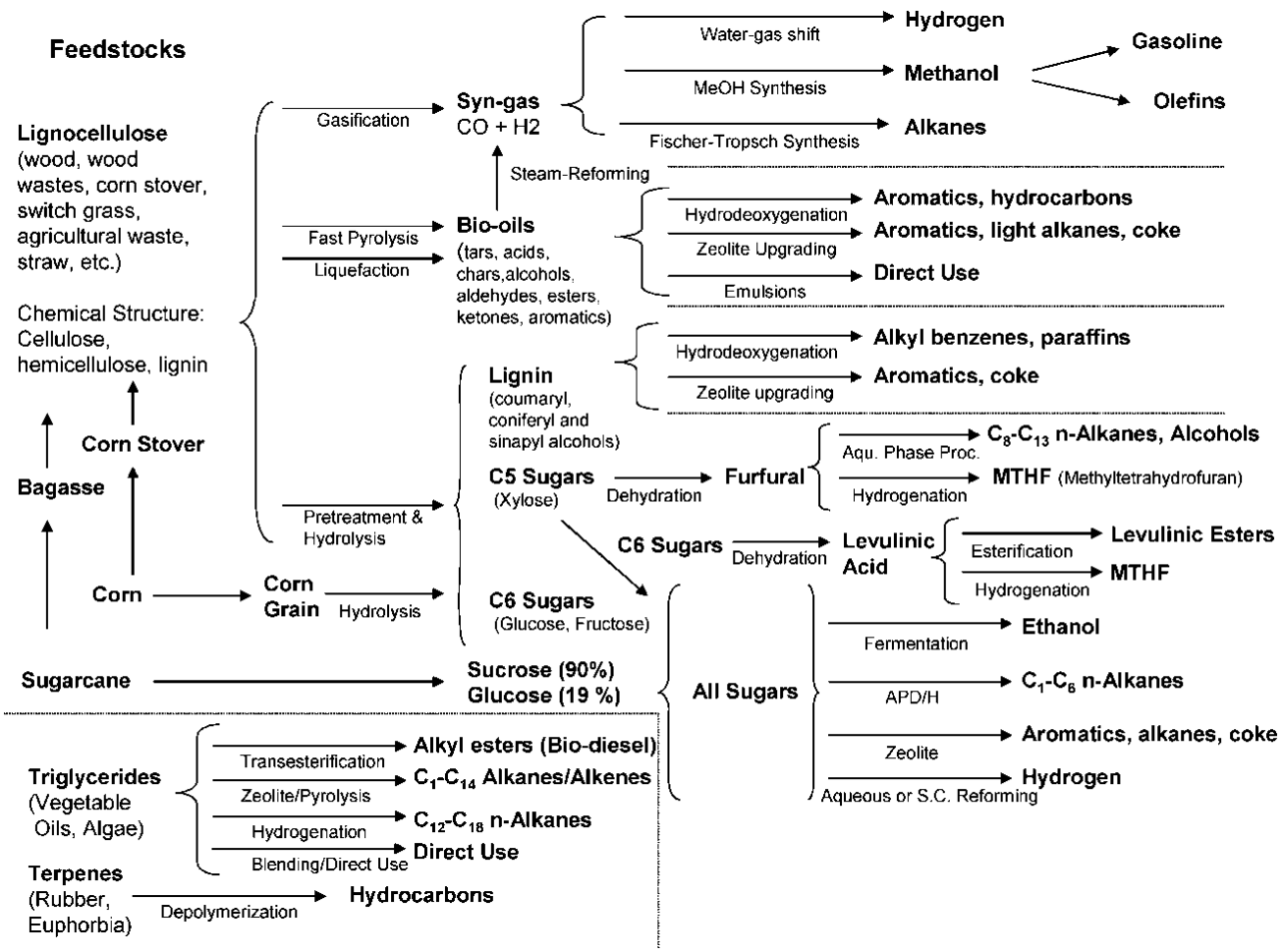

Figure 1-6. Chemical refinery of biomass-derived carbohydrates to chemicals and fuels. Reprinted with permission from [9]. Copyright (2006) American Chemical Society.

1.3.1.1 Glucose isomerization to Fructose in water

The isomerization of glucose into fructose is a very important industrial reaction catalyzed by immobilized enzyme for production of high fructose corn syrup. In recent years, the reaction is considered as a crucial intermediate step for the synthesis of platform chemicals from glucose [69-72]. For example, fructose, obtained by isomerization of cellulose-derived glucose, can be dehydrated by Brönsted acid into 5-hydroxymethylfurfural (HMF), an important chemical intermediate (Scheme 1-12) [13,73,74]. However, current enzymatic fructose production system has some drawbacks: strict pH adjustment, temperature control, high reactant purity and addition of large amounts of unreusable catalyst are requested. Thus, development of more stable, robust and versatile catalyst for the glucose isomerization contributes to the construction of comprehensive biomass-based chemical production.

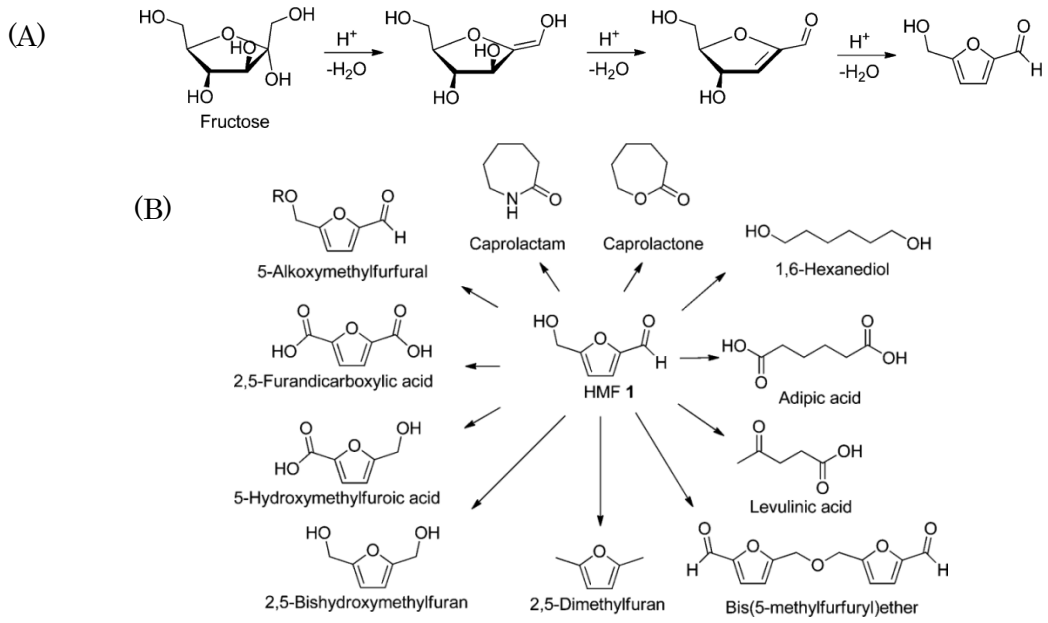

Scheme 1-12. (A) Fructose dehydration to HMF. (B) HMF as platform chemical. Reprinted with permission from [13]. Copyright (2013) American Chemical Society.

Two types of reaction mechanisms have been reported for the isomerization of glucose into fructose, base catalyzed proton transfer through enolate intermediates and Lewis acid (or metal) catalyzed hydride transfer (Scheme1-13) [54,55]. Because of the promotion of side reactions by base catalysts, Lewis acid catalyzed hydride transfer reaction is preferable for the selective fructose production. Lewis acid catalyzed isomerization proceeds through 3 stage mechanisms, (i) ring opening of glucose to form acyclic form, (ii) hydride transfer from C2 to C1 assisted by Lewis acid center, (iii) ring closing to form cyclic fructose.

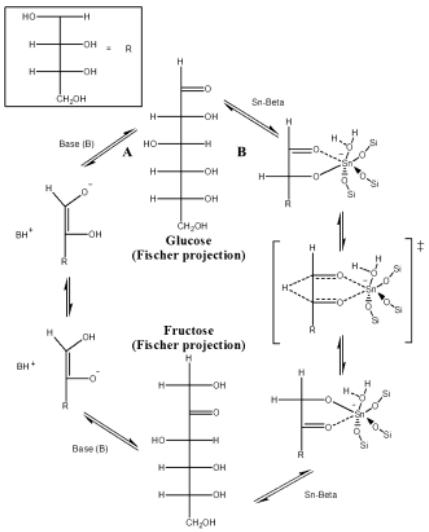

Scheme 1-13. Schematic representation of the glucose isomerization mechanisms. Reproduced from [55] with permission of John Wiley & Sons.

One pot synthesis of HMF from glucose via fructose intermediate with $CrCl_2$ in ionic liquid was reported by Zhao and coworkers (Scheme1-14) [75]. Under the optimized condition, HMF yield reached near 70 %, however addition of water strongly suppresses the reaction. In practical application, conventional catalytic system in water by using reusable solid acid has been desirable for direct production of HMF from glucose.

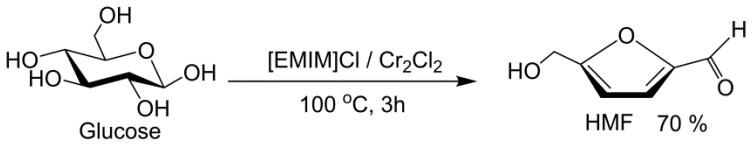

Scheme 1-14. One-pot HMF synthesis from glucose in ionic liquid [75].

In 2010, Davis and co-workers reported that Sn-Beta zeolite catalyzes glucose isomerization into fructose in water (Scheme 1-13) [54-56]. According to their isotopic labeled experiment using ^{13}C solid state NMR measurement, it was confirmed that the reaction proceeds through intramolecular hydride transfer mechanism, similar to the enzyme, D-xylose isomerase XI. The reaction proceeds even in the acidic solutions (pH=2), high glucose concentration (45 wt %), and wide temperature range (343–413 K). It should be noted that HMF can be effectively obtained in this reaction system by the addition of appropriate Brönsted acid catalyst and organic co-solvent to extract HMF from an aqueous reaction phase.

1.3.1.2 Lactic acid synthesis

Lactic acid, one of the "new top chemicals" listed by Bozell and Petersen, is known as an organism-origin chemical, and an intermediate for production of alkyl lactates, acrylic acid, propylene oxide and polylactic acid (Scheme 1-15) [14,68,76]. It is commercially produced by glucose fermentation using micro-organisms with 90% calcium lactate yield, which is produced by neutralization of lactic acid containing cultivating medium with calcium sulfate to maintain appropriate pH. This means that micro-organism system produces large amounts of $CaSO_4$ as a by-product in parallel with lactic acid production.

Efforts have been made to develop chemo-catalytic process for the production of lactic acid from biomass-derived substrates by using solid catalysts for replacement of the environmental unfriendly fermentation system [77-82]. In recent years, trioses, 1,3-dihydroxyacetone (DHA) and glyceraldehyde which can be synthesized by retro-aldol condensation from sugars or oxidation of glycerol, is attracting much attention as a feedstock for lactic acid production (Scheme 1-15) [80-82]. Isomerization of DHA into lactic acid is energetically favored (24 kcal mol^{-1}) [14]. The conversion of trioses into lactic acid proceeds via following two steps (Scheme 1-16) [82]; first, dehydration of trioses to form pyruvaldehyde, and then self-hydration of pyruvaldehyde followed by the hydride

transfer of mono-hydrated form to give lactic acid [32,83,84].

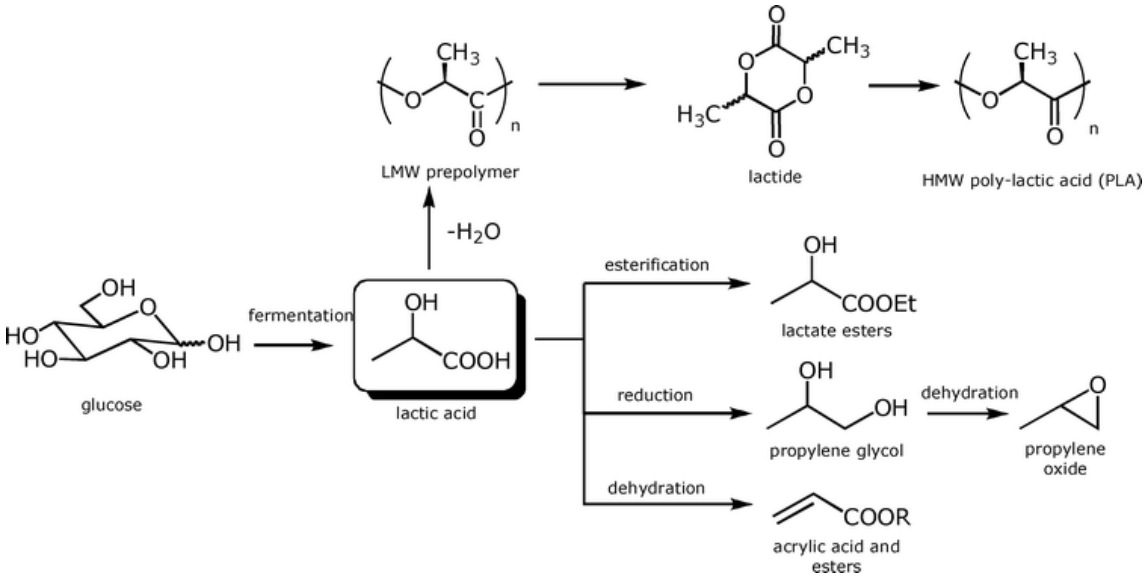

Scheme 1-15. Lactic acid conversion. Reproduced from [68] with permission of The Royal Society of Chemistry.

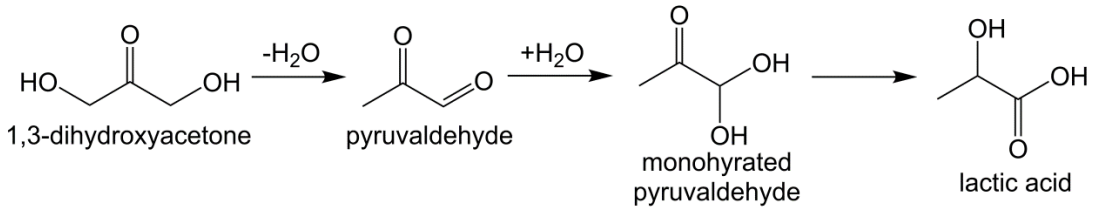

Scheme 1-16. Lactic acid synthesis from 1,3-dihydroxyacetone.

A lot of homogeneous catalysts, such as H_2SO_4, $ZnSO_4$, $Ca(OH)_2$, $AlCl_3$, $SnCl_4$ have been reported for the conversion of DHA to lactic acid [14,77-79]. Among them, Lewis acid catalysts showed high lactic acid yield. On the other hands, efficient heterogeneous catalysts are also reported for the conversion of DHA to lactic acid [80-82]. Taarning et al. found that Sn-Beta zeolite is a highly active catalyst for the production of lactic acid and methyl lactate from triose sugars [80,81]. Lactic acid in 90 % yield was obtained from DHA in aqueous medium at 125 °C. Desilicated commercial ZSM-5 zeolite is also found to be an effective catalyst for the reaction by Dapsens and co-workers: lactic acid yield exceeds 90 % [82]. In either case, Lewis acidity of the catalysts plays an important role for the efficient and selective conversion. It should be noted that these catalysts also promote alkyl lactate synthesis from DHA in alcohol medium, such as methanol or ethanol (scheme 1-17) [80-82,85,86]. Alkyl lactates are considered as next generation “green” solvents for versatile application.

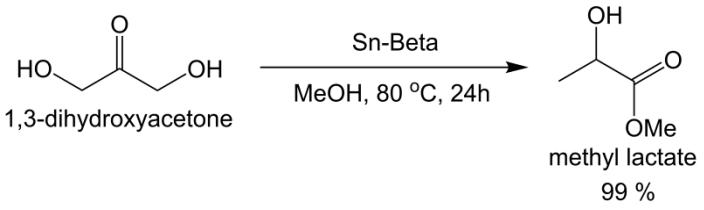

Scheme 1-17. Formation of Methyl lactate in methanol catalyzed by Sn-Beta [81].

1.3.2 Lewis acid catalyzed organic synthesis in water

1.3.2.1 Effect of water on the carbon-carbon forming reaction

Water, an abundant resource in nature, is a "green" solvent. It is essential for water-compatible Lewis acid catalysts to develop an environmental benign chemical production. Note that the use of water as a solvent was found to improve the product selectivity and reaction rate. In 1980, Rideout and Breslow reported the acceleration and increase of selectivity for Diels-Alder reaction in water: the reaction was accelerated more than 700-fold in water as compared with aprotic nonpolar solvent, 2,2,4-trimethylpentane (Scheme 1-18) [87]. Drastic acceleration of the reaction rate was explained by the hydrophobic effect to form emulsions of reactants in water medium. Breslow also pointed that enhanced *endo/exo* selectivity can be attributed to the hydrophobic effect to stabilize more compact *endo* transition state [88]. On the other hands, Gajewski reported the importance of hydrogen bonding donating ability of water for the transition state [89]. Otto and Engberts summarized recent progress of the aqueous Diels-Alder reactions including results of computational chemistry and concluded the effect of water as follows [90]. About the rate enhancement, hydrophobic interactions of substrates raise the initial state, and hydrogen bonding interactions stabilize transition state. The high *endo/exo* ratio is attributed to the three nature of water to form endo adduct, ability to donate hydrogen bond, polarity and hydrophilicity.

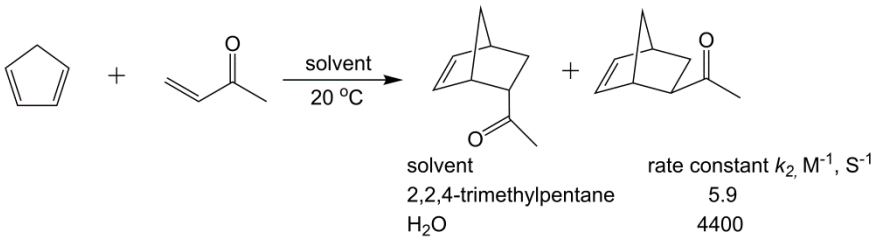

Scheme 1-18. Diels alder reaction accelerated by water [87].

Otto and co-workers reported that reaction rate of the Diels-Alder reaction is largely enhanced in water using water-tolerant Lewis acid catalyst [91,92]. Lewis acid catalyst, $Cu(NO_3)_2$, accelerates the reaction in water much more effectively than in acetonitrile. These reports show clear potential for the combination of water solvent and Lewis acid catalyst in order to develop a variety of carbon-carbon bond forming reaction systems.

1.3.2.2 Mukaiyama aldol reaction

The Mukaiyama-aldol condensation is an essential reaction for the chemoselective synthesis of β-hydroxycarbonyl compounds from silyl enol ether and aldehyde [93-97]. The Mukaiyama-aldol reaction starts by activation of carbonyl group in reactant (aldehyde) by Lewis acid catalysts ($TiCl_4$, for example), and gives cross-aldol adduct with high selectivity. Isolable and stable silyl enol ether is a useful nucleophilic reagent for promoting cross-aldol reaction.

The reaction rate of the Mukaiyama aldol reaction is enhanced by water. Libineau and coworkers reported that the Mukaiyama aldol reaction between benzaldehyde and enolate derived from cyclohexanone proceeds in water without any Lewis acid catalysts, although no reaction occurred in dichloromethane (Table 1-5) [98,99]. It should be noted that the diastereoselectivity of the products was completely opposite in comparison with Lewis acid catalyzed reaction in dichloromethane. This can be attributed to the preferable formation of more compact *syn* transition state in water medium. Acceleration of the reaction by water was also reported by Loh and coworkers [100]. The Mukaiyama aldol reaction of ketene silyl acetal and 2-pyridinecarboxyaldehyde in water was 4 times faster than in tetrahydrofuran or dichloromethane.

Table 1-5. Mukaiyama-aldol reaction accelerated by water. Reproduced from [101] with permission of John Wiley & Sons.

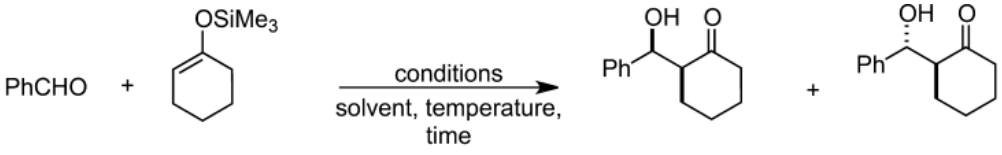

X	Solvent	Temperature [°C]	Conditions[a]	Time	Yield[b] [%]	*syn*/*anti*
1	CH_2Cl_2	20	$TiCl_4$	2 h	82	25/75
1	CH_2Cl_2	60	10 kbar	9 d	90	75/25
2	H_2O	20	stirring[c]	5 d	45 (43)[d]	74/26

Lewis acid catalyzed aqueous Mukaiyama aldol reactions using lanthanide triflates were found in 1991, by Kobayashi et al (Scheme 1-5) [34]. The reactions with $Yb(OTf)_3$ in water-tetrahydrofuran mixture proceeded smoothly, and gave aldol adduct (*syn*) in high yield. Addition of water to reaction system is necessary to obtain the desired product effectively (Scheme 1-19) [35]. Recently, Morokuma et al. studied the role of water for aqueous Eu^{3+} catalyzed Mukaiyama aldol reaction using computational chemistry and concluded as follows (Figure 1-7) [102]. The reaction proceeds via 3 steps mechanism: first C-C bond between substrates is formed, then, proton transfers from water to benzaldehyde, and finally bulk water molecules attack trimethylsilyl group to

dissociate. Without water, the reverse reaction, C-C bond cleavage, occurs easily. Furthermore, water stabilizes *syn* transition state better than anti transition state. These effects of water give characteristic acceleration and selectivity to aqueous Mukaiyama aldol reaction.

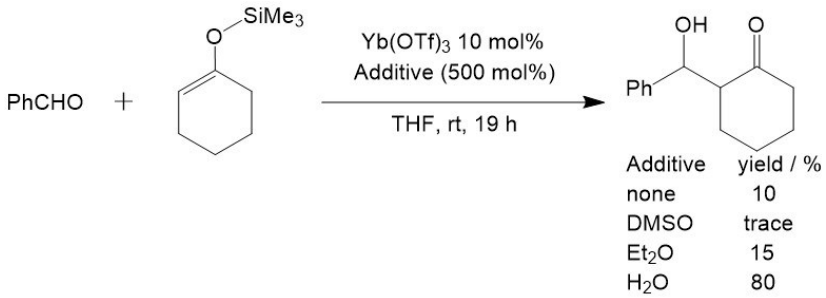

Scheme 1-19. Effect of solvent for Mukaiyama-aldol reaction. [35]

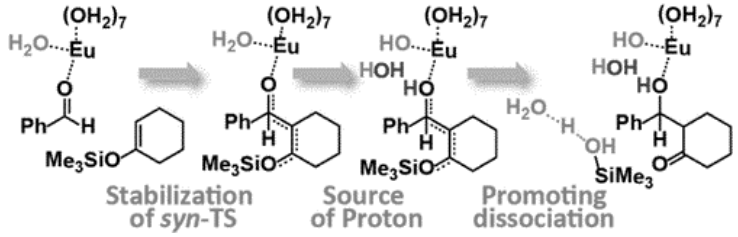

Figure 1-7. Schematic image of the role of water in Mukaiyama-aldol reaction. Reprinted with permission from reference [102]. Copyright (2013) American Chemical Society.

Another advantage of aqueous Mukaiyama aldol reaction is usage of aqueous reactant solution, such as formalin [34,35]. Kobayashi et al. demonstrated the lanthanide triflates catalyzed hydroxymethylation using formalin as carbon source (Scheme 1-20). Formaldehyde is a useful reagent for the hydroxymethylation in organic synthesis. However, due to the instability of formaldehyde, formalin (aqueous solution of formaldehyde) or paraformaldehyde (polymer of formaldehyde) are commercially available formaldehyde source. This finding succeeded in avoiding troublesome procedure such as pyrolysis of paraformaldehyde.

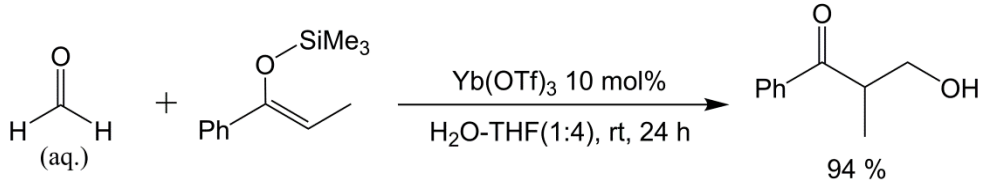

Scheme 1-20. Hydroxymethylation of silyl enol ether using formaldehyde solution [35].

Kobayashi et al. also developed some aqueous Mukaiyama aldol reaction systems using lanthanide based catalysts [36,37]. The micellar reaction systems, containing pure water as reaction medium and surfactants such as sodium dodecyl sulfate and triton X-100, enables the use of hydrophobic reactant in water (Scheme 1-21). Lewis acid surfactant combined catalyst (LASC), such as Scandium tris(dodecyl sulfate), is a lanthanide complex containing surfactant molecule as a ligand and can form small hydrophobic spheres in reaction mixture that can incorporate hydrophobic reactants. The incorporated reactant molecules can easily access to catalytically active metal center, thus promoting the Mukaiyama-aldol reaction.

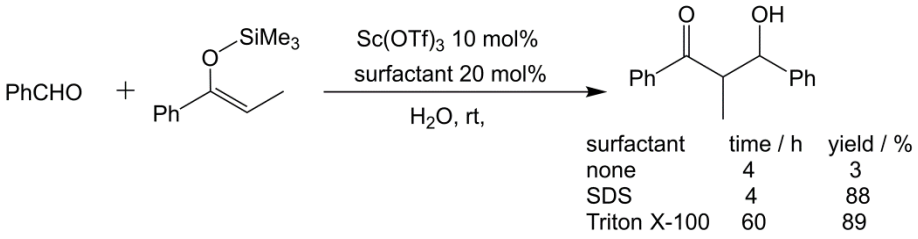

Scheme 1-21. Effect of surfactants for Mukaiyama-aldol reaction in water [36].

Many attempts have been devoted to develop solid acid catalyzed Mukaiyama aldol reaction so far [103-111]. For example, aluminum-montmorillonite, aluminium-MCM-41, titanium-MCM-41 are found to function as solid catalysts for the reaction in organic solvents, such as dichloromethane, toluene or acetonitrile (Scheme 1-22). However, solid acid catalyzed aqueous Mukaiyama aldol reaction has not been reported.

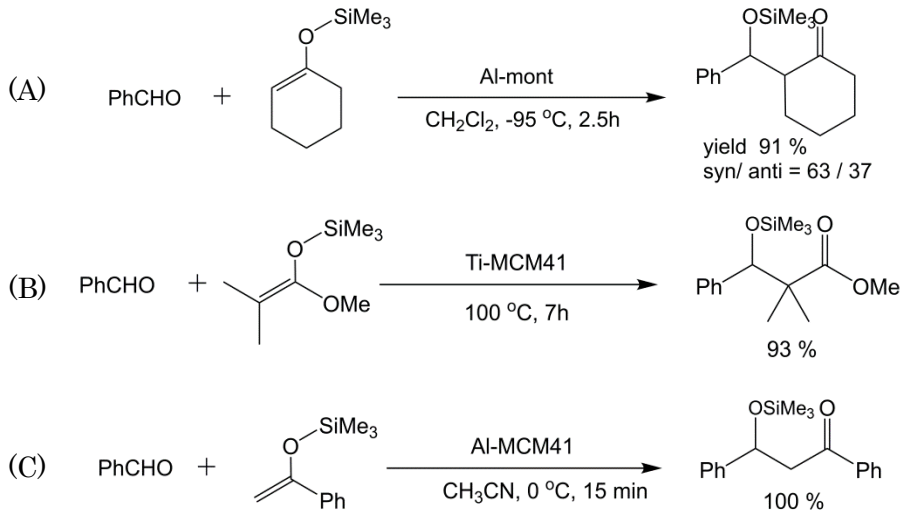

Scheme 1-22. Solid acid catalyzed Mukaiyama aldol rection (A) Aluminum-montmorillonite [103], (B) Titanium-MCM-41 [108] and (C) Aluminium-MCM-41 [111].

1.4 Outline of this thesis

Lewis acid catalyzed reactions are industrially useful for the production of bulk and fine chemicals. The developments of easy separable, recyclable and water compatible solid Lewis acid catalysts using earth abundant elements enable us to establish environmental benign chemical process.

The main objective of this thesis is design of solid Lewis acid catalysts and their catalytic application for aqueous-phase organic reactions. In this study, to develop versatile solid catalysts, I focused on mesoporous silica as a support, and titanium tetrahedron as Lewis acid site, because porous structure and large surface area of silica support are beneficial for the access of bulk reactant molecules in water to the active sites, and titanium tetrahedra are promising water tolerant Lewis acid sites. I studied the synthesis and structural characterization of titanium deposited mesoporous silicas (TDMS), and their catalytic activity for the triose conversion reaction into lactic acid and surfactant assisted Mukaiyama aldol reaction in water. Furthermore, to develop Mukaiyama aldol reaction in pure water medium, I also designed surfactant-free Mukaiyama-aldol condensation reaction in water with hydrophobic TDMS as a solid Lewis acid catalyst.

Chapter 2

TDMS prepared by post-grafting was investigated as a water tolerant Lewis acid catalyst. Lewis acidity and catalysis of TDMS was examined by FT-IR measurement using carbon monoxide as basic molecular probes, and hydride transfer reaction of pyruvaldehyde and surfactant assisted aqueous Mukaiyama aldol reaction, respectively.

Chapter 3

Co-condensation method and post-grafting method were studied for the development of highly active TDMS catalyst. While co-condensation method restrict homogeneous dispersion of titanium species due to the formation of titanium oxide, post-grafting method can produce highly dispersed TiO_4 tetrahedra on the surface of mesoporous silica.

Chapter 4

Hydrophobic TDMS was prepared by surface modification of TDMS with various organic functional groups and tested for surfactant free aqueous Mukaiyama aldol reaction of benzaldehyde with 1-(trimethylsilyloxy)cyclohexene. Surface hydrophobicity enhances adsorption of reactant molecule in water, which results in high catalytic performance even in the absence of surfactant. In addition, the reaction cannot be promoted in any organic solvent, meaning that water also plays an important role for the reaction.

References

[1] C. H. Bartholomew, R. J. Farrauto, *Fundamentals of Industrial Catalytic Processes*, Wiley-VCH, Hoboken, **2006**.

[2] M. Poliakoff1, J. M. Fitzpatrick, T. R. Farren, P. T. Anastas, *Science* **2002**, *297*, 807–810.

[3] G. Busca, *Chem. Rev.* **2007**, *107*, 5366–5410.

[4] A. Corma, H. Garcia, *Chem. Rev.* **2003**, *103*, 4307–4365.

[5] A. Corma, *Curr. Opin. Solid State Mater. Sci.* **1997**, 2, 63–75

[6] P. T Anastas, M. M. Kirchhoff, *Acc. Chem. Res*. **2002**, *35*, 686–694.

[7] T. Setoyama, M. Kobayashi, Y. Kabata, T. Kawai, A. Nakanishi, *Catal. Today* **2002**, *73*, 29–37.

[8] T. Setoyama, T. Ookoshi, I. Ono, *Catal. Surv. Asia* **2003**, *7*, 183–187.

[9] G. W. Huber, S. Iborra, A. Corma, *Chem. Rev.* **2006**, *106*, 4044–4098.

[10] D. M. Alonso, S. G. Wettstein, J. A. Dumesic, *Chem. Soc. Rev.* **2012**, *41*, 8075–8098.

[11] D. M. Alonso, J. Q. Bond, J. A. Dumesic. *Green Chem.* **2010**, *12*, 1493–1513.

[12] N. Sun, H. Rodríguez, M. Rahman, R. D. Rogers, *Chem. Commun.* **2011**, *47*, 1405–1421.

[13] R. J. Putten, J. C. van der Waal, E. D. Jong, C. B. Rasrendra, H. J. Heeres, J. G. Vries, *Chem. Rev*. **2013**, *113*, 1499–1597

[14] P. M. Arvela, I. L. Simakova, T. Salmi, D. Y. Murzin, *Chem. Rev.* **2014**, *114*, 1909–1971.

[15] U. M. Lindström (Eds.), Organic Reactions in Water: Principles, Strategies and Applications, Wiley-Blackwell, Oxford, **2007**.

[16] T.Okuhara, *Chem.Rev.* **2002***, 102,*3641–3666.

[17] S. Kobayashi, K.Manabe, *Acc. Chem. Res.* **2002**, *35*, 209–217.

[18] Li, C.-J. *Chem. Rev.* **2005**, *105*, 3095–3166.

[19] S. Narayan, J. Muldoon, M. G. Finn, V. V. Fokin, H. C. Kolb, K. B. Sharpless, *Angew. Chem. Int. Ed.* **2005**, *44*, 3275–3279.

[20] R.N. Butler, A.G.Coyne, *Chem. Rev.* **2010**, *110***,** 6302–6337.

[21] R. I. Masel, *Principles of Adsorption and Reaction on Solid Surfaces*, Wiley, New York, **1996**.

[22] J. W. Niemantsverdriet, *Spectroscopy in Catalysis, an Introduction*, Wiley-VCH, Weinheim, **2000**.

[23] W. E. Farneth, R.J. Gorte, *Chem. Rev.* **2005**, *95*, 615–635.

[24] R. J. Cvetanovic, Y. Amemiya, *Adv. Catal.* **1967**, *17*, 103–149.

[25] A. Zheng, S.-J. Huang, S.-B. Liu F. Deng, *Phys. Chem. Chem. Phys.* **2011**, *13*, 14889–14901.

[26] A. Zhenga, S.-B. Liub, F. Deng, *Solid State Nuclear Magnetic Resonance* **2013**, *55*, 12–27.

[27] R. G. Pearson, *J. Am. Chem. Soc.* **1963**, *85*, 3533–3539.

[28] R. G. Pearson, *J. Chem. Educ.* **1968**, *45*, 581–586.

[29] R. G. Pearson, *J. Chem. Educ.* **1968**, *45*, 643–648.

[30] J. E. McMurry, *Organic Chemistry 6th edition*, Cengage Learning, Hampshire, **2007**.

[31] F. Fringuelli, F. Pizzo, L. Vaccaro, *J. Org. Chem.* **2001**, *66,* 4719–4722.

[32] Y. Hayashi, Y. Sasaki, *Chem. Commun.* **2005**, 2716–2718.

[33] C. B. Rasrendra, B. A. Fachri, I. G B. N. Makertihartha, S. Adisasmito, H. J. Heeres, *ChemSusChem* **2011**, *4*, 768–777.

[34] S. Kobayashi, *Chem. Lett.* **1991**, 2187–2190.

[35] S. Kobayashi, I. Hachiya, *J. Org. Chem.* **1994**, *59*, 3590–3596.

[36] S. Kobayashi, T. Wakabayashi, S. Nagayama, H. Oyamada, *Tetrahedron Lett.* **1997**, *38*, 4559–4562.

[37] S. Kobayashi, T. Busujima, S. Nagayama, *Chem. Commun.* **1998**, 19–20.

[38] S. Kobayashi, S. Nagayama, T. Busujima, *J. Am. Chem. Soc.* **1998**, *120*, 8287–8288.

[39] P. Dissanayake, M. J. Allen, *J. Am. Chem. Soc.* **2009**, *131*, 6342–6343.

[40] D. J. Averill, P. Dissanayake, M. J. Allen, *Molecules* **2012**, *17*, 2073–2081.

[41] J. A. Martens, P. A. Jacobs, *Stud. Surf. Sci. Catal.* **2001**, *137*, 633–671.

[42] A. Primo, H. Garcia, *Chem. Soc. Rev.* **2014**, *43*, 7548–7561.

[43] E. Beerdsen, D. Dubbeldam, B. Smit, *J. Phys. Chem. C* **2006**, *110*, 22754–22772.

[44] I. N. Senchenya, V. B. Kazanskii, S. Beran, *J. Phys. Chem.* **1986**, *90*, 4857–4859.

[45] M.Taramasso, G. Perego, B. Notari, US patent 4410501, **1983**.

[46] B. Notari, *Adv. Catal*. **1996**, *41*, 253–334.

[47] A. Corma, H. Garcia, *Chem. Rev.* **2002**, *102*, 3837–3892.

[48] C. Li, G. Xiong, Q. Xin, J. K. Liu, P. L. Ying, Z. C. Feng, J. Li,W. B. Yang, Y. Z. Wang, G. R. Wang, X. Y. Liu, M. Lin, X. Q. Wang, E. Z. Min, *Angew. Chem. Int. Ed.* **1999**, *38*, 2220–2222.

[49] Q. Guo, K. Sun,Z. Feng,G. Li, M. Guo, F. Fan, C. Li, *Chem. Eur. J.* **2012**, *18*, 13854–13860.

[50] A. Corma, L. T. Nemeth, M. Renz, S. Valencia, *Nature* **2001**, *412*, 423–425.

[51] A. Corma, M. E. Domine, L. Nemeth, S. Valencia, *J. Am. Chem. Soc.* **2002**, *124*, 3194–3195.

[52] A. Corma, V. Fornés, S. Iborra, M. Mifsud, M. Renz, *J. Catal.* **2004**, *221*, 67–76.

[53] A. Corma, F. X. Llabrés i Xamena, C. Prestipino, M. Renz, S. Valencia, *J. Phys. Chem. C* **2009**, *113*, 11306–11315.

[54] M. Moliner, Y. Román-Leshkov, M. E. Davis, *Proc. Natl. Acad. Sci. U.S.A.* **2010**, *107*, 6164–6168.

[55] Y. Román-Leshkov, M. Moliner, J. A. Labinger, M. E. Davis, *Angew. Chem. Int. Ed.* **2010**, *49*, 8954–8956.

[56] R. Bermejo-Deval, R. S. Assary, E. Nikolla, M. Moliner, Y. Romań-Leshkov, S.-J. Hwang, A. Palsdottir, D. Silverman, R. F. Lobo, L. A. Curtiss, M. E. Davis, *Proc. Natl. Acad. Sci. U.S.A.*

2012, *109*, 9727–9732.

[57] R. Bermejo-Deval, M. Orazov, R. Gounder, S.-J. Hwang, M. E. Davis, *ACS Catal*. **2014**, *4*, 2288–2297.

[58] Z. Chen, T. Iizuka, K.Tanabe, *Chem. Lett*. **1984**, 1085–1088.

[59] K. Hanaoka, T. Takeuchi, T. Matsuzaki, Y. Sugi, *Catal. Today* **1990**, *8*, 123–132.

[60] K. Nakajima, Y. Baba, R. Noma, M. Kitano, J. N. Kondo, S. Hayashi, M. Hara, *J. Am. Chem. Soc.* **2011**, *133*, 4224–4227.

[61] K.Nakajima, R. Noma, M. Kitano, M. Hara, *J. Phys. Chem. C* **2013**, *117*, 16028–16033.

[62] Y. Wang, F. Wang, Q. Song, Q. Xin, S. Xu, J. Xu, *J. Am. Chem. Soc.* **2013**, *135*, 1506–1515.

[63] S. Nagayama, S. Kobayashi, *J. Org. Chem.* **1996**, *61*, 2256–2257.

[64] S. Kobayashi, S. Nagayama, *J. Am. Chem. Soc.* **1998**, *120*, 2985–2986.

[65] S. Nagayama, S. Kobayashi, *Angew. Chem. Int. Ed.* **2000**, *39*, 567–569.

[66] T. Kawabata, T. Mizugaki, K. Ebitani, K. Kaneda, *J. Am. Chem. Soc.* **2003**, *125*, 10486–10487.

[67] T. Kawabata, M. Kato, T. Mizugaki, K. Ebitani, K. Kaneda, *Chem. Eur. J.* **2005**, *11*, 288–297.

[68] J. J. Bozell, G. R. Petersen, *Green Chem.* **2010**, *12*, 539–554.

[69] Y. Román-Leshkov, M. E. Davis, *ACS Catal.* **2011**, *1*, 1566–1580.

[70] R.Gounder, *Catal. Sci. Technol.* **2014**, *4*, 2877–2886.

[71] M. Moliner, *Dalton Trans*. **2014**, *43*, 4197–4208.

[72] S. Saravanamurugan, M. Paniagua, J. A. Melero, A. Riisager, *J. Am. Chem. Soc.* **2013**, *135* 5246–5249.

[73] M. A. Lilga, R. T. Hallen, R. T. Gray, *Top Catal*. **2010**, *53*, 1264–1269.

[74] S. Subbiah, S. P. Simeonov, J. M. S. S. Esperança, L. P. N. Rebelo, C. A. M. Afonso, *Green Chem.* **2013**,*15*, 2849–2853.

[75] H. Zhao, J. E. Holladay, H. Brown, Z. C. Zhang, *Science* **2007**, *316*, 1597–1600.

[76] R. E. Drumright, P. R. Gruber, D. E. Henton, *Adv. Mater*. **2000**, *12*, 1841–1846.

[77] M. Bicker, S. Endres, L. Ott, H. Vogel, *J. Mol. Catal. A* **2005**, *239*, 151–157.

[78] L.Kong, G. Li, H. Wang, W. He, F. Ling, *J. Chem. Technol. Biotechnol.* **2008**, *83*, 383–388.

[79] F. Chambon, F. Rataboul, C. Pinel, A. Cabiac, E. Guillon, N. Essayem, *Appl. Catal. B* **2011**, *105*, 171–181.

[80] E.Taarning, S. Saravanamurugan, M. S. Holm, J. Xiong, R. M. West, C. H. Christensen, *ChemSusChem* **2009**, *2*, 625–627.

[81] M. S. Holm, S. Saravanamurugan, E. Taarning, *Science* **2010**, *328*, 602–605.

[82] P. Y. Dapsens, C. Mondelli, J. Prez-Ramrez, *ChemSusChem* **2013**, *6*, 831–839.

[83] I. Nemet, D. Vikić-Topić, L. Varga-Defterdarović, *Bioorg. Chem.* **2004**, *32*, 560–570.

[84] Y. Koito, K. Nakajima, M. Kitano, M. Hara, *Chem. Lett.* **2013**, *42*, 873–875.

[85] P. P. Pescarmona, K. P. F. Janssen, C. Delaet, C. Stroobants, K. Houthoofd, A. Philippaerts, C. De Jonghe, J. S. Paul, P. A. Jacobs, B. F. Sels, *Green Chem*. **2010**, *12*, 1083–1089.

[86] L. Li, C. Stroobants, K. Lin, P. A. Jacobs B. F. Sels, P. P. Pescarmona, *Green Chem.* **2011**,*13*, 1175–1181.

[87] D. Rideout, R. Breslow, *J. Am. Chem. Soc.* **1980**, *102*, 7816–7817.

[88] R. Breslow, U. Maitra, D. Rideout, *Tetrahedron Lett.* **1983**, *24*, 1901–1904.

[89] J. J. Gajewski, *J. Org. Chem.* **1992**, *57*, 5500–5506.

[90] S. Otto, B. F. N. Engberts, *Pure. Appl. Chem.* **2000**, *72*, 1365–1372.

[91] S. Otto, G. Boccaletti, J. B. F. N. Engberts. *J. Am. Chem. Soc.* **1998,** *120*, 4238–4238.

[92] S. Otto, J. C. T. Kwak, J. B. F. N. Engberts. *J. Am. Chem. Soc.* **1998**, *120*, 9517–9525.

[93] T. Mukaiyama, K. Narasaka, K. Banno, *Chem. Lett.* **1973**, *2*, 1011–1014.

[94] T. Mukaiyama, K. Banno, K. Narasaka, *J. Am. Chem. Soc.* **1974**, *96*, 7503–7509.

[95] S. B. J. Kan, K. K.-H. Ng, I. Paterson, *Angew. Chem. Int. Ed.* **2013**, *52*, 9097–9108.

[96] S. E. Denmark, S. B. D. Winter, X. Su, K.-T. Wong, *J. Am. Chem. Soc.* **1996**, *118*, 7404–7405.

[97] H. Fujisawa, T. Mukaiyama, *Chem. Lett.* **2002**, *31,* 182–183.

[98] A. Lubineau, *J. Org. Chem.* **1986**, *51*, 2142–2144.

[99] A. Lubineau, E. Meyer, *Tetrahedron* **1988**, *44*, 6065–6070.

[100] T.-P. Loh, L.-C. Feng, L.-L. Wei, *Tetrahedron* **2000**, *56*, 7309–7312.

[101] T. Kitanosono, S. Kobayash, *Adv. Synth. Catal.* **2013**, *355*, 3095–3118.

[102] M. Hatanaka, K. Morokuma, *J. Am. Chem. Soc.* **2013**, *135*, 13972–13979.

[103] M. Kawai, M. Onak, Y. Izumi, *Chem. Lett*. **1986**, *15*, 1581–1584.

[104] M. Sasidharan, S. V. N. Raju, K. V. Srinivasan, V. Pau, R. Kumar, *Chem. Commun.* **1996**, 129–130.

[105] T.-P. Loh, X.-R. Li, *Tetrahedron* **1999**, *55,* 10789–10802.

[106] H. Matsuhashi, M. Tanaka, H. Nakamura, K. Arata, *Appl. Catal. A* **2001**, *208*, 1–5.

[107] H. Ishitani, M. Iwamoto, *Tetrahedron Lett.* **2003**, *44*, 299–301.

[108] R. Garro, M. T. Navarro, J. Primo, A. Corma, *J. Catal.* **2005**, *233*, 342–350.

[109] T. R. Gaydhankar, P. N. Joshi, P. Kalita, R. Kumar, *J. Mol. Catal. A* **2007**, *265*, 306–315.

[110] S. Ito, H. Yamaguchi, Y. Kubota, M. Asami, *Chem. Lett.* **2009**, *38*, 700–701.

[111] S. Ito, A. Hayashi, H. Komai, Y. Kubota, M. Asami, *Tetrahedron Lett.* **2010**, *51*, 4243–4245.

Chapter 2

Lewis Acid Catalysis of TiO_4 Deposited Mesoporous Silica in Water

2.1 Abstract

TiO_4-deposited mesoporous silica (TDMS) was studied as a water-tolerant solid Lewis acid catalyst. TDMS prepared by a simple post-grafting technique using Ti(OPr-*i*)$_4$ has a large BET surface area (ca. 450 m^2 g^{-1}) and ordered mesoporous structure. Ultraviolet-visible diffuse reflectance spectroscopy (UV-Vis DRS), X-ray absorption near edge structure (XANES), and CO adsorption measurements with Fourier transform infrared (FTIR) spectroscopy revealed that isolated TiO_4 tetrahedra on TDMS have Lewis acidity, even in the presence of water. Lewis acid centers on TDMS exhibit higher catalytic performance for the hydride transfer of pyruvaldehyde to lactic acid and the Mukaiyama-aldol condensation of benzaldehyde with 1-trimethylsilyloxy-cyclohexene in water than that of conventional heterogeneous and homogeneous Lewis acids, including scandium(III) triflate ($Sc(OTf)_3$), which also work even in water. The high catalytic performance of TDMS can be attributed to Lewis acid catalysis of isolated TiO_4 tetrahedra in water.

2.2 Introduction

Lewis acids, such as $AlCl_3$ and $TiCl_4$, are essential catalysts for the production of a variety of petroleum-derived chemicals, such as polymers and pharmaceuticals [1,2]. However, the use of conventional Lewis acids require strictly anhydrous conditions because they are decomposed and/or completely deactivated by water. In addition, excess amounts of Lewis acid are often necessary for efficient Lewis acid-catalyzed reactions, accompanied with the production of corrosive acid waste by neutralization [3]. Some attempts have been made to develop water-compatible and easily separable solid Lewis acid catalysts to reduce the environmental impact of reaction systems. For example, polymer-supported lanthanide triflates have been studied as heterogeneous Lewis acid catalysts for various water-participating organic reactions, such as aldol condensation and the Diels-Alder reaction, under mild conditions [4,5]. The Sn center on Sn-Beta zeolite can act as a water-tolerant Lewis acid site to promote the Baeyer-Villiger oxidation of ketones with hydrogen peroxide [6,7]. The unique catalysis with Sn-Beta zeolite is attributed not only to the selective activation of hydrogen peroxide, but also to the carbonyl group in the reactant; the activated carbonyl group on a

Lewis acid site preferentially reacts with hydrogen peroxide to form lactone in the presence of water. Sn-Beta zeolite also effectively catalyzes the hydride transfer of glucose into fructose in water [8.9] and methyl lactate production from 1,3-dihydroxyacetone in methanol [10]. However, the utility of polymer supported lanthanide triflates and Sn-Beta zeolte have been limited by the scarcity of lanthanide and the narrow reaction spaces of zeolites, respectively.

We have recently reported that some early transition metal oxides, such as Nb_2O_5 and TiO_2, can work in water as insoluble Lewis acid catalysts and are applicable to the conversion of glucose into 5-hydroxymethylfurfural and lactic acid production from pyruvaldehyde in water [11-13]. The Lewis acid sites of these oxides are considered to be unsaturated coordination species, such as tetrahedrally coordinated niobium and titanium species on the surface [11,12]. In this study, we have focused on Lewis acid catalysis of TiO_4-deposited mesoporous silica (TDMS). It has been reported that the introduction of titanium species onto the silica surface would preferentially result in the formation of TiO_4 tetrahedra [14-17], but the Lewis acid catalysis for such species in water has not yet been studied. Here, we report that isolated TiO_4 tetrahedra dispersed on mesoporous silica exhibit high catalytic performance that is distinct from that of TiO_2.

2.3 Experimental

2.3.1 Catalyst Preparation

Mesoporous silica SBA-15 was synthesized with an amphiphilic block copolymer P123 (Aldrich, M_W=5800) as a structure directing agent and tetramethyl orthosilicate (TMOS) as a silica source [18,19]. In a typical synthesis, 4 g of P123 was dissolved in a mixed solution of distilled water (90 g) and HCl (4 M, 60 mL) at 313 K. After addition of TMOS (6.2 g) into the clear solution, the mixture was stirred at 313 K for 20 h, followed by heating at 373 K for 24 h under static conditions. Calcination of the resultant white precipitate at 823 K for 5 h in air resulted in mesoporous silica SBA-15.

Impregnation of titanium species onto SBA-15 was performed by a simple post-grafting method [15]. SBA-15 (5 g) was added to a mixture of distilled water (145 g) and ethanol (15 g) at room temperature. After the pH of the solution was adjusted to 10.0 with diluted ammonia, a mixture of ethanol (5 g), Ti(OPr-*i*)$_4$ (TTIP) and acetyl acetone (AA) (AA/TTIP =3.1) was slowly added to the mixture at 278 K and then stirred for 2 h. After filtration and repeated washing with ethanol, the material was calcined at 823 K for 3 h to immobilize the titanium species on the silica surface. The resulting TiO_4-deposited mesoporous silica (TDMS) samples with various titanium content are denoted as Ti-x/SBA-15 (x=Ti atom%).

For comparison, bulk anatase TiO_2 and titanosilicate zeolite (TS-1) were used as reference catalysts. TiO_2 was synthesized by a sol-gel method using Ti(OPr-*i*)$_4$ as a precursor [12]. TS-1 was supplied from the Catalysis Society of Japan and was used as received.

2.3.2 Catalyst Characterization

The titanium content of the samples was determined using X-ray fluorescence spectroscopy (XRF; ZSX100e, Rigaku). Powder X-ray diffraction patterns were obtained with a diffractometer (Ultima IV, Rigaku) using Cu Kα radiation (40 kV, 40 mA) over the 2θ range of 0.7–70°. Nitrogen adsorption-desorption isotherms were measured at 77 K with a surface area analyzer (Nova-4200e, Quantachrome). Prior to measurement, the samples were heated at 473 K for 1 h under vacuum to remove physisorbed water. The Brunauer-Emmett-Teller (BET) surface areas were estimated over a relative pressure (P/P_0) range of 0.05-0.30. Pore size distributions were obtained from the adsorption branch of the isotherms using the Barrett-Joyner-Halenda (BJH) method. X-ray absorption spectra at the Ti-K edge were acquired at BL-9C of the Photon Factory of the Institute for Material Structure Science (PF-IMSS, KEK, Proposal no. 2012G101). TS-1 and TDMS were pressed into 20 mm diameter self-supporting disks, and TiO_2 was pressed with boron nitride into a 20 mm diameter disk. Dehydrated samples were sealed in polyethylene bags under a nitrogen atmosphere. Data reduction was performed using the REX2000 program (Rigaku). The acid site density of the samples was estimated by Hammett indicator titration based on the Benesi method in dry benzene [20,21]. n-butylamine and 4-phenylazo-1-naphthylamine (p*K*a = +4.0) were used as titrant and color indicator, respectively.

Fourier transform-infrared (FT-IR) spectra were obtained at a resolution of 4 cm^{-1} using a spectrometer (FT/IR-6100, Jasco) equipped with an extended KBr beam splitting device and a mercury cadmium telluride (MCT) detector. A total of 32 scans were averaged for each spectrum. The samples were pressed into self-supporting disks (20 mm diameter, 20 mg) and placed in an IR cell attached to a closed glass-circulation system. The disks were dehydrated by heating at 573 K for 1 h under vacuum to remove physisorbed water. For experiments with hydrated samples, the dehydrated disks were exposed to 20 Torr of water vapor at room temperature for 1 h, followed by evacuation for 5 min to remove weakly adsorbed water. CO was adsorbed as a basic probe molecule on the dehydrated or hydrated sample disks in the IR cell under cooling with liquid N_2 (measured temperature, 100 K). Each IR spectrum was measured after adsorbed CO and CO in the gas phase reached equilibrium. IR spectra of the samples measured at 100 K before CO adsorption were used as backgrounds for difference spectra by subtraction from the spectra measured for the CO-adsorbed samples.

The acid strength of the hydrated samples was also investigated by ^{31}P MAS NMR using trimethylphosphine oxide (TMPO) as a basic probe molecule. Samples were exposed to saturated water vapor at 298 K for 24 h, and then added to a TMPO-dissolved dichloromethane solution for an additional 24 h. After evacuation of dichloromethane solution, the samples were packed into a 4 mm rotor. ^{31}P MAS NMR spectra for the TMPO-adsorbed samples were measured at room temperature at a Larmor frequency of 162.0 MHz using a single-pulse sequence with high-power proton

decoupling. A Bruker MAS probehead was used with a 4 mm zirconia rotor. The spinning rate of the sample was 10 kHz. The ^{31}P chemical shift was referenced to 85% H_3PO_4 at 0.0 ppm. $(NH_4)_2HPO_4$ was used as a second experimental reference material with the signal set at 1.33 ppm.

2.3.3 Catalytic Reactions

Lewis acid catalysis of the prepared mesoporous titanosilicates was examined by the hydride transfer of pyruvaldehyde to lactic acid and the Mukaiyama-aldol condensation benzaldehyde with 1-trimethylsilyloxy-cyclohexene in water. In the typical hydride transfer reaction, a mixture of pyruvaldehyde solution (2 mL, 0.1 M) and catalyst (0.1 g) was heated in a sealed Pyrex glass vial at 383 K for 2 h. The solution was analyzed after reaction using high-performance liquid chromatography (HPLC; LC-2000 plus, Jasco) with a refractive index detector.

For the Mukaiyama-aldol condensation, a mixture of benzaldehyde (0.4 mmol), 1-trimethysilyloxy-cyclohexene (0.6 mmol), sodium dodecyl sulfate (0.08 mmol), water (3 mL), and catalyst (100 mg) was stirred at 298 K for 2 h. The product isolated by solvent extraction with ethyl acetate was analyzed using ^1H nuclear magnetic resonance spectroscopy (NMR; Biospin AvanceIII 400 MHz, Bruker). Dioxane was used as an internal standard.

2.4 Results and Discussion

2.4.1 Structure of TDMS

The mesoporous structure and mesoporosity of the samples were examined by X-ray diffraction (XRD) measurement and N_2 adsorption analysis and the results are shown in Figures 2-1 and 2-2. All samples, including bare SBA-15, have well-defined XRD peaks at 0.9, 1.5, and 1.8° in Figure 2-1(A). These peaks are assignable to (100), (110), and (200) diffraction of the two-dimensional hexagonal *(P6mm)* symmetry of mesopores [18,19]. The lack of clear diffractions in the wide-angle range suggests that the titanium species are highly dispersed onto the mesoporous surface, even after calcination at 823 K (Figure 2-1(B)). The samples have a typical type-IV N_2 adsorption-desorption isotherm with an H1-type hysteresis loop that is characteristic of a mesoporous solid with uniform and large mesopores (Figure 2-2) [18,19]. Table 2-1 summarizes the physicochemical properties of the samples. Although there is a slight decrease in the BET surface area and pore volumes of SBA-15 after immobilization of the titanium species, the samples still have large BET surface areas (432-483 $m^2\ g^{-1}$), pore volumes (0.74-0.80 mL g^{-1}), and uniform mesopores (ca. 9 nm) that are beneficial for catalytic applications. The titanium content of the samples increases continuously with the initial Ti(OPr-*i*)$_4$ concentration and reaches 0.35 mmol g^{-1} for Ti-2/SBA-15.

The coordination environment of the titanium species was evaluated using ultraviolet-visible diffusive reflectance spectroscopy (UV-Vis DRS) and X-ray absorption near edge structure (XANES) of the Ti K-edge. Figure 2-3 shows UV-Vis DRS spectra for bare SBA-15 and

the TDMS samples, in addition to that for a titanosilicate zeolite (TS-1) for comparison. SBA-15 shows no absorption band in the UV region; however, TS-1 and TDMS have an intense and narrow absorption band at 200-250 nm, which is assignable to the charge transfer of isolated TiO_4 tetrahedra [14-17,22,23]. It has been reported that TiO_4 tetrahedra in zeolite are stabilized by coordination of two H_2O molecules, forming octahedrally coordinated Ti species, $TiO_4(H_2O)_2$ [24,25]. This suggests that octahedrally coordinated Ti species such as $TiO_4(H_2O)_2$ are also formed on TDMS in the presence of water. The band intensity and absorption edge of the TiO_4 tetrahedra for TDMS increases and shifts to longer wavelength with increasing introduced titanium content, and the band edge reaches ca. 300 nm for Ti-2/SBA-15. This can be attributed to the formation of TiO_6 octahedra: the adsorption band of TiO_6 octahedra appears at longer wavelength than that of TiO_4 tetrahedra. The absence of a strong and wide absorption band up to ca. 400 nm for anatase TiO_2 (Figure 2-3(f)) indicates that TDMS has no bulk TiO_2 particles.

The formation of TiO_4 tetrahedra is also supported by XANES measurement. Figure 2-4 shows Ti K-edge XANES spectra of Ti-0.5/SBA-15, Ti-2/SBA-15, TS-1, and anatase TiO_2. TDMS has a similar pre-edge peak to that of TS-1, where a sharp pre-edge peak appears at around 4967 eV, which is attributed to the transition from the Ti 1s to Ti 3d mixed with O 2p of tetrahedrally coordinated titanium species [24,26,27]. In contrast, anatase TiO_2 shows typical weak pre-edge peaks assignable to the transition of octahedrally coordinated titanium centers. The UV-Vis DRS results are compatible with the XANES spectra in terms of the formation of isolated TiO_4 tetrahedra on the mesopore surfaces. It was estimated from the XANES spectra for TS-1 and anatase TiO_2 that about half of the introduced titanium species are deposited as TiO_4 tetrahedra on SBA-15 in Ti-0.5/SBA-15 and Ti-2/SBA-15.

2.4.2 Lewis Acid property of TDMS

Lewis acid site density for TDMS samples was also examined by Hammett indicator titration based on the Benesi method (Table 2-1). The density clearly increases with increase in introduced titanium species, and reaches 0.16 mmol g^{-1} for Ti-2/SBA-15. Table 2-1 also shows that 40–60 % of introduced titanium species function as Lewis acid sites on all prepared TDMS samples: half of the introduced Ti species show no Lewis acidity. This is in good agreement with the results of XANES. In UV-Vis DRS measurement, the absorption band edge of the TiO_4 tetrahedra for TDMS shifts to longer wavelength with increasing introduced titanium content, suggesting the formation of TiO_6 octahedra even at low Ti content. As a result, both of unsaturated coordination TiO_4 tetrahedra and saturated coordination TiO_6 octahedra would be formed even at low Ti (OPr-*i*)$_4$ concentration.

The Lewis acid properties of the samples were investigated using FT-IR measurements with CO as a basic probe molecule (Figure 2-5). Figure 2-5(A) shows difference FT-IR spectra for CO-adsorbed hydrated anatase TiO_2. The intensities of the three bands at 2137, 2152, and 2178 cm^{-1}

that are assigned to physisorbed CO, hydrogen-bonded CO with surface Ti-OH group [28], and CO adsorbed on Lewis acid sites, respectively, increase with the amount of introduced CO. Therefore, anatase TiO_2 has Lewis acid sites that are active in the presence of water, which is in good agreement with the previous report [12]. Figures 2-5(B) and 2-5(C) show FT-IR spectra for CO-adsorbed dehydrated and hydrated Ti-2/SBA-15. Ti-2/SBA-15 also has three intense bands at 2137, 2156, and 2182 cm^{-1}, due to physisorbed CO, hydrogen-bonded CO with surface Si-OH group, and coordinated CO on Lewis acid sites, respectively, even in the presence of physisorbed water. This band for coordinated CO on Lewis acid sites is not observed for bare SBA-15 (Figure 2-5(D)): the bands at 2137 and 2156 cm^{-1} are derived from physisorbed CO and hydrogen-bonded CO with surface Si-OH group, respectively [29-31]. Thus, Lewis acid sites on TDMS samples can work even in the presence of water. Considering that TiO_4 tetrahedra on TDMS exist as octahedrally coordinated $TiO_4(H_2O)_2$ in the presence of water molecules, it is expected that coordinated H_2O molecules of the Lewis acid sites are replaced by CO, due to weak H_2O-Lewis acid interaction. It should be noted that the band position for coordinated CO on hydrated Ti-2/SBA-15 (2182 cm^{-1}) is somewhat higher than that of hydrated anatase TiO_2 (2178 cm^{-1}), which suggests that there is a difference in acid strength between hydrated Ti-2/SBA-15 and anatase TiO_2.

The Lewis acidity of Ti-2/SBA-15 was also evaluated by ^{31}P MAS NMR measurements with trimethylphosphine oxide (TMPO) as a basic probe molecule [32,33]. Prior to the TMPO immersion, the sample was contacted with saturated water vapor to clarify the effect of adsorbed water on the interaction between TMPO and Lewis acid site. Figure 2-6 shows ^{31}P MAS NMR spectra for hydrated SBA-15 and Ti-2/SBA-15 after TMPO adsorption. The peak at around 50 ppm in pure silica SBA-15 (Figure 2-6(A)) is derived from TMPO physisorbed on the hydrated silica surface (Figure 2-6(A)). The peak for Ti-2/SBA-15 can be divided into the two peaks (Figure 2-6 (B)): the intense peak at 50 ppm is due to physisorbed TMPO that can be observed for SBA-15, and the shoulder peak at around 60 ppm can be assignable to the TMPO adsorbed on Lewis acid site. These results are good consistent with FT-IR measurement: water molecules coordinated with Lewis acid sites on TDMS can be exchangeable with TMPO, a basic molecule.

2.4.3 Lewis Acid catalysis of TDMS

Lewis acid catalysis with TDMS was examined through the hydride transfer of pyruvaldehyde to lactic acid and the Mukaiyama-aldol condensation of benzaldehyde with 1-trimethylsilyloxy-cyclohexene. Pyruvaldehyde is present in water as the original aldehyde, monohydrate, and dihydrate forms with typical equilibrium distributions of trace level, 57%, and 43%, respectively [34]. Monohydrate pyruvaldehyde can be converted into lactic acid on a water-tolerant Lewis acid catalyst through the intramolucular Meerwein-Ponndorf-Verley (MPV) mechanism (Table 2-2) [13]. Table 2-2 shows the catalytic activities of the samples and reference

catalysts for this reaction. H_2SO_4 as a Brönsted acid is not effective for the reaction; however, scandium(III) triflate ($Sc(OTf)_3$) [35-37], a highly active and soluble water-tolerant Lewis acid catalyst, gave a high yield (94%) of lactic acid [13]. Therefore, $Sc(OTf)_3$ functions as an effective catalyst to promote hydride transfer in water. It has been reported that TiO_4 tetrahedra on anatase TiO_2 can function as water-tolerant Lewis acid sites, and anatase TiO_2 showed 100% conversion and 49% lactic acid yield [12]. The low lactic acid selectivity is due to simultaneous side reactions that proceed on the TiO_2 surface. The high lactic acid yield (82%) for TS-1 indicates that TiO_4 tetrahedra can act as active and selective sites for hydride transfer in water. Table 2-2 indicates that bare SBA-15 does not catalyze the reaction at all, and that TDMS effectively catalyzes the reaction as well as TS-1; the pyruvaldehyde conversion and lactic acid yield for TDMS samples increase with the amount of Lewis acid sites and reached 90% yield over Ti-2/SBA-15. Table 2-3 summarizes the turnover frequency (TOF) for each catalyst at a pyruvaldehyde conversion of ca. 50%. While the Lewis acid sites on TiO_2 have the largest TOF, on the basis of pyruvaldehyde conversion, these are quite inferior to those of other catalysts with lactic acid selectivity. $Sc(OTf)_3$, TS-1, and TDMS (Ti > 0.5 atom%) exhibit high lactic acid selectivity and yield, and there is no large difference in lactic acid selectivity and yield shown in Table 2-2. However, Table 2-3 reveals that TOF for TDMS under optimal conditions (Ti-0.5/SBA-15) is more than 2 to 6 times higher than those of $Sc(OTf)_3$ and TS-1. This indicates that TiO_4 tetrahedra on TDMS are not only selective for the hydride transfer conversion of pyruvaldehyde, but also more active than $Sc(OTf)_3$ and the TiO_4 tetrahedra of TS-1. TDMS samples were readily separated from the reaction mixture by simple decantation or filtration. No significant decrease in lactic acid yield was observed even after three reuses of the samples (Figure 2-7).

TDMS was also evaluated by the Mukaiyama-aldol reaction of benzaldehyde with 1-trimethylsilyloxy-cyclohexene in water. It has been reported that the product yield of this reaction increases significantly in a water/tetrahydrofuran (THF) mixture or in a water-surfactant reaction system [35-37]. Water and sodium dodecyl sulfate (SDS) were adopted as a solvent and dispersing agent, respectively, for this study. Table 2-4 summarizes the acid site density, product yield, and turnover number (TON) of the samples and some reference catalysts. $Sc(OTf)_3$ exhibits a high product yield (82%), which is comparable to that for $Sc(OTf)_3$ in a water/THF reaction system [35]. TS-1 and anatase TiO_2 with TiO_4 tetrahedra Lewis acid sites do not work as effective catalysts for the Mukaiyama-aldol reaction. The difference in activity for the hydride transfer of pyruvaldehyde and the Mukaiyama-aldol reaction between TS-1 and TDMS might be due to microporous structure. The micropores of TS-1 can prevent diffusion of reactants and products, limiting the catalysis of a high density of TiO_4 tetrahedra in TS-1. In contrast to TS-1 and TiO_2, the TDMS samples have product yields comparable to that of $Sc(OTf)_3$ and TON that are larger than that of $Sc(OTf)_3$. Tables 2-3 and 2-4 also show that Ti-0.5/SBA-15 exhibits the highest TOF for the hydride transfer of

pyruvaldehyde into lactic acid and the largest TON for the Mukaiyama-aldol reaction. However, Ti-2/SBA-15 that has a higher Lewis acid density than Ti-0.5/SBA-15 is inferior to Ti-0.5/SBA-15 in TOF and TON for both reactions, indicating that the Lewis acid sites of the former have lower reactivity than those of the latter. The absorption band intensity and absorption edge of the TiO_4 tetrahedra for TDMS increases and shifts to longer wavelength with increasing introduced titanium content as shown in UV-Vis DRS for TDMS (Figure 2-3). This is due to the formation of TiO_6 octahedra that has an absorption band at longer wavelength than that of TiO_4 tetrahedra. Increase in TiO_6 species or aggregation of TiO_6 species might decrease the activity of Lewis acid sites on TDMS.

To summarize, TDMS exhibits higher catalytic performance for the tested Lewis acid-catalyzed reactions in the presence of water than TiO_2 and TS-1: the catalytic activity of TDMS is comparable to that of $Sc(OTf)_3$, a highly active homogeneous Lewis acid catalyst. Such high catalytic performance of solid acid catalysts have been often attributed to either porous structure or acid strength, or both [38,39]. While mesoporous structure may facilitate diffusion and access of reactant molecules to the active sites, poor catalytic activity of TiO_2 for the Mukaiyama-aldol reaction cannot be explained solely by mesoporous structure. It should be noted that in the presence of water the IR band for CO-adsorbed Lewis acid sites on TDMS is observed at higher wavenumber (2182 cm^{-1}) than that of TiO_2 (2178 cm^{-1}) in CO adsorption experiment (Figure 2-5). This is due to the replacement of H_2O with CO on Ti species such as octahedral coordination $TiO_4(H_2O)_2$ in zeolites and suggests that there is a difference in reactivity or H_2O-CO replacement capability between Lewis acid sites of TDMS and TiO_2. One possible explanation for the difference is an essential distinction in TiO_4 Lewis acid sites between both materials. The Lewis acid sites on TiO_2 are regarded as Ti-O unsaturated coordination spheres and positive charges in the Lewis acid centers can be compensated by delocalized electrons throughout the conduction band based on Ti3d orbital. On the other hand, it has been reported that in transition metal-exchanged zeolite, metal cations in an insulator, the positive charges of metal cations are compensated by negative charges localized on the framework, suggesting that such local charge separation also occurs on TDMS surface [40]. As a result, the Lewis acid sites of both materials are expected to differ in environment, electronic state, and this may cause the difference in catalysis between TDMS and TiO_2. The details are currently under investigation.

2.5 Conclusion

TDMS prepared by post-grafting method was investigated as solid Lewis acid catalyst in water. FTIR measurement reveals that TiO_4 tetrahedra on mesoporous silica can interact with carbon monoxide even in the presence of water. The TiO_4 tetrahedra deposited on mesoporous silica exhibit Lewis acid catalysis distinct from that of TiO_4 tetrahedra on TiO_2, and they act as highly selective

and active sites for the hydride transfer of pyruvaldehyde to lactic acid and the Mukaiyama-aldol condensation of benzaldehyde with 1-trimethylsilyloxy-cyclohexene.

References

[1] A. Corma, A, H. García, *Chem. Rev.* **2003**, *103*, 4307–4366.

[2] H. Yamamoto, Ed. *Lewis Acid in Organic Synthesis*; Wiley-VCH: Weinheim, **2000**.

[3] P. T. Anastas, M. M. Kirchhoff, *Acc. Chem. Res*. **2002**, *35*, 686–694.

[4] S. Nagayama, S. Kobayashi, *Angew. Chem. Int. Ed.* **2000**, *39*, 567–569.

[5] W. Gu, W.-J. Zhou, D. L.Gin, *Chem. Mater.* **2001**, *13*, 1949–1951.

[6] A.Corma, L. T. Nemeth, M. Renz, S. Valencia, *Nature* **2001**, *412*, 423–425.

[7] A.Corma, V. Fornés, S. Iborra, M. Mifsud, M. Renz, *J. Catal.* **2004**, *221*, 67–76.

[8] M. Moliner, Y. Román-Leshkov, M. E. Davis, *Proc. Natl. Acad. Sci. USA* **2010**, *107*, 6164–6168.

[9] Y. Román-Leshkov, M. Moliner, J. A. Labinger, M. E. Davis, *Angew. Chem. Int. Ed.* **2010**, *49*, 8954–8957.

[10] P. P. Pescarmona, K. P. F. Janssen, C. Delaet, C. Stroobants, K. Houthoofd, A. Philippaerts, C. De Jonghe, J. S. Paul, P. A. Jacobs, B. F. Sels, *Green Chem.* **2010**, *12*, 1083–1089.

[11] K.Nakajima, Y. Baba, R. Noma, M. Kitano, J. N. Kondo, S. Hayashi, M. Hara, *J. Am. Chem. Soc.* **2011**, *133*, 4224–4227.

[12] K. Nakajima, R. Noma, M. Kitano, M. Hara, *J. Phys. Chem. C.* **2013**, *117*, 16028–16033.

[13] Y. Koito, K. Nakajima, M. Kitano, M. Hara, *Chem. Lett.* **2013**, *42,* 873–875.

[14] F. Bérubé, B. Nohair, F. Kleitz, S. Kaliaguine, *Chem. Mater.* **2010**, *22*, 1988–2000.

[15] T.-W. Kim, M.-J. Kim, F. Kleitz; M. M. Nair; R. Guillet-Nicolas, K.-E. Jeong, H.-J.Chae. C.-U. Kim, S.-Y. Jeong, *ChemCatChem* **2012**, *4*, 687–697.

[16] M. C. Capel-Sanchez, G. Blanco-Brieva, J. M. Campos-Martin, M. P. de Frutos, W. Wen, J. A. Rodriguez, J. L. G. Fierro, *Langmuir* **2009**, *25*, 7148–7155.

[17] P. Wu, T. Tatsumi, T. Komatsu, T. Yashima, *Chem. Mater.* **2002**, *14*, 1657–1664.

[18] D. Zhao, J. Feng, Q. Huo, N. Melosh, G. H.Fredrickson, B. F. Chmelka, G. D. Stucky, *Science* **1998**, *279*, 548–552.

[19] D. Zhao, J. Sun, Q. Li, G. D. Stucky, *Chem. Mater.* **2000**, *12*, 275–279.

[20] H. A. Benesi, *J. Am. Chem. Soc.* **1956**, *78*, 5490–5494.

[21] H. A. Benesi, *J. Phys. Chem.* **1957**, *61*, 970–973.

[22] M. C. Capel-Sanchez, V. A. de la Peña-O'Shea, J. M. Campos-Martin, J. L. G. Fierro, *Top. Catal.* **2006**, *41*, 27–34.

[23] A. Zecchina, G. Spoto, S. Bordiga, A. Ferrero, G. Petrini, G. Leofanti, M. Padovan, *Stud. Surf. Sci. Catal.* **1991**, *69*, 251–258.

[24] S. Bordiga, F. Bonino, A. Damin, C. Lamberti, *Phys. Chem. Chem. Phys.* **2007**, *9*, 4854–4878.

[25] S. Bordiga, A. Damin, F. Bonino, G. Ricchiardi, A. Zecchina, R. Tagliapietra, C. Lamberti, *Phys. Chem. Chem. Phys.* **2003**, *5*, 4390–4393.

[26]S.-Y. Chen, C.-Y. Tang, J.-F. Lee, L.-Y. Jang, T. Tatsumi, S. Cheng, *J. Mater. Chem.* **2011**, *21*, 2255–2265.

[27]F. Farges, G. E. Brown, J. J. Rehr, *Phys. Rev. B* **1997**, *56*, 1809–1819.

[28]K. I. Hadjiivanov, D. G. Klissurski, *Chem. Soc. Rev.*, **1996**, *25*, 61–69

[29]T. P. Beebe, P. Gelin, J. T. Yates, *Surf. Sci*. **1984**, *148*, 526–550.

[30]O. Cairon, T. Chevreau, J.-C. Lavalley, *J. Chem. Soc. Faraday Trans.* **1998**, *94*, 3039–3047.

[31]Y. Matsunaga, H.Yamazaki, T. Yokoi, T. Tatsumi, J. N. Kondo, *J. Phys. Chem. C* **2013**, *117*, 14043–14050.

[32]A. Zheng, S.-J. Huang, S.-B. Liu F. Deng, *Phys. Chem. Chem. Phys.* **2011**, *13*, 14889‑14901.

[33]A. Zhenga, S.-B. Liub, F. Deng, *Solid State Nuclear Magnetic Resonance* **2013**, *55*, 12‑27.

[34]I. Nemet, D. Vikić-Topić, L.Varga-Defterdarović, *Bioorg. Chem.* **2004**, *32*, 560–570.

[35]S. Kobayashi, I. Hachiya, *J. Org. Chem.* **1994**, *59*, 3590–3596.

[36]S. Kobayashi, T. Wakabayashi, S. Nagayama, H. Oyamada, *Tetrahedron Lett.* **1997**, *38*, 4559–4562.

[37]S. Kobayashi, S. Nagayama, T. Busujima, *J. Am. Chem. Soc.* **1998**, *120*, 8287–8288.

[38]C. Tagusagawa, A. Takagaki, A. Iguchi, K. Takanabe, J. N. Kondo, K. Ebitani, T. Tatsumi, K. Domen, *Chem. Mater.* **2010**, *22*, 3072–3078.

[39]Y. Rao, M. Trudeau, D. Antonelli, *J. Am. Chem. Soc.* **2006**, *128*, 13996–13997.

[40]R. Schoonheydt, P. Geerlings, E. Pidko, R. A. Santen, *J. Mater. Chem.* **2012**, *22*, 18705–18717.

[41]H. Shintaku, K. Nakajima, M. Kitano, N. Ichikuni, M. Hara, *ACS Catal.* **2014**, *4*, 1198–1204.

Table 2-1. Physicochemical properties of TDMS samples.

Catalyst	S_{BET} / m^2 g^{-1}	Pore volume / cm^2 g^{-1}	Pore diameter / nm	Ti content[a] / mmol g^{-1}	Surface Ti density / nm^{-2}	Lewis acid site density[b] / mmol g^{-1}
SBA-15	742	0.90	9.3	-	-	-
Ti-0.1/SBA-15	455	0.80	9.2	0.020	0.03	0.01[b]
Ti-0.25/SBA-15	429	0.78	9.4	0.049	0.07	0.02[b]
Ti-0.5/SBA-15	432	0.80	9.3	0.085	0.12	0.03[b]
Ti-1/SBA-15	483	0.77	9.4	0.170	0.21	0.11[b]
Ti-2/SBA-15	481	0.74	9.4	0.353	0.44	0.16[b]

[a]Determined from XRF measurements. [b]Hammett indicator titration based on the Benesi method.

Table 2-2. Catalytic activities of the samples and reference catalysts for the hydride transfer of pyruvaldehyde to lactic acid in water.

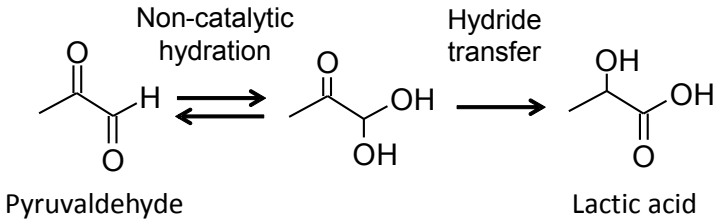

Catalyst	Lewis acid site density / mmol g^{-1}	Conv. (%)	Yield (%)	Selec. (%)
H_2SO_4	-	16	2	13
$Sc(OTf)_3$	2.0	100	94	94
TiO_2	0.26[a]	100	49	49
TS-1	0.36[b]	95	82	86
SBA-15	-	29	0	-
Ti-0.1/SBA-15	0.01[b]	51	45	88
Ti-0.25/SBA-15	0.02[b]	74	68	92
Ti-0.5/SBA-15	0.03[b]	86	80	92
Ti-1/SBA-15	0.11[b]	92	89	97
Ti-2/SBA-15	0.16[b]	91	90	98

Reagents and conditions: pyruvaldehyde, 0.2 mmol; catalyst, 100 mg; water, 2 mL; temperature, 383 K; time, 2h. [a]FT-IR measurement using pyridine as a basic probe molecule. [b]Hammett indicator titration based on the Benesi method.

Table 2-3. TOF values for hydride transfer conversion of pyruvaldehyde to lactic acid in water.

Catalyst	Lewis acid site density / mmol g^{-1}	Catalyst weight / g	Reaction time / min	Conversion / %	TOF / h^{-1}
$Sc(OTf)_3$	2.0	0.05	5	47	11
TiO_2	0.26[a]	0.05	5	53	98
TS-1	0.36[b]	0.05	15	57	25
Ti-0.1/SBA-15	0.01[b]	0.1	120	51	51
Ti-0.25/SBA-15	0.02[b]	0.1	60	43	43
Ti-0.5/SBA-15	0.03[b]	0.1	30	46	61
Ti-1/SBA-15	0.11[b]	0.1	30	50	18
Ti-2/SBA-15	0.16[b]	0.1	30	45	11

Reagents and conditions: pyruvaldehyde, 0.2 mmol; water, 2 mL; temperature, 383 K. [a]FT-IR measurement using pyridine as a basic probe molecule. [b]Hammett indicator titration based on the Benesi method.

Table 2-4. Catalytic activities of the samples and reference catalysts for the Mukaiyama-aldol reaction of benzaldehyde with 1-trimethylsilyloxy-cyclohexene in water.

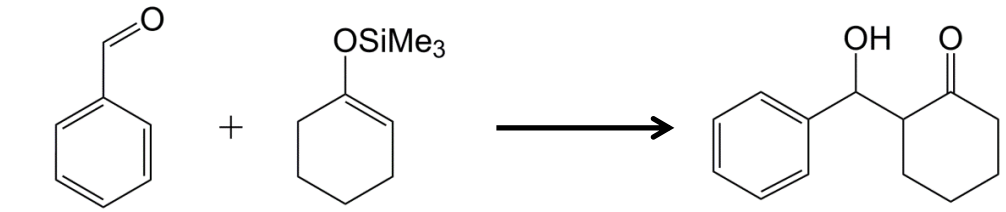

Benzaldehyde 1-(trimethylsilyloxy) cyclohexene

Catalyst	Lewis acid site density / mmol g^{-1}	Yield[a] (%)	TON
$Sc(OTf)_3$	2.0	82	1.6
TiO_2	0.26[b]	3	0.5
TS-1	0.36[c]	9	1.0
SBA-15	-	2	-
Ti-0.1/SBA-15	0.01[c]	17	68
Ti-0.5/SBA-15	0.03[c]	67	89
Ti-2/SBA-15	0.16[c]	93	23

Reagents and conditions: benzaldehyde, 0.4 mmol; 1-trimethylsilyloxy-cyclohexene, 0.6 mmol; SDS, 0.08 mmol; water, 3 mL; catalyst, 100 mg; temperature, 298 K; time, 2 h. [a]*Syn/anti* ratio for all tested catalysts was estimated to be ca. 7/3. [b]Determined by pyridine-adsorption experiment using FT-IR. [c]Determined by Hammett indicator titration based on the Benesi method.

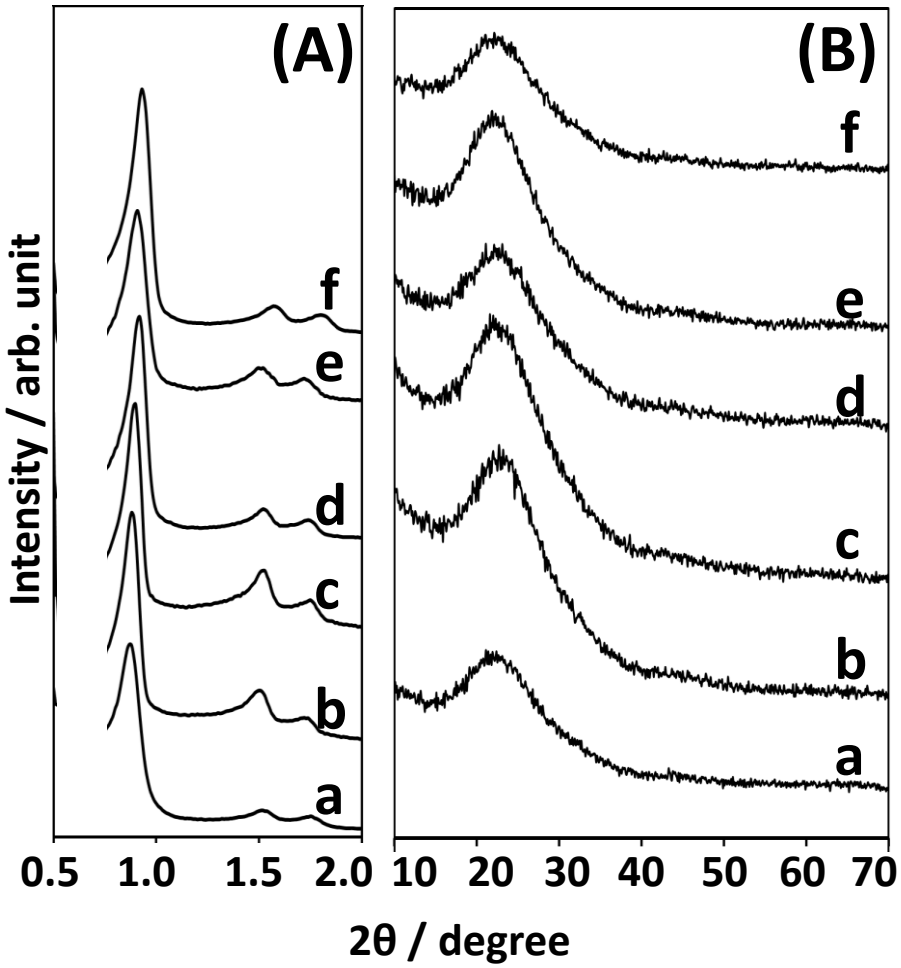

Figure 2-1. (A) Low-angle and (B) wide-angle XRD patterns for (a) bare SBA-15, (b) Ti-0.1/SBA-15, (c) Ti-0.25/SBA-15, (d) Ti-0.5/SBA-15, (e) Ti-1/SBA-15, and (f) Ti-2/SBA-15. Reprinted with permission from reference [41]. Copyright (2014) American Chemical Society.

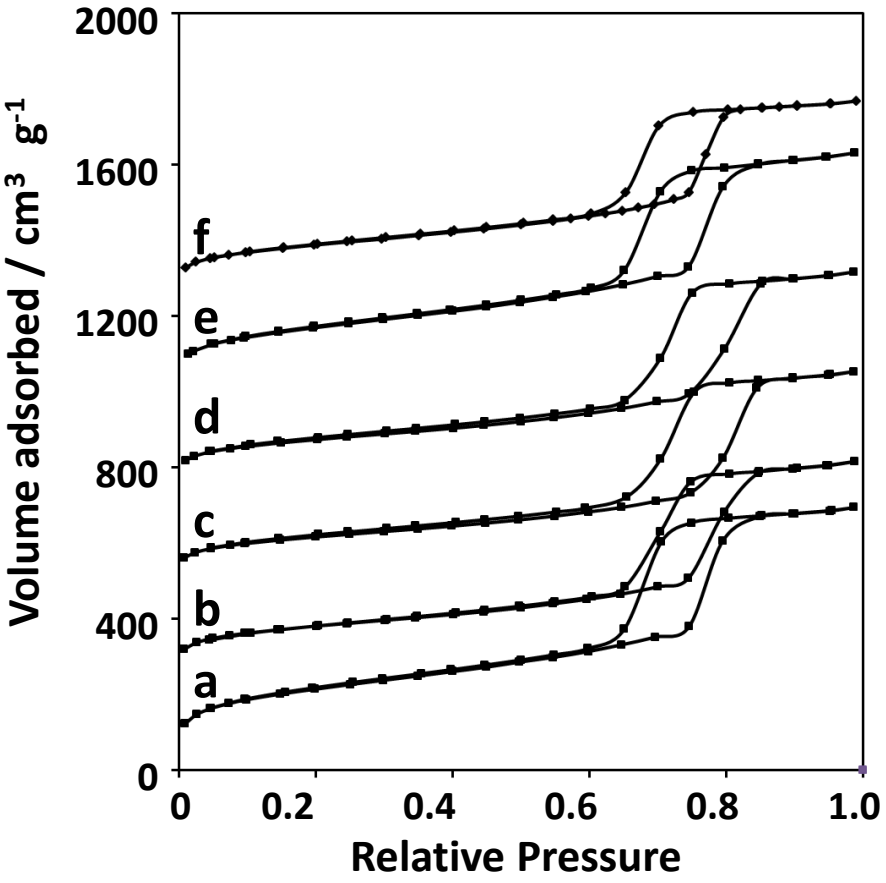

Figure 2-2. N_2 adsorption-desorption isotherms for (a) SBA-15, (b) Ti-0.1/SBA-15, (c) Ti-0.25/SBA-15, (d) Ti-0.5/SBA-15, (e) Ti-1/SBA-15, and (f) Ti-2/SBA-15. Each isotherm is vertically offset with 250 cm^3 g^{-1}. Reprinted with permission from reference [41]. Copyright (2014) American Chemical Society.

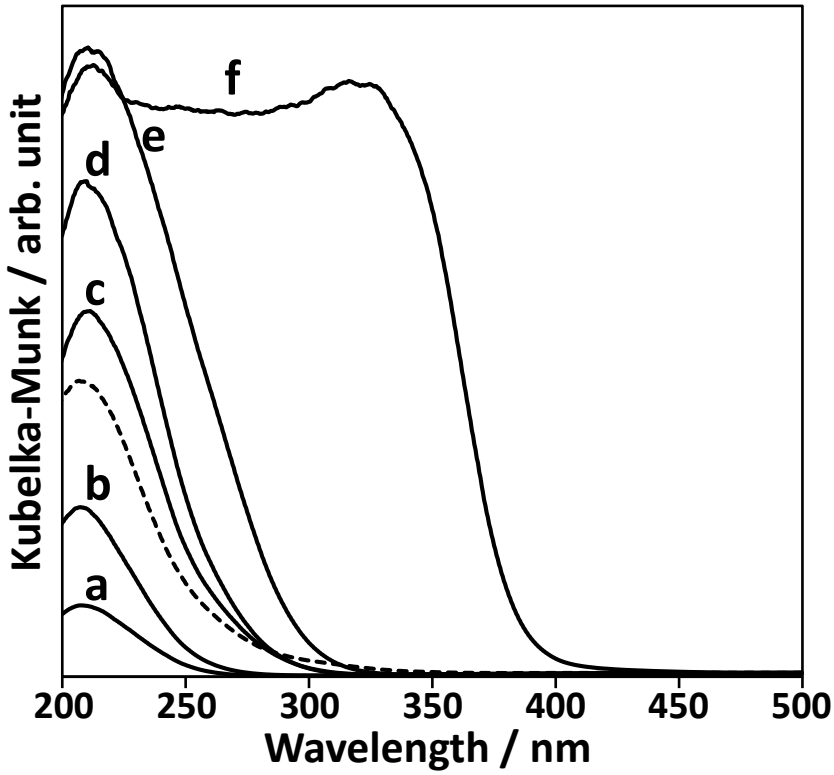

Figure 2-3. UV-Vis DRS spectra of TDMS with various titanium content, TS-1 and anatase TiO_2. (a) Ti-0.1/SBA-15, (b) Ti-0.25/SBA-15, (c) Ti-0.5/SBA-15, (d) Ti-1/SBA-15, (e) Ti-2/SBA-15, and (f) anatase TiO_2. The spectrum for TS-1 is given as a dashed line. Reprinted with permission from reference [41]. Copyright (2014) American Chemical Society.

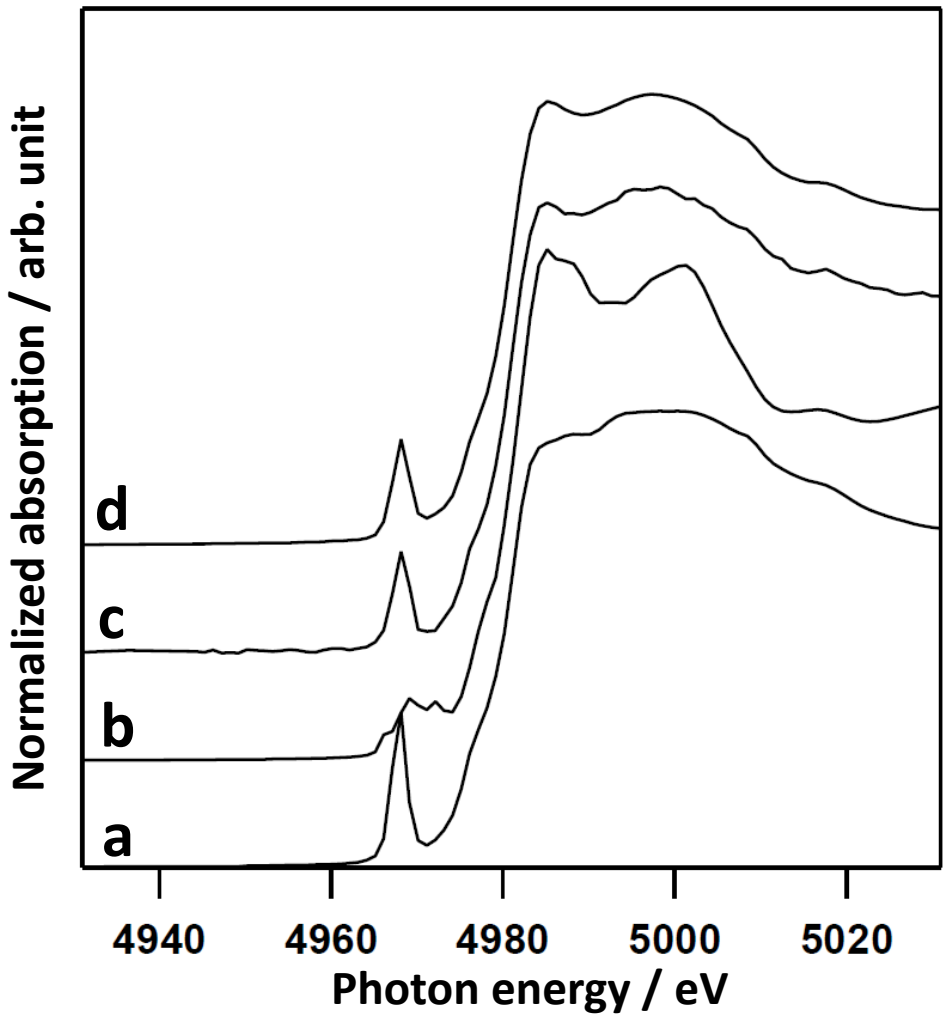

Figure 2-4. Ti K-edge XANES spectra for (a) TS-1, (b) TiO_2, (c) Ti-0.5/SBA-15, and (d) Ti-2/SBA-15. Reprinted with permission from reference [41]. Copyright (2014) American Chemical Society.

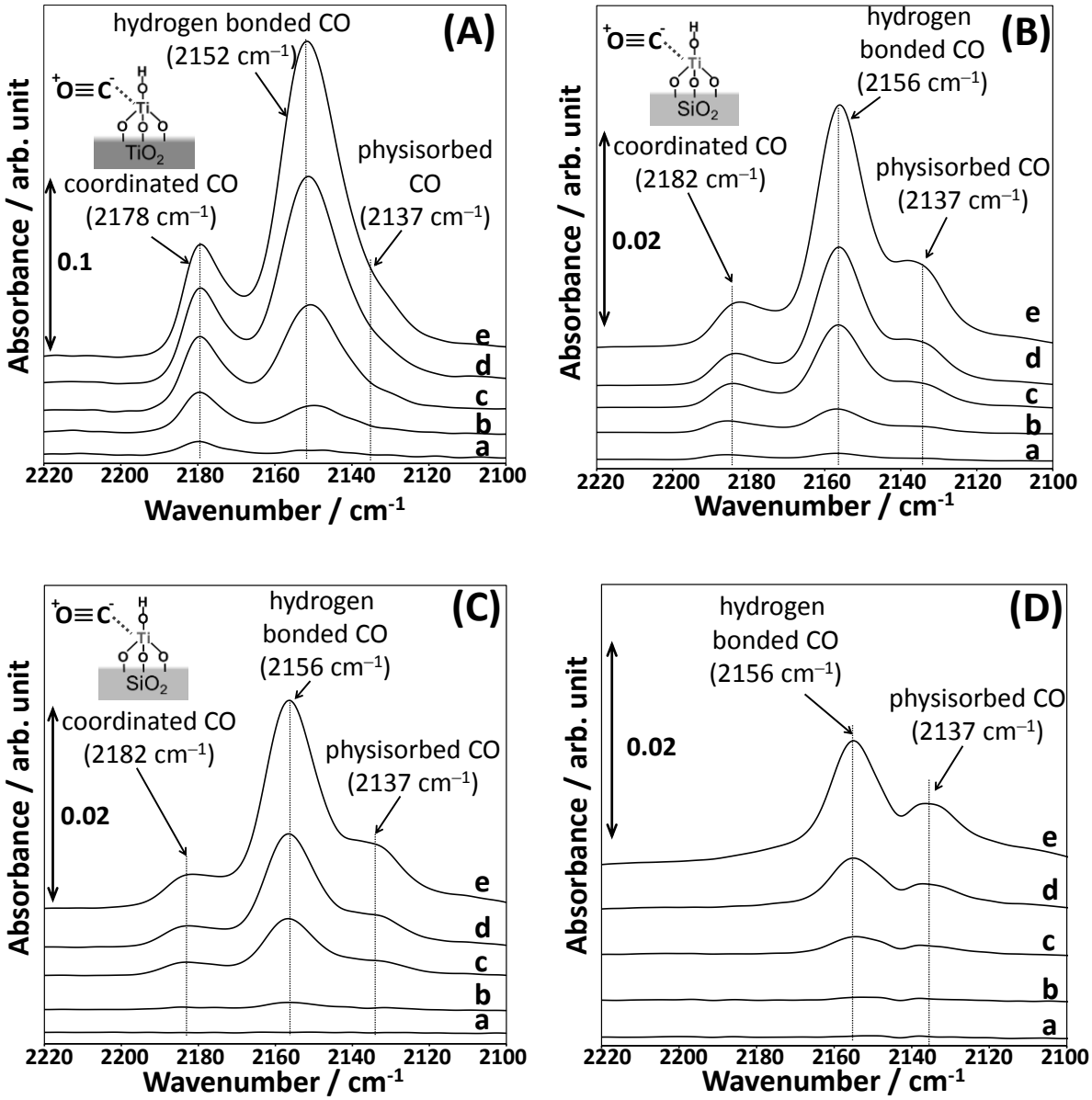

Figure 2-5. FT-IR difference spectra of CO-adsorbed (A) hydrated TiO_2, (B) dehydrated Ti-2/SBA-15, (C) hydrated Ti-2/SBA-15 and (D) dehydrated SBA-15 at 100 K. CO pressures for spectra a, b, c, d, and e correspond to 0.1, 0.2, 0.5, 1.0, and 2.0 Torr, respectively. Reprinted with permission from reference [41]. Copyright (2014) American Chemical Society.

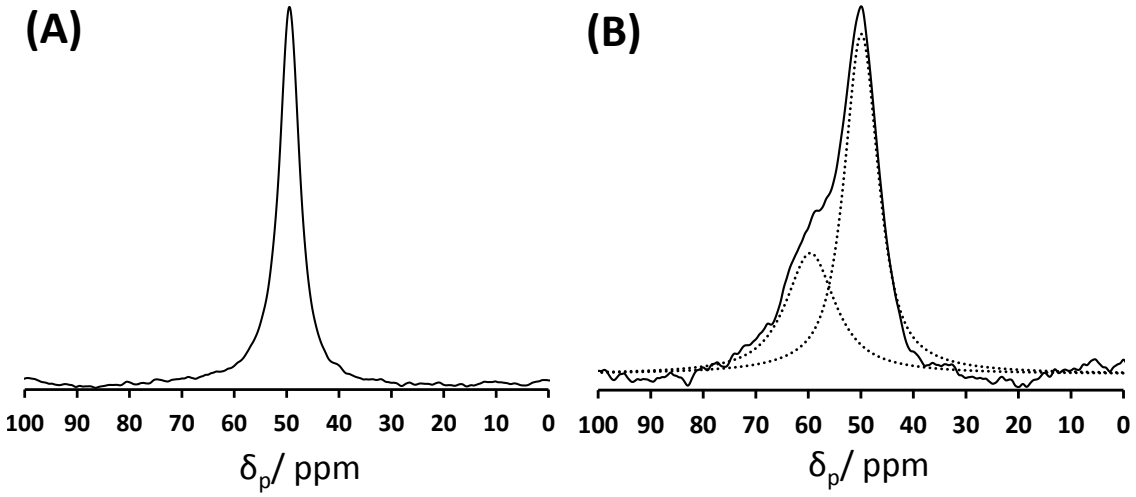

Figure 2-6. ^{31}P NMR spectra of TMPO-adsorbed hydrated (A) SBA-15 and (B) Ti-2/SBA-15. The deconvoluted spectra for hydrated Ti-2/SBA-15 is given as a dashed line.

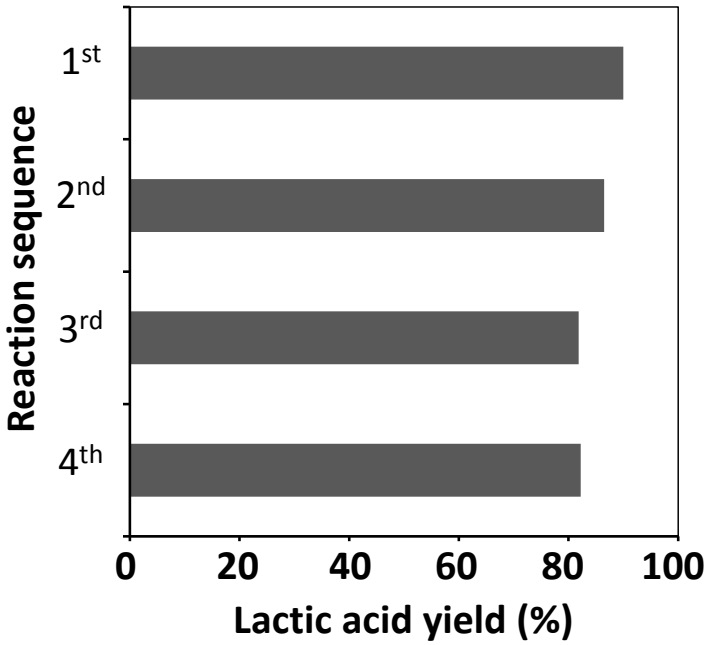

Figure 2-7. Catalyst reuse experiment using Ti-2/SBA-15 for the hydride transfer conversion of pyruvaldehyde to lactic acid in water at 383 K for 2 h. Reprinted with permission from reference [41]. Copyright (2014) American Chemical Society.

Chapter 3

Lewis acid catalysis of TiO_4 deposited mesoporous silica prepared by co-condensation method

3.1 Abstract

TiO_4 deposited Mesoporous silica (TDMS) was prepared by co-condensation of silicon alkoxide and titanium alkoxide in the presence of an amphiphilic block copolymer as a structure directing agent. The resulting catalysts have ordered mesopores and higher surface areas than TDMS prepared by post-grafting method. Ti content in the final material can be controlled by intial concentration of titanium alkoxide. However, due to the difference in hydrolysis rate between silicone and titanium alkoxide, titania nanoparticles were also simultaneously formed for TDMS with high titanium contents: band intensity for TiO_6 octahedra, main component for bulk TiO_2 particle, in Ultraviolet-visible diffuse reflectance spectra (UV-Vis DRS) spectra increases with the increase in titanium content. While all TDMS samples synthesized by co-condensation method can catalyze hydride transfer reaction of pyruvaldehyde into lactic acid water, TDMS with high Ti content show low lactic acid selectivity. This would be due to TiO_2 nanoparticles that contain active site for by-product formation.

3.2 Introduction

Lewis acids catalysts, represented by $AlCl_3$ and $TiCl_4$, are attractive compounds for the production of wide range of chemicals including fine chemicals, polymers, pharmaceuticals and so on [1-3]. Especially, the interest in the water tolerant Lewis acid catalyst has been much growing due to the potential application as catalysts for biomass-derived sugar conversion into raw chemicals [4-8]. Furthermore, other excellent characters of water as solvents, non-toxicity and nature abundance has made Lewis acid catalysts in water attractive from the ecological point of view [9]. Therefore, there has been increasing demand for the development of Lewis acid catalysts in water. However, most of conventional homogeneous and heterogeneous Lewis acid catalysts readily undergo hydrolysis or deactivation by water molecules.

In recent years, some water tolerant Lewis acids have been reported. Heterogeneous Lewis acids such as tin or titanium containing Beta zeolite (Sn-Beta or Ti-Beta) and titanium containing MFI zeolite (TS-1) are found to be promising Lewis acids for aqueous sugar conversion reactions [4-8,10,11]. For example, the unsaturated Sn species in Beta zeolite framework function as Lewis acid sites in water. The conversion of glucose into fructose, an intramolecular hydride transfer

reaction, is effectively promoted by Sn-beta through activation carbonyl and hydroxyl group of glucose in water, and hydrophobic environment in micropores is also essential for the highly efficient sugar conversion [4-8]. Sn-Beta also functions as an effective catalyst for the Bayer-Villiger oxidation and the Meerwein-Ponndorf-Verley reduction [12,13]. TS-1 zeolite is known as an effective catalyst for the propylene oxidation with hydrogen peroxide [14]. Titanium tetrahedral species function as Lewis acid sites even in the presence of water for activation of hydrogen peroxide into Ti-OOH. However, zeolite based catalysts with restricted micropores cannot be used for the conversion of large-sized organic substrates.

We focused on Lewis acidity of metal oxides [15,16], and have found that coordinately unsaturated tetrahedral titanium species formed on mesoporous silica are active Lewis acid sites for the hydride transfer reaction of pyruvaldehyde into lactic acid and the Mukaiyama-aldol reaction of benzaldehyde with 1-(trimethylsilyloxy)cyclohexene in water [17]. TDMS was prepared by the post grafting method of preformed mesoporous silica, SBA-15 [18,19]. Mesoporous structure and high surface area of the TDMS are beneficial for the effective diffusion of the reactants compared to zeolite catalyst. While post-grafting method using a mixture of Ti(OPr-*i*)$_4$ and acetylacetone in water can be suitable for the formation of TiO_4 tetrahedra on silica surface, the amount of titanium content deposited on the surface is limited below ca. 0.4 mmol g^{-1}. In contrast, co-condensation method is a simple sol-gel reaction system that can produce TDMS (CC-TDMS) with a wide range of titanium contents, as compared with TDMS synthesized by post-grafting method (PG-TDMS). Acid catalysis of the CC-TDMS samples has been studied through the hydride transfer reaction of triose in water.

3.3 Experimental

3.3.1 Catalyst Preparation

Mesoporous silica SBA-15 was synthesized with an amphiphilic block copolymer P123 (Aldrich, M_W=5800) as a structure directing agent and tetramethyl orthosilicate (TMOS) as a silica source [20]. In a typical synthesis, 4 g of P123 was dissolved in a mixed solution of distilled water (90 g) and HCl (4 M, 60 mL) at 313 K. After addition of TMOS (6.2 g) into the clear solution, the mixture was stirred at 313 K for 20 h, followed by heating at 373 K for 24 h under static conditions. Calcination of the resultant white precipitate at 823 K for 5 h in air resulted in mesoporous silica SBA-15.

CC-TDMS samples were prepared by a simple sol-gel reaction of TMOS and Ti(OPr-*i*)$_4$ in the presence of P123. In a typical synthesis, 4 g of P123 was dissolved in a mixture of distilled water (90 g) and HCl (4 M, 60 mL) at 313 K. After addition of TMOS (6.2 g) and Ti(OPr-*i*)$_4$ simultaneously to the solution, the mixture was stirred at 313 K for 20 h, followed by heating at 373 K for 24 h under static conditions. Calcination of the resultant white powders at 823 K for 5 h in air resulted in CC-TDMS samples, which are denoted as CC-Ti-x/SBA-15 (x=Ti atom% for initial

condition).

In the case of post-grafting method, impregnation of titanium species onto SBA-15 was performed by a simple grafting method [17-19]. SBA-15 (5 g) was added to a mixture of distilled water (145 g) and ethanol (15 g) at room temperature. After the pH of the solution was adjusted to 10.0 with diluted ammonia, a mixture of ethanol (5 g), Ti(OPr-*i*)$_4$ (TTIP) and acetyl acetone (AA) (AA/TTIP =3.1) was slowly added to the mixture at 278 K and then stirred for 2 h. After filtration and repeated washing with ethanol, the material was calcined at 823 K for 3 h to immobilize the titanium species on the silica surface. The resulting TDMS samples with various titanium content are denoted as PG-Ti-x/SBA-15 (x=Ti atom% forinitial condition).

For comparison, bulk anatase TiO_2 and titanosilicate zeolite (TS-1) were used as reference catalysts. TiO_2 was synthesized by a sol-gel method using Ti(OPr-*i*)$_4$ as a precursor [16]. TS-1 was supplied from the Catalysis Society of Japan and was used as received.

3.3.2 Catalyst Characterization

The titanium content of the samples was determined using X-ray fluorescence spectroscopy (XRF; ZSX100e, Rigaku). Powder X-ray diffraction patterns were obtained with a diffractometer (Ultima IV, Rigaku) using Cu Kα radiation (40 kV, 40 mA) over the 2θ range of 0.7–70°. Nitrogen adsorption-desorption isotherms were measured at 77 K with a surface area analyzer (Nova-4200e, Quantachrome). Prior to measurement, the samples were heated at 473 K for 1 h under vacuum to remove physisorbed water. The Brunauer-Emmett-Teller (BET) surface areas were estimated over a relative pressure (P/P_0) range of 0.05-0.30. Pore size distributions were obtained from the adsorption branch of the isotherms using the Barrett-Joyner-Halenda (BJH) method. Ultraviolet-visible diffuse reflectance spectra (UV-Vis DRS) of the TDMS samples were measured with spectrophotometer (V-670, Jasco).

3.3.3 Catalytic Reactions

Lewis acid catalysis of the prepared TDMS samples was examined by the hydride transfer of pyruvaldehyde to lactic acid in water. In the typical hydride transfer reaction, a mixture of pyruvaldehyde solution (2 mL, 0.1 M) and catalyst (0.1 g) was heated in a sealed Pyrex glass vial at 383 K for 2 h. The solution was analyzed after reaction using high-performance liquid chromatography (HPLC; LC-2000 plus, Jasco) with a refractive index detector.

3.4 Results and Discussion

3.4.1 Preparation and Structure of TDMS

The composition and textural properties of the CC-TDMS and PD-TDMS samples are shown in Table 3-1. Titanium content for CC-TDMS can be controlled by initial Ti(OPr-*i*)$_4$

concentration, which varies from 0.04 to 0.78 mmol g^{-1}. However, Si/Ti ratios for the CC-TDMS samples are not equal to those for the initial reaction solutions. In the case of CC-Ti-5/SBA-15, for example, only 20 % of titanium species remained intact in the final material. This is likely attributed to the formation of water-soluble titanium species and/or clusters that cannot be stabilized on silica surface. Structural information of the prepared TDMS was investigated by N_2 adsorption desorption isotherm analysis and X-ray diffraction (XRD) measurement. The XRD patterns for the CC-TDMS and PG-Ti-2/SBA-15 are shown in Figure 3-1. CC-TDMS and PG-Ti-2/SBA-15 have well-defined XRD peaks at 0.9, 1.5, 1.8° in lower angle region, indicating that prepared materials have ordered mesoporous structure similar to the SBA-15 [17-20]. The diffractions in the wide-angle region of CC-Ti-7/SBA-15 are assignable to the titania anatase crystal. This is direct evidence for the formation of titania nanocrystal. On the other hands, other samples showed no clear diffractions due to anatase TiO_2, suggesting the absence of large TiO_2 nanocrystal. Figure 3-2 shows N_2 adsorption-desorption isotherms of the samples. All isotherms are a type-IV isotherm with a H1-type hysteresis loop, typical of the mesoporous materials with cylindrical pores [17-20]. CC-TDMS catalysts have large BET surface areas of ca. 770 m^2 g^{-1} and uniform mesopores of ca. 9 nm even after incorporation of large amounts of titanium species (CC-Ti7/SBA-15). The decrease in BET surface area is observed for PG-Ti2/SBA-15 samples (ca. 450 m^2 g^{-1}) compared with parent SBA-15. This is probably due to the deposition of titanium species only on mesoporous silica surface which accompanies pore closing of micropores and partial degradation of original porous system by the weak alkaline treatment during surface modification. However, mesopores originated from the parent SBA-15 almost retained after deposition (pore size of PG-Ti2/SBA-15, ca. 9 nm). Thus, both CC-TDMS and PG-TDMS have large mesopores which enhance the diffusion of the reactants in water medium.

The coordination environment and dispersion of the titanium species in the prepared samples were studied by ultraviolet-visible diffusive reflectance spectroscopy (UV-Vis DRS) [21-24]. Figure 3-3 shows UV-Vis DRS spectra for the TDMS samples. UV-Vis DRS spectra of titania and titanosilicate zeolite (TS-1) are also shown for comparison. A strong and wide absorption band up to 400 nm was observed for TiO_2, which is associated with the band structure of anatase titania crystal [17,21-24]. On the other hands, TS-1 has an intense and narrow absorption band at 200-250 nm that can be assignable to the ligand to metal charge transfer (LMTC) of isolated titanium tetrahedral species in zeolite framework [21-24]. CC-Ti-1/SBA-15 shows a narrow peak centered at 210 nm, indicating that tetrahedrally ccordinated titanium species are presented on or in the mesoporous silica framework. While the intensity of the band increases with the increase in the titanium content, an additional broad adsorption up to 350 nm appears for CC-Ti5/SBA-15 and CC-Ti7/SBA-15, which means the formation of titania octahedral species. According to the XRD and UV-Vis DRS measurement, CC-TDMS with high titanium contents contains both highly dispersed and isolated

titanium tetrahedra in/on mesoporous silica framework and TiO_6 octahedra consisting of titania nanocrystal on mesoporous silica particles. On the other hands, PG-Ti-2/SBA-15 shows only a narrow peak centered at 210 nm, indicating that most of the titanium species are regarded as TiO_4 tetrahedra. Slight shift of the adsorption edge to longer wavelength observed in PG-Ti-2/SBA-15 is due to the formation of TiO_6 octahedra [17]. Incorporation of titanium species in the silica wall and formation of large amounts of TiO_6 octahedra due to TiO_2 nanocrystal for CC-TDMS catalysts would result in the decrease in effective Lewis acid sites, TiO_4 tetrahedra. Therefore, co-condensation method is not suitable for the preparation of TDMS with isolated titanium species.

Figure 3-4 shows SEM images of the SBA-15, CC-Ti-3/SBA-15, CC-Ti-7/SBA-15 and PG-Ti-2/SBA-15. Characteristic rod-like particles with ordered mesoporous structures similar to the SBA-15 are evident in all samples, which are well consistent with the results of N_2 adsorption desorption isotherm and XRD [20]. The formation of aggregated nanoparticles can be observed on the surface of CC-Ti-7/SBA-15. From the XRD patterns and UV-Vis DRS spectra of the CC-Ti-7/SBA-15, these particles are expected as titania nanoparticles.

3.4.2 Lewis Acid catalysis of TDMS

The catalytic performance of the prepared TDMS samples was investigated by hydride transfer of pyruvaldehyde into lactic acid in water. The reaction proceeds in aqueous medium by Lewis acid catalyzed intramolecular Meerwein-Ponndorf-Verley (MPV) reduction mechanism of mono-hydrated pyruvaldehyde [25]. We have already reported that PG-TDMS catalysts show high conversion and selectivity for the reaction [17]. In this experiment, the same amount of the catalysts was used in all experiments (0.1 g). The results are summarized in Table 2-2. As previously reported, water tolerant Lewis acid catalysts, $Sc(OTf)_3$, TiO_2 and PG-Ti-2/SBA-15 promotes the reaction effectively, while conventional liquid Brönsted acid catalyst, H_2SO_4 shows poor catalysis [15,17,25]. It should be noted that the lactic acid selectivity of titania is moderate, due to the simultaneous formation of by-product on titania surface. Koito et al. reported that the side reactions involve aldol condensation among pyruvaldehyde molecules to form polymerized species, which is catalyzed by basic sites on titania surface [26]. CC-TDMS also catalyzed the reaction: the pyruvaldehyde conversion and lactic acid yield increases with the increase in the titanium content, and lactic acid yield reached 61 % with high selectivity (88 %) for CC-Ti-5/SBA-15. TiO_4 tetrahedra for CC-TDMS can work as water tolerant Lewis acid sites for the hydride transfer reaction. However, catalytic performance for CC-Ti-7/SBA-15 largely decreases (lactic acid yield 30 % and selectivity 63 %) in spite of its high titanium content (Ti/Si = 4.7 %). According to the results of XRD, SEM and UV-Vis DRS, most of the titanium species in the CC-Ti-7/SBA-15 are present as TiO_6 octahedra in titania particle form, and cannot work as Lewis acid sites for the reaction. Low lactic acid selectivity can be therefore explained by the formation of basic sites on titania particles that enhance by-product

formation. PG-Ti-2/SBA-15 show higher catalytic performance (lactic acid yield and selectivity) than the tested heterogeneous catalysts here. Thus, surface modification by post-grafting method is effective on comparison with co-condensation method for the introduction of tetrahedra on mesoporous silica surface.

3.5 Conclusion

In summary, TDMS catalysts were also prepared by one pot co-condensation of silicon alkoxide and titanium alkoxide in the presence of an amphiphilic block copolymer as a structure directing agent. CC-TDMS has ordered mesoporous structure with high surface area, and TiO_4 tetrahedra which can work as water tolerant Lewis acid sites. However, it is difficult for co-condensation method to control the coordination environment of titanium species, due to the formation of titania nanoparticles under high Ti(OPr-*i*)$_4$ concentration. CC-TDMS can work as water tolerant Lewis acid catalyst for the hydride transfer of pyruvaldehyde into lactic acid, while side reaction is also promoted by titania particle on CC-TDMS with high titanium content. Therefore, post-grafting method is superior method to prepare TDMS catalyst with isolated titanium tetrahedral species.

References

[1] A. Corma, A, H. García, *Chem. Rev.* **2003**, *103*, 4307–4366.

[2] H. Yamamoto, Ed. *Lewis Acid in Organic Synthesis* Wiley-VCH, Weinheim, **2000**.

[3] P. T. Anastas, M. M. Kirchhoff, *Acc. Chem. Res*. **2002**, *35*, 686–694.

[4] M. Moliner, Y. Román-Leshkov, M. E. Davis, *Proc. Natl. Acad. Sci. USA* **2010**, *107*, 6164–6168.

[5] Y. Román-Leshkov, M. Moliner, J. A. Labinger, M. E. Davis, *Angew. Chem. Int. Ed.* **2010**, *49*, 8954–8957.

[6] Y. Román-Leshkov, M. E. Davis, *ACS Catal.* **2011**, *1*, 1566–1580.

[7] R.Gounder, *Catal. Sci. Technol.* **2014**, *4*, 2877–2886.

[8] M. Moliner, *Dalton Trans*. **2014**, *43*, 4197–4208.

[9] U. M. Lindström, Ed. *Organic Reactions in Water,* Wiley-Blackwell, Oxford, **2007**.

[10] A.Corma, V. Fornés, S. Iborra, M. Mifsud, M. Renz, *J. Catal.* **2004**, *221*, 67–76.

[11] A. Corma, F. X. Llabrés i Xamena, C. Prestipino, M. Renz, S. Valencia, *J. Phys. Chem. C* **2009**, *113*, 11306–11315.

[12] A.Corma, L. T. Nemeth, M. Renz, S. Valencia, *Nature* **2001**, *412*, 423–425.

[13] A. Corma, M. E. Domine, L. Nemeth, S. Valencia, *J. Am. Chem. Soc.* **2002**, *124*, 3194–3195.

[14] A. Corma, H. Garcia, *Chem. Rev.* **2002**, *102*, 3837–3892.

[15] K.Nakajima, Y. Baba, R. Noma, M. Kitano, J. N. Kondo, S. Hayashi, M. Hara, *J. Am. Chem. Soc.* **2011**, *133*, 4224–4227.

[16] K. Nakajima, R. Noma, M. Kitano, M. Hara, *J. Phys. Chem. C.* **2013**, *117*, 16028–16033.

[17] H. Shintaku, K. Nakajima, M. Kitano, N. Ichikuni, M. Hara, *ACS Catal.* **2014**, *4*, 1198–1204.

[18] F. Bérubé, B. Nohair, F. Kleitz, S. Kaliaguine, *Chem. Mater.* **2010**, *22*, 1988–2000.

[19] T.-W. Kim, M.-J. Kim, F. Kleitz; M. M. Nair; R. Guillet-Nicolas, K.-E. Jeong, H.-J.Chae. C.-U. Kim, S.-Y. Jeong, *ChemCatChem* **2012**, *4*, 687–697.

[20] D. Zhao, J. Feng, Q. Huo, N. Melosh, G. H.Fredrickson, B. F. Chmelka, G. D. Stucky, *Science* **1998**, *279*, 548–552.

[21] M. C. Capel-Sanchez, V. A. de la Peña-O'Shea, J. M. Campos-Martin, J. L. G. Fierro, *Top. Catal.* **2006**, *41*, 27–34.

[22] A. Zecchina, G. Spoto, S. Bordiga, A. Ferrero, G. Petrini, G. Leofanti, M. Padovan, *Stud. Surf. Sci. Catal.* **1991**, *69*, 251–258.

[23] M. C. Capel-Sanchez, G. Blanco-Brieva, J. M. Campos-Martin, M. P. de Frutos, W. Wen, J. A. Rodriguez, J. L. G. Fierro, *Langmuir* **2009**, *25*, 7148–7155.

[24] P. Wu, T. Tatsumi, T. Komatsu, T. Yashima, *Chem. Mater.* **2002**, *14*, 1657–1664.

[25] Y. Koito, K. Nakajima, M. Kitano, M. Hara, *Chem. Lett.* **2013**, *42,* 873–875.

[26] Y, Koito, Tokyo Institute of Technology Doctor Thesis, **2014**.

Table 3-1. Physicochemical properties of TDMS samples.

Catalyst	S_{BET} / m^2 g^{-1}	Pore volume / cm^2 g^{-1}	Pore diameter / nm	Ti/Si molar ratio for preparation (%)	Final Ti/Si molar ratio of catalyst (%)	Ti content / mmol g^{-1}
SBA-15	742	0.90	9.3	-	-	-
PG-Ti-2/SBA-15	481	0.74	9.4	2.0	2.19[a]	0.35[a]
CC-Ti-1/SBA-15	774	0.91	9.5	1.0	0.25[b]	0.04[b]
CC-Ti-3/SBA-15	782	0.94	9.4	3.0	0.36[b]	0.06[b]
CC-Ti-5/SBA-15	777	0.92	9.4	5.0	1.08[b]	0.18[b]
CC-Ti-7/SBA-15	755	0.94	9.4	7.0	4.78[b]	0.78[b]

[a] XRF measurements. [b]ICP-AES measurements.

Table 3-2. Catalytic activities of the samples and reference catalysts for the hydride transfer of pyruvaldehyde to lactic acid in water.

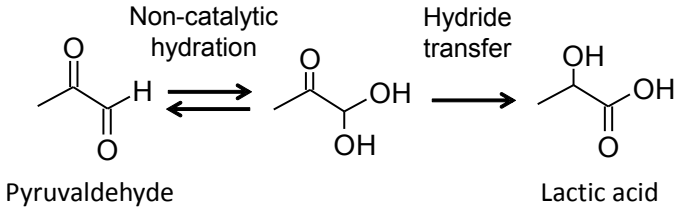

Pyruvaldehyde Lactic acid

Catalyst	Conv. (%)	Yield (%)	Selec. (%)
H_2SO_4	16	2	13
$Sc(OTf)_3$	100	94	94
TiO_2	100	49	49
SBA-15	29	0	-
PG-Ti-2/SBA-15	89	87	97
CC-Ti-1/SBA-15	33	15	44
CC-Ti-3/SBA-15	60	49	82
CC-Ti-5/SBA-15	70	61	88
CC-Ti-7/SBA-15	49	30	63

Reagents and conditions: pyruvaldehyde, 0.2 mmol; catalyst, 100 mg; water, 2 mL; temperature, 383 K; time, 2 h.

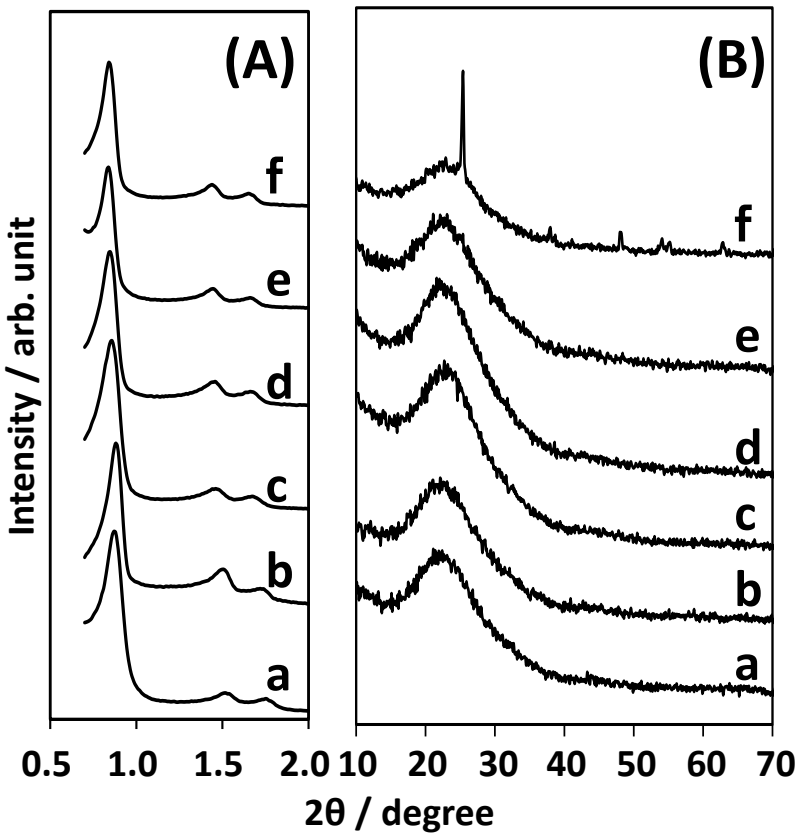

Figure 3-1. (A) Low-angle and (B) wide-angle XRD patterns for (a) bare SBA-15, (b) PG-Ti-2/SBA-15, (c) CC-Ti-1/SBA-15, (d) CC-Ti-3/SBA-15, (e) CC-Ti-5/SBA-15, and (f) CC-Ti-7/SBA-15.

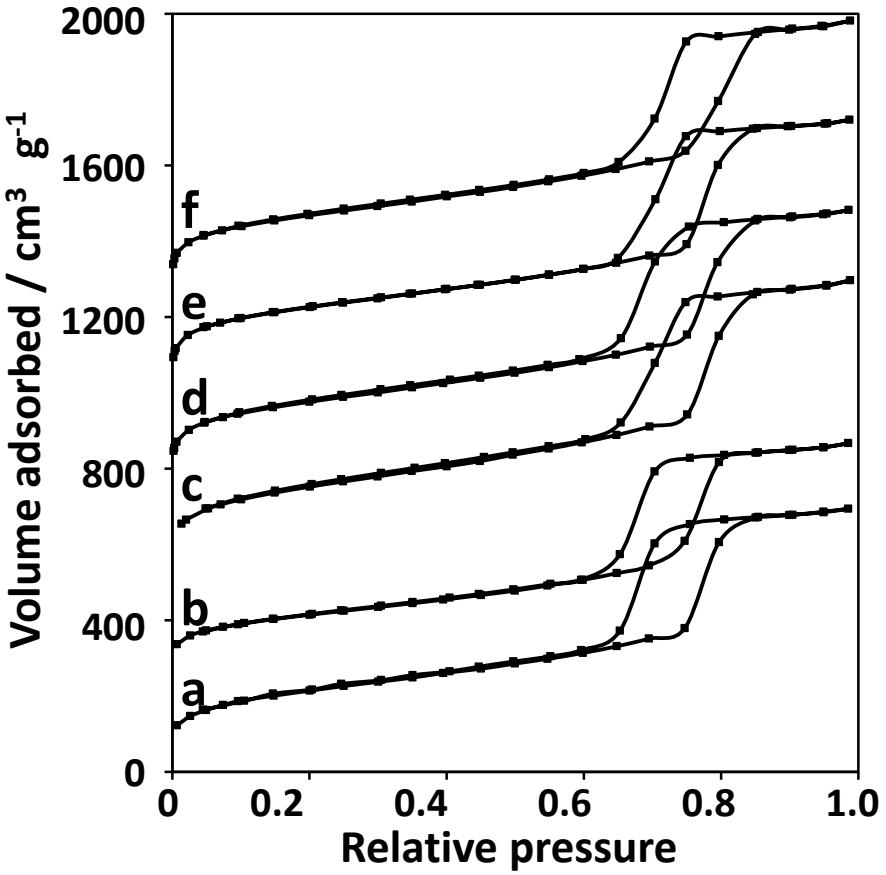

Figure 3-2. N_2 adsorption-desorption isotherms for (a) bare SBA-15, (b) PG-Ti-2/SBA-15, (c) CC-Ti-1/SBA-15, (d) CC-Ti-3/SBA-15, (e) CC-Ti-5/SBA-15, and (f) CC-Ti-7/SBA-15. Each isotherm is vertically offset with 250 cm^3 g^{-1}.

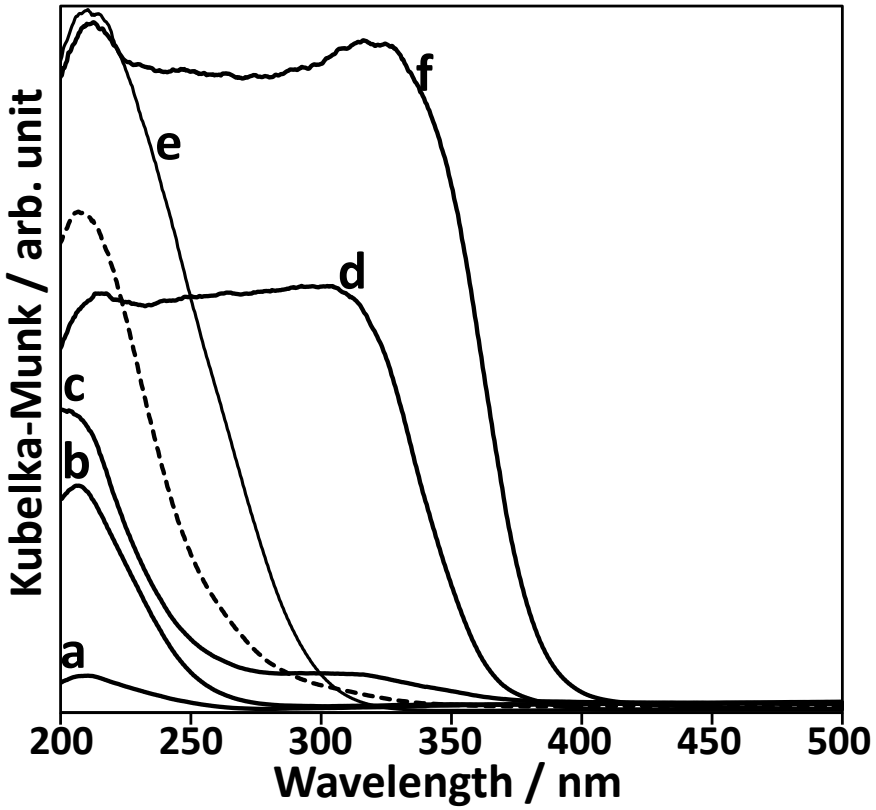

Figure 3-3. UV-Vis DRS spectra of TDMS with various titanium content, TS-1 and anatase TiO_2. (a) CC-Ti-1/SBA-15, (b) CC-Ti-3/SBA-15, (c) CC-Ti-5/SBA-15, (d) CC-Ti-7/SBA-15, (e) PG-Ti-2/SBA-15, and (f) anatase TiO_2. The spectrum for TS-1 is given as a dashed line.

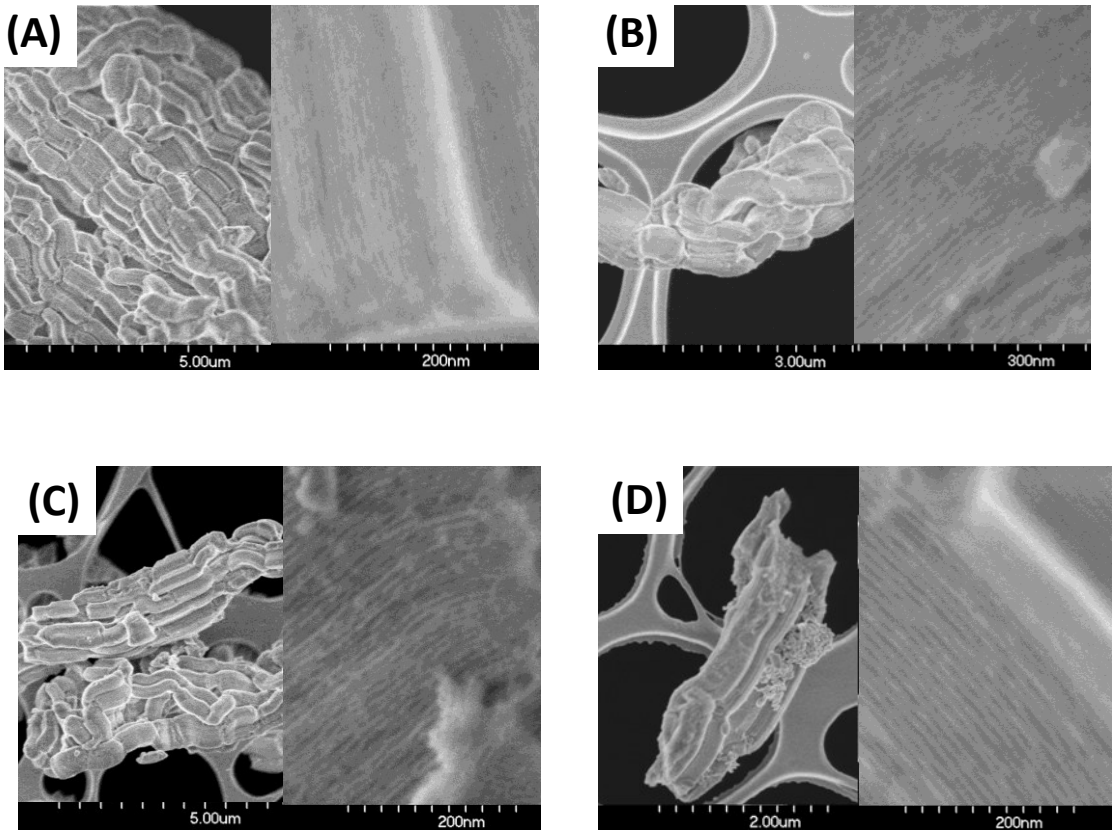

Figure 3-4. SEM images of TDMS catalysts. (a) SBA-15, (b) PG-Ti-2/SBA-15, (c) CC-Ti-3/SBA-15, and (d) CC-Ti-7/SBA-15.

Chapter 4

Efficient Mukaiyama Aldol Reaction in Water with TiO_4 Tetrahedra on Hydrophobic Mesoporous Silica Surface

Reproduced from H. Shintaku, K. Nakajima, M. Kitano, M. Hara, *Chem commun.* **2015**, 13473–13476, with permission of The Royal Society of Chemistry

4.1 Abstract

A new heterogeneous catalyst, hydrophobic TiO_4-deposited mesoporous silica, has been designed for the efficient Mukaiyama-aldol condensation, a water-participating Lewis acid-catalyzed reaction between hydrophobic carbonyl compound and silyl enol ether. Prepared catalyst suspended in water exhibited high catalytic performance as a reusable catalyst for the reaction without a surfactant.

4.2 Introduction

The Mukaiyama-aldol condensation is an essential reaction for the chemoselective synthesis of β-hydroxycarbonyl compounds, and adopts stable and isolable enol ethers as enolizable carbonyl compounds [1]. Enol ethers with at least one acidic hydrogen atom in the α-position act as nucleophiles and react with activated carbonyl compounds (aldehydes or ketones) in the presence of a Lewis acid/base [1-6]. A variety of homogeneous and heterogeneous catalysts have been investigated for this reaction [1-16]. Kobayashi et al. reported that some metal triflates, such as $Sc(OTf)_3$, can act as Lewis acids in water to promote the Mukaiyama-aldol reaction of silyl enol ethers with aldehydes and ketones in an organic solvent-water mixture or pure water containing an appropriate surfactant [17-19]. However, the low solubility of the hydrophobic reactant in pure water necessitates the addition of large amounts of surfactant to enhance the accessibility of hydrophobic reactant molecules to the homogeneous Lewis acid in solution. It has already been reported that resins used to immobilize metal triflates can function as heterogeneous Lewis acid catalysts that are workable even in water [20-22], and homogeneous catalysts composed of Lewis acids and surfactants are effective for reactions of hydrophobic molecules in water [18,19]. However, heterogeneous catalysts available for the reaction without surfactants have not been devised to date. Any heterogeneous Lewis acid catalysts derived from ubiquitous, abundant starting materials that efficiently promote such a reaction in water without the addition of surfactants would be applicable to the environmentally benign production of various chemicals on a large scale.

Recently, some unsaturated metal species, such as Sn [23-27], Zr [27,28], Ta [27,28],

Nb[27-29] , and Ti [27,30,31], formed on oxide surfaces have been reported to act as water-tolerant Lewis acid sites to promote various organic reactions in water or organic solvent-water mixtures. We have reported that unsaturated titanium species, tetrahedral TiO_4, formed on mesoporous silica are active Lewis acid sites for the Mukaiyama-aldol reaction of benzaldehyde with 1-(trimethylsilyloxy)cyclohexene in a water-surfactant system [31]. The mesoporous structure of TiO_4-deposited mesoporous silica (TDMS) effectively enhances the access of reactant molecules to TiO_4 Lewis acid sites which exhibit high catalytic activity for the reaction, comparable to that of $Sc(OTf)_3$. However, sodium dodecyl sulfate (SDS) is necessary in the reaction system to disperse the hydrophobic substrates in water: both $Sc(OTf)_3$ and TDMS have poor catalytic activity for the reaction in the absence of SDS. Here, the introduction of various hydrophobic organic functional groups was examined on TDMS to realize a surfactant-free aqueous reaction system for the reaction.

4.3 Experimental

4.3.1 Catalyst Preparation

TiO_4-deposited mesoporous silica (TDMS) was prepared by the simple impregnation of a titanium complex on mesoporous silica (SBA-15) [31-33]. SBA-15 (5 g) was added to a mixture of distilled water (145 g) and ethanol (15 g). After pH adjustment of the suspension to 10 with diluted ammonia, a mixture of ethanol (5 g), titanium isopropoxide ($Ti(OPr\text{-}i)_4$; TTIP), and acetyl acetone (AA) (AA/TTIP =3.1) was slowly added to the mixture at 278 K and stirred for 2 h. The solid material recovered by filtration was washed repeatedly with ethanol and then calcined at 823 K for 3 h in air to produce TDMS (Ti/Si=1.8 mol%).

Surface modification with hydrophobic organic groups was performed by treatment of the TDMS with various silane coupling agents: $CH_3(CH_2)_2Si(OCH_3)_3$ (propyltrimethoxysilane; Propyl), $CH_3(CH_2)_{11}Si(OCH_3)_3$ (dodecyltrimethoxysilane; Dodecyl), $C_6H_5CH_2Si(OCH_3)_3$ (benzyltrimethoxysilane; Benzyl), or $CF_3(CF_2)_5(CH_2)_2$ $Si(OCH_3)_3$ ((1H,1H,2H,2H-tridecafluoro-n-octyl)trichlorosilane; Tridecafluoro). In a typical synthesis, TDMS was heated at 573 K for 1 h to remove physisorbed water. The dehydrated TDMS was then added to a mixture of toluene (25 ml) and an adequate amount of silane coupling agent (0.2-0.4 mmol). After the solution was stirred under reflux for 12 h, the resulting material was recovered by filtration and washed repeatedly with toluene, ethanol, and water, and dried in air at 353 K overnight. The TDMS samples modified with propyl, benzyl, dodecyl, and tridecafluoro-n-octyl groups are denoted as Propyl-TDMS, Benzyl-TDMS, Dodecyl-TDMS, and Tridecafluoro-TDMS, respectively.

4.3.2 Catalyst Characterization

The titanium content of the samples was determined using X-ray fluorescence spectroscopy (XRF; ZSX100e, Rigaku). Powder X-ray diffraction patterns were obtained with a

diffractometer (Ultima IV, Rigaku) using Cu Kα radiation (40 kV, 40 mA) over the 2θ range of 0.7–70°. Nitrogen adsorption-desorption isotherms were measured at 77 K with a surface area analyzer (Nova-4200e, Quantachrome). Prior to measurement, the samples were heated at 473 K for 1 h under vacuum to remove physisorbed water. The Brunauer-Emmett-Teller (BET) surface areas were estimated over a relative pressure (P/P_0) range of 0.05–0.30. Pore size distributions were obtained from the adsorption branch of the isotherms using the Barrett-Joyner-Halenda (BJH) method. Ultraviolet-visible diffuse reflectance spectra (UV-Vis DRS) of the TDMS samples were measured with spectrophotometer (V-670, Jasco). The densities of organic functional groups were estimated from the carbon content determined by elemental analysis (varioMICRO cube, Elementar). The acid site densities of the samples were examined by NH_3 temperature-programmed desorption (TPD; BEL-CAT, BEL JAPAN) with helium as a carrier gas. Fourier transform-infrared (FTIR) spectra were obtained at a resolution of 4 cm^{-1} using a spectrometer (FT/IR-6100, Jasco) equipped with an extended KBr beam splitting device and a mercury cadmium telluride (MCT) detector. The samples were pressed into self-supporting disks (20 mm diameter, 0.02 g), placed in an IR cell attached to a closed glass-circulation system and dehydrated by heating at 473 K for 1 h under vacuum. Prior to CO-adsorbed FT-IR measurements, all samples were exposed to water vapor (20 Torr), followed by evacuation for 5 min to remove weakly physisorbed water, and then exposed to CO (1.0 Torr) for adsorption.

4.3.3 Catalytic Reactions

Lewis acid catalyst (0.1 g) was added to a mixture of benzaldehyde (0.4 mmol), 1-(trimethylsilyloxy)cyclohexene (0.6 mmol), and water (3 mL) at 298 K. After stirring the solution at 298 K for 2 h, the product was isolated by extraction with ethyl acetate and analyzed using ^1H nuclear magnetic resonance (NMR) spectroscopy (Biospin AvanceIII 400 MHz, Bruker) with dioxane used as an internal standard.

4.4 Results ans Discussion

4.4.1 Catalysts Characterization

TDMS was prepared by a simple impregnation procedure with titanium isopropoxide and acetylacetone [31-33]. The catalytic activity of TDMS depends largely on Ti content. In this study, TDMS (Ti/Si=0.018) was adopted because it exhibits high catalytic performance for the Mukaiyama-aldol reaction in SDS-water system among tested TDMS samples [31]. The density of TiO_4 tetrahedra on the TDMS was estimated to be 0.44 TiO_4 nm^{-2} which is smaller than monolayer coverage. Surface modification with hydrophobic organic groups bonded to TDMS through surface silanol groups was conducted using $(CH_3(CH_2)_2Si(OCH_3)_3$ (propyltrimethoxysilane; Propyl), $CH_3(CH_2)_{11}Si(OCH_3)_3$ (dodecyltrimethoxysilane; Dodecyl), $C_6H_5CH_2Si(OCH_3)_3$

(benzyltrimethoxysilane, Benzyl), and $CF_3(CF_2)_5(CH_2)_2Si(OCH_3)_3$ ((1H,1H,2H,2H-tridecafluoro-n-octyl)trichlorosilane, Tridecafluoro). The TDMS samples with propyl, benzyl, dodecyl, and tridecafluoro-n-octyl groups are denoted as Propyl-TDMS, Benzyl-TDMS, Dodecyl-TDMS, and Tridecafluoro-TDMS, respectively.

Figure 4-1 shows small and wide angle X-ray diffraction (XRD) patterns of the samples. All samples have three intense peaks at around 0.9, 1.5, and 1.8° in the small angle region (Figure 4-1(A)), which are assignable to (100), (110), and (200) diffractions, respectively, of a two-dimensional hexagonal *(P6mm)* symmetry structure [31-35]. No diffractions were observed in the large angle region (Figure 4-1(B)), which indicates the absence of large crystalline TiO_2 domains on mesoporous silica. N_2 adsorption-desorption measurements of the samples in Figure 4-2 show typical type-IV isotherms with an H1-type hysteresis loop that is characteristic of a mesoporous solid with uniform and cylindrical mesopores [31-35]. Immobilization of organic functional groups (ca. 0.3 nm^{-2} for each sample) on a mesoporous surface results in a slight decrease in the original Brunauer-Emmett-Teller (BET) surface area, pore volume and average pore size (Table 4-1). There is no significant differences in the XRD patterns and N_2 adsorption isotherms between the bare and modified TDMS samples, which suggests that the original mesoporosity and periodic mesoporous structure remain intact even after the introduction of various organic functionalities by a simple surface modification technique.

TDMS samples were also evaluated using Fourier transform infrared (FTIR) spectroscopy. FTIR spectra of the modified TDMS samples are shown in Figure 4-3. Prior to measurement, the samples were heated at 473 K for 1 h to remove physisorbed water. Propyl and Dodecyl-TDMS have several bands for the CH stretching mode (2820-3000 cm^{-1}) and one band for the CH asymmetric bending mode (1465 cm^{-1}) that are due to methylene and methyl moieties of the propyl and dodecyl groups on the silica surface (Figures 4-3(b) and 4-3(c)). Benzyl-TDMS has specific bands for the methylene group (several bands at 2820-3000 cm^{-1}: CH stretching mode) and benzene ring (several bands at 3000-3095 cm^{-1}: CH stretching mode, three bands at 1605, 1495, and 1453 cm^{-1}: C=C-C stretching mode), which indicates the successful introduction of the benzyl group onto the silica surface. A CF stretching band at 1350 cm^{-1} is observed as a shoulder peak for Tridecafluoro-TDMS, in addition to bands for the CH stretching (2820-3000 cm^{-1}) and bending (1445 cm^{-1}) modes. These results clearly indicate that certain amounts of organic functional groups are successfully embedded on the silica surface. The densities of organic functional groups for Propyl-, Dodecyl-, Benzyl-, and Tridecafluoro-TDMS were estimated to be 0.28, 0.32, 0.31, and 0.33 nm^{-2}, respectively (Table 4-1), from BET surface area measurements and CHNS elemental analysis. The modified TDMS samples still have large amounts of silanol group on the surface, due to low organic functional group densities.

The coordination environment of the titanium species was investigated using

ultraviolet-visible diffusive reflectance spectroscopy (UV-Vis DRS) [31-33,36-39]. Figure 4-4 shows UV-Vis DRS spectra for the TDMS samples. TDMS has a narrow absorption band centered at ca. 210 nm, which is assigned to the charge transfer of isolated TiO_4 tetrahedra on the silica framework. The surface-modified TDMS samples also have a similar absorption band, which indicates that TiO_4 tetrahedra on the silica surface remain intact after surface modification, i.e., the introduction of hydrophobic groups onto TDMS does not affect the TiO_4 Lewis acid sites. In the case of Benzyl-TDMS, a shoulder band also appears at around 250 nm, which is attributed to the $\pi \rightarrow \pi^*$ transition of the benzene ring. As a result, TiO_4 tetrahedra on the modified TDMS are expected to function as Lewis acid sites in water [31].

The Lewis acidity of the modified TDMS samples was examined using CO adsorption measurements with FTIR spectroscopy. Figure 4-5 shows difference FTIR spectra for the CO adsorbed TDMS samples. Prior to measurement, the samples were exposed to saturated water vapor to introduce an excess amount of physisorbed water onto the surface. All modified samples have a band at 2182 cm^{-1} due to CO coordinated on Lewis acid sites [31]. This band is not present in the spectrum for bare mesoporous silica (SBA-15) without TiO_4 deposition, which indicates that the TiO_4 tetrahedra function as Lewis acid sites and bond to CO even in the presence of water.

The Lewis acid site densities for the samples were estimated from NH_3 temperature-programmed desorption (TPD) measurements. There were no significant differences in the effective Lewis acid densities of TDMS and the modified TDMS samples (Table 4-1). Therefore, water-tolerant Lewis acid sites on TDMS are considered to be preserved, even after the introduction of various organic functional groups.

4.4.2 Catalytic Reactions

The TDMS samples were applied as catalysts to the Mukaiyama-aldol condensation of benzaldehyde with 1-(trimethylsilyloxy)cyclohexene in water in the absence of a surfactant. The catalytic activities of the tested catalysts are summarized in Table 4-2. HCl, a homogeneous liquid acid does not catalyze the reaction at all due to rapid hydrolysis of 1-(trimethylsilyloxy)cyclohexene by the Brönsted acid. $Sc(OTf)_3$ has a high catalytic activity for the reaction in the presence of sodium dodecyl sulfate (SDS) as a surfactant, and the yield of 2-(hydroxy(phenyl)methyl)cyclohexanone reaches 83% after 2 h. However, $Sc(OTf)_3$ is not an effective catalyst for the reaction without SDS, as shown in Table 4-2. TDMS without surface modification also has high catalytic activity in the presence of SDS with a product yield comparable to that for $Sc(OTf)_3$. However, the catalytic activity of TDMS in the absence of SDS is significantly decreased in the same manner as that for $Sc(OTf)_3$ without SDS. Propyl- and Benzyl-TDMS have similar catalytic activity to bare TDMS, whereas Dodecyl- and Tridecafluoro-TDMS work as effective catalysts for the reaction, even in the absence of SDS. In particular, Tridecafluoro-TDMS has the highest catalytic performance without

SDS among the tested catalysts. After the reaction, the TDMS catalysts could be readily separated from the reaction solution by filtration. The results of catalyst reuse experiment for Tridecafluoro-TDMS are presented in Figure 4-6. No decrease in activity was observed even after two reuses of the sample, and it was confirmed that there was no elution of Ti species or hydrophobic functional groups from TDMS. Therefore, Tridecafluoro-TDMS is a stable, reusable, and highly active solid Lewis acid catalyst for SDS-free Mukaiyama-aldol condensation.

While both Dodecyl and Tridecafluoro-TDMS samples have hydrophobic surfaces that are suitable for adsorption of hydrophobic reactant in water, Tridecafluoro-TDMS shows higher catalytic performance for the SDS-free reaction system than Dodecyl-TDMS (Table 4-2). It was confirmed that this difference in activity between Dodecyl and Tridecafluoro-TDMS remains unaltered even when the density of dodecyl groups is increased. Dodecyl-TDMS with a higher density of dodecyl groups (0.44 nm^{-2}) gave a yield of 44%. Although this value is larger than that (35%) of Dodecyl-TDMS in Table 4-2 (dodecyl density: 0.32 nm^{-2}), Dodecyl-TDMS sample is still inferior to Tridecafluoro-TDMS (0.33 nm^{-2}) in activity.

4.4.3 Hydrophobicity of Catalysts

The prepared TDMS catalysts can be classified into two groups with respect to the catalytic activity of the SDS-free system; Dodecyl- and Tridecafluoro-TDMS are distinct from bare, Propyl-, and Benzyl-TDMS. The high catalytic performance of the former SDS-free systems can be attributed to the hydrophobic organic layer formed on the silica surface, which enhances the accessibility of hydrophobic reactants to the TiO_4 Lewis acid sites. The hydrophobicity and hydrophilicity of the TDMS samples were examined using a simple method. Figure 4-7 (A) shows a photograph of the TDMS samples suspended in a water-benzene (1:1 vol%) mixture. Most of the Propyl-, and Benzyl-TDMS particles are present in the lower water phase. In contrast, the Dodecyl- and Tridecafluoro-TDMS particles are observed in the upper benzene phase, which indicates that Dodecyl- and Tridecafluoro-TDMS are more hydrophobic than the other TDMS samples. Water vapor adsorption-desorption isotherms were measured to determine the hydrophobic characteristics of the TDMS samples and the results are shown in Figure 4-8. In the case of the SBA-15 silica support, the adsorption of water vapor starts at P/P_0=0.78. Although water adsorption on bare, Propyl-, and Benzyl-TDMS is accelerated at ca. P/P_0=0.78, steep water uptake is not observed up to P/P_0=0.85 in Dodecyl-and Tridecafluoro-TDMS. The large shift in P/P_0 indicates that Dodecyl- and Tridecafluoro-TDMS are more hydrophobic than bare, Propyl-, and Benzyl-TDMS, which results in the higher catalytic activity of Dodecyl- and Tridecafluoro-TDMS. Both TiO_4 Lewis acid sites and SBA-15 as a support are primarily hydrophilic materials because of Lewis acidity and silanol groups. As a result, strong hydrophobic functional groups such as dodecyl and tridecafluoro groups are required to enhance the hydrophobicity of TDMS. The difference in catalytic performance between

Dodecyl-TDMS and Tridecafluoro-TDMS can be also attributed to surface hydrophobicity. Figure 4-7 (B) shows a photograph of the Docecyl- and Tridecafluoro-TDMS suspended in a water-ethanol (4:1 vol%) mixture. Although most of Tridecafluoro-TDMS particles float on the liquid level, Dodecyl-TDMS particles were dispersed in the solution, suggesting that Tridecafluoro-TDMS is more hydrophobic than Docecyl-TDMS. It has been reported that fluorocarbon moiety is more hydrophobic than normal hydrocarbon chains such as dodecyl group [40].

It should be noted that water is essential for the Mukaiyama-aldol condensation of benzaldehyde with 1-(trimethylsilyloxy)cyclohexene [20,41,42]. This reaction is regarded as a Lewis acid-catalyzed reaction of hydrophobic molecules requiring water and is therefore largely enhanced by the addition of a surfactant. Table 4-3 shows the catalytic activities of bare dehydrated TDMS for the Mukaiyama-aldol condensation at 1 h conducted in various solvents. The SDS-water system is the most suitable for the reaction. While hydrophobic reactants are readily dissolved in polar (tetrahydrofuran and acetonitrile), nonpolar (dichloromethane and toluene), and protonic (ethanol) solvents, bare TDMS has only moderate catalytic activity in these solvents. The effect of water in the Mukaiyama-aldol reaction was further examined through the reaction for bare TDMS in various aqueous THF solutions. The results are shown in Figure 4-9. Bare TDMS shows no catalysis in pure THF without water. However, the product yield increases with increasing water content, reaching a maximum at 17 vol%. Further increase of water content decreases product yield, due to phase separation: hydrophilic TDMS and hydrophobic reactants are preferentially dispersed in water and THF phase, respectively, which prevent access of reactant molecules with TiO_4 tetrahedra on TDMS. This means that a certain amount of water is indispensable for the efficient Mukaiyama-aldol reaction. Recently, Hatanaka et al. reported that water molecules contribute largely to the stabilization of a transition state formed between activated aldehyde with a Lewis acid and silyl enol ether and the dissociation of trimethylsilyl groups, which results in an increase of the overall reaction rate [43]. Reactions of hydrophobic molecules that require water, in addition to the Mukaiyama-aldol condensation, have often been reported, and such reactions increases in importance [44-46]. Lewis acids that are workable in the presence of water and surfactants are indispensable for such reactions. The results presented in this study suggest that heterogeneous catalysts prepared from abundant and ubiquitous starting materials could be applied to such complex reactions.

4.5 Conclusion

In conclusion, TDMS catalysts modified with various organic functional groups were investigated as a new type of heterogeneous catalyst for efficient Mukaiyama-aldol condensation of benzaldehyde with 1-(trimethylsilyloxy)cyclohexene. The introduction of dodecyl- and tridecafluoro-groups onto TDMS induced strong hydrophobicity to the material, which resulted in high catalytic activity for the reaction without the addition of SDS as a surfactant. For

Tridecafluoro-TDMS, the yield of 2-(hydroxy(phenyl)methyl)cyclohexanone reached 85% after 2 h, even without SDS, which is comparable to that for bare TDMS and $Sc(OTf)_3$ with SDS. The high catalytic performance of hydrophobic TDMS can be attributed to both TiO_4 tetrahedra Lewis acid sites that are workable in water and a highly hydrophobic organic layer that facilitates access of the reactant and water molecules to the Lewis acid sites.

References

[1] T. Mukaiyama, K. Narasaka, K. Banno, *Chem. Lett.* **1973**, *2*, 1011–1014.

[2] T. Mukaiyama, K. Banno, K. Narasaka, *J. Am. Chem. Soc.* **1974**, *96*, 7503–7509.

[3] S. B. J. Kan, K. K.-H. Ng, I. Paterson, *Angew. Chem. Int. Ed.* **2013**, *52*, 9097–9108.

[4] G. L. Beutner, S. E. Denmark, *Angew. Chem. Int. Ed.* **2013**, *52,* 9086–9096.

[5] H. Fujisawa, T. Mukaiyama, *Chem. Lett.* **2002**, *31,* 182–183.

[6] S. E. Denmark, S. B. D. Winter, X. Su, K.-T. Wong, *J. Am. Chem. Soc.* **1996**, *118*, 7404–7405.

[7] R. Flowers, X. Xu, C. Timmons, G. Li, *Eur. J. Org. Chem.* **2004**, 2988–2990.

[8] M. Kawai, M. Onaka, Y. Izumi, *Chem. Lett*. **1986**, *15*, 1581–1584.

[9] M. Sasidharan, S. V. N. Raju, K. V. Srinivasan, V. Paul, R. Kumar, *Chem. Commun.* **1996**, 129–130.

[10] T.-P. Loh, X.-R. Li, *Tetrahedron* **1999**, *55,* 10789–10802.

[11] H. Matsuhashi, M. Tanaka, H. Nakamura, K. Arata, *Appl. Catal. A* **2001**, *208*, 1–5.

[12] H. Ishitani, M. Iwamoto, *Tetrahedron Lett.* **2003**, *44*, 299–301.

[13] R. Garro, M. T. Navarro, J. Primo, A. Corma, *J. Catal.* **2005**, *233*, 342–350.

[14] T. R. Gaydhankar, P. N. Joshi, P. Kalita, R. Kumar, *J. Mol. Catal. A* **2007**, *265*, 306–315.

[15] S. Ito, H. Yamaguchi, Y. Kubota, M. Asami, *Chem. Lett.* **2009**, *38*, 700–701.

[16] S. Ito, A. Hayashi, H. Komai, Y. Kubota, M. Asami, *Tetrahedron Lett.* **2010**, *51*, 4243–4245.

[17] S. Kobayashi, I. Hachiya, *J. Org. Chem.* **1994**, *59*, 3590–3596.

[18] S. Kobayashi, T. Wakabayashi, S. Nagayama H. Oyamada, *Tetrahedron Lett.* **1997**, *38*, 4559–4562.

[19] S. Kobayashi, T. Busujima. S. Nagayama, *Chem. Commun.* **1998**, 19–20.

[20] S. Kobayashi, S. Nagayama, *J. Am. Chem. Soc.* **1998**, *120*, 2985–2986.

[21] S. Nagayama, S. Kobayashi, *Angew. Chem. Int. Ed.* **2000**, *39*, 567–569.

[22] W. Gu, W.-J. Zhou, D. L. Gin, *Chem. Mater.* **2001**, *13*, 1949–1951.

[23] A. Corma, L. T. Nemeth, M. Renz, S. Valencia, *Nature* **2001**, *412*, 423–425.

[24] A. Corma, V. Fornés, S. Iborra, M. Mifsud, M. Renz, *J. Catal.* **2004**, *221*, 67–76.

[25] M. Moliner, Y. Román-Leshkov, M. E. Davis, *Proc. Natl. Acad. Sci. U.S.A.* **2010**, *107*, 6164–6168.

[26] Y. Román-Leshkov, M. Moliner, J. A. Labinger, M. E. Davis, *Angew. Chem. Int. Ed.* **2010**, *49*, 8954–8957.

[27] A. Corma, H. Garcia, *Chem. Rev.* **2002**, *102*, 3837–3892.

[28] A. Corma, F. X. Llabrés i Xamena, C. Prestipino, M. Renz, S. Valencia, *J. Phys. Chem. C* **2009**, *113*, 11306–11315.

[29] K. Nakajima, Y. Baba, R. Noma, M. Kitano, J. N. Kondo, S. Hayashi, M. Hara, *J. Am. Chem. Soc.* **2011**, *133*, 4224–4227.

[30] K. Nakajima, R. Noma, M. Kitano, M. Hara, *J. Phys. Chem. C* **2013**, *117*, 16028–16033.

[31] H. Shintaku, K. Nakajima, M. Kitano, N. Ichikuni, M. Hara, *ACS Catal.* **2014**, *4*, 1198–1204.

[32] F. Bérubé, B. Nohair, F. Kleitz, S. Kaliaguine, *Chem. Mater.* **2010**, *22*, 1988–2000.

[33] T. -W. Kim, M. -J. Kim, F. Kleitz, M. M. Nair, R. Guillet-Nicolas, K. -E. Jeong, H. -J. Chae, C. -U. Kim, S. -Y. Jeong, *ChemCatChem* **2012**, *4*, 687–697.

[34] D. Zhao, J. Feng, Q. Huo, N. Melosh, G. H. Fredrickson, B. F. Chmelka, G. D. Stucky, *Science* **1998**, *279*, 548–552.

[35] D. Zhao, J. Sun, Q. Li, G. D. Stucky, *Chem. Mater.* **2000**, *12*, 275–279.

[36] M. C. Capel-Sanchez, G. Blanco-Brieva, J. M. Campos-Martin, M. P. de Frutos, W. Wen, J. A. Rodriguez, J. L. G. Fierro, *Langmuir* **2009**, *25*, 7148–7155.

[37] P. Wu, T. Tatsumi, T. Komatsu, T. Yashima, *Chem. Mater.* **2002**, *14*, 1657–1664.

[38] M. C. Capel-Sanchez, V. A. de la Peña-O'Shea, J. M. Campos-Martin, J. L. G. Fierro, *Top. Catal.* **2006**, *41*, 27–34.

[39] A. Zecchina, G. Spoto, S. Bordiga, A. Ferrero, G. Petrini, G. Leofanti, M. Padovan, *Stud. Surf. Sci. Catal.* **1991**, *69*, 251–258.

[40] V. H. Dalvi, P. J. Rossky, *Proc. Natl. Acad. Sci. U.S.A.* **2010**, *107*, 13603–13607.

[41] P. anayake, M. J. Allen, *J. Am. Chem. Soc.* **2009**, *131*, 6342–6343.

[42] D. J. Averill, P. Dissanayake, M. J. Allen, *Molecules* **2012**, *17*, 2073–2081.

[43] M. Hatanaka, K. Morokuma, *J. Am. Chem. Soc.* **2013**, *135*, 13972–13979.

[44] R. N. Butler, A. G. Coyne, *Chem. Rev.* **2010**, *110*, 6302–6337.

[45] A. Chanda, V. V. Fokin, *Chem. Rev.* **2009**, *109*, 725–748

[46] S. Narayan, J. Muldoon, M. G. Finn, V. V. Fokin, H. C. Kolb, K. B. Sharpless, *Angew. Chem. Int. Ed.* **2005**, *44*, 3275–3279.

[47] H. Shintaku, K. Nakajima, M. Kitano, M. Hara, *Chem commun.* **2015**, 13473–13476.

Table 4-1. Physicochemical properties of the TDMS samples.

Catalyst	S_{BET} / $m^2\ g^{-1}$	Pore volume / $cm^3\ g^{-1}$	Pore diameter / nm	Organic functional group density[a] / nm^{-2}	Lewis acid site density[b] / mmol g^{-1}
TDMS	535	0.74	9.3	-	0.16
Propyl-TDMS	485	0.73	8.4	0.28	0.17
Dodecyl-TDMS	436	0.66	7.8	0.32	0.16
Benzyl-TDMS	493	0.71	9.1	0.31	0.16
Tridecafluoro-TDMS	419	0.68	9.1	0.33	0.17

[a]Determined by elemental analysis. [b]Determined by NH_3 TPD measurement.

Table 4-2. Catalytic activities of the TDMS samples and reference catalysts for the Mukaiyama-aldol reaction of benzaldehyde with 1-(trimethylsilyloxy)cyclohexene in water.

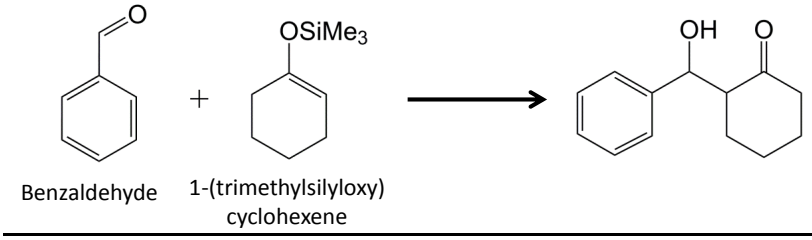

Catalyst	Lewis acid site density[a] / mmol g^{-1}	Yield[b] (%)
1 mol/L HCl	-	0
$Sc(OTf)_3$	2.0	19
$Sc(OTf)_3$-SDS[c]	2.0	83
TDMS	0.16	7
TDMS-SDS[c]	0.16	87
Propyl-TDMS	0.17	3
Dodecyl-TDMS	0.16	35
Benzyl-TDMS	0.16	3
Tridecafluoro-TDMS	0.17	85

Reagents and conditions: benzaldehyde, 0.4 mmol; 1-(trimethylsilyloxy)cyclohexene, 0.6 mmol; water, 3 mL; catalyst, 0.1 g; temperature, 298 K; time, 2 h. [a] Determined by NH_3-TPD measurement. [b] *Syn/anti* ratio for all tested catalysts was estimated to be ca. 7/3. [c] Reaction in the presence of SDS (0.023 g).

Table 4-3. Influence of solvent on the Mukaiyama-aldol reaction of benzaldehyde with 1-(trimethylsilyloxy)cyclohexene.

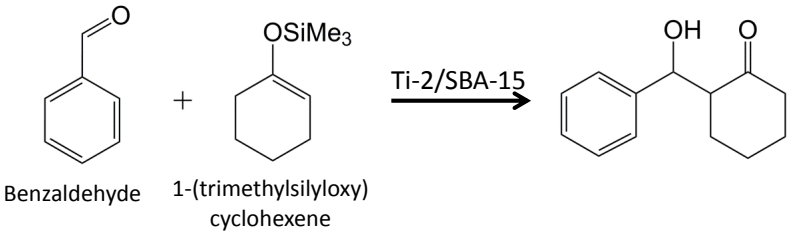

Solvent	Yield (%)
Water	3
Water-SDS[a]	14[b]
Ethanol	1
Tetrahydrofuran	1
Acetonitrile	0
Dichloromethane	0
Toluene	0
Neat	0

Reagents and conditions: benzaldehyde, 0.4 mmol; 1-(trimethylsilyloxy)cyclohexene, 0.6 mmol; water, 3 mL; catalyst(Ti-2/SBA-15), 0.02 g; temperature, 298 K; time, 1 h. [a] Reaction in the presence of dodecyl sodium sulfate (SDS) (0.023 g) in reaction solution. [b]*Syn/anti* ratio was estimated to be ca. 7/3.

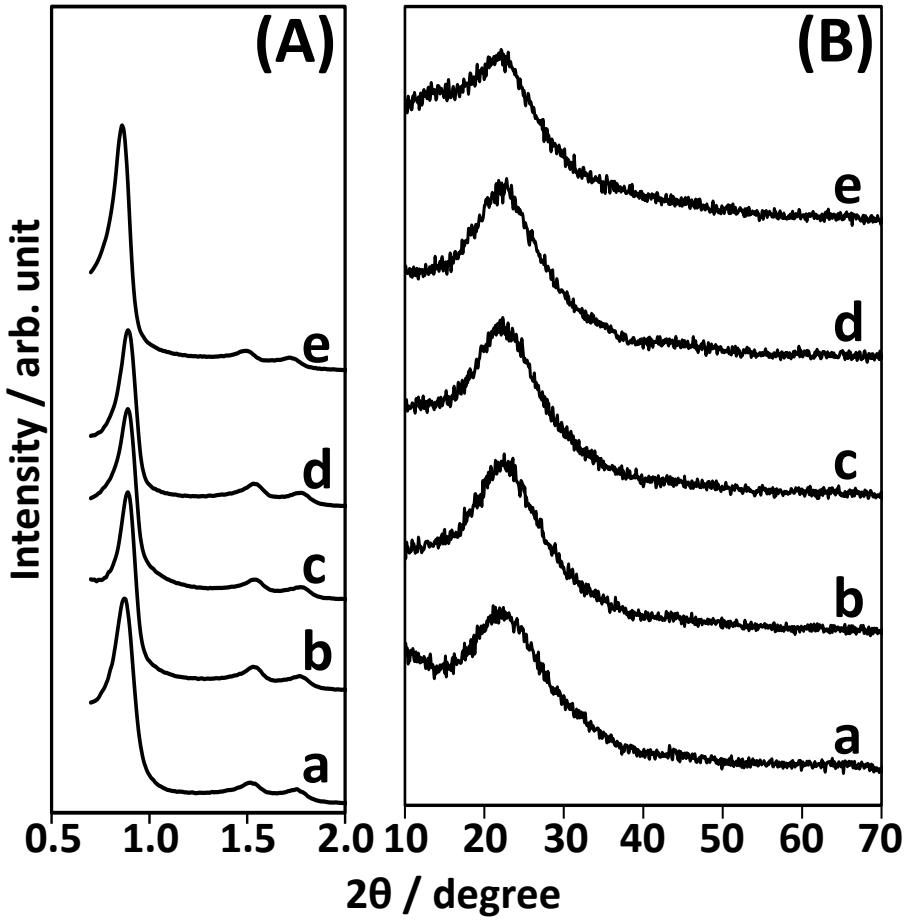

Figure 4-1. (A) Small-angle and (B) wide-angle XRD patterns for (a) TDMS, (b) Propyl-TDMS, (c) Dodecyl-TDMS, (d) Benzyl-TDMS, and (e) Tridecafluoro-TDMS. Reproduced from [47] with permission of The Royal Society of Chemistry.

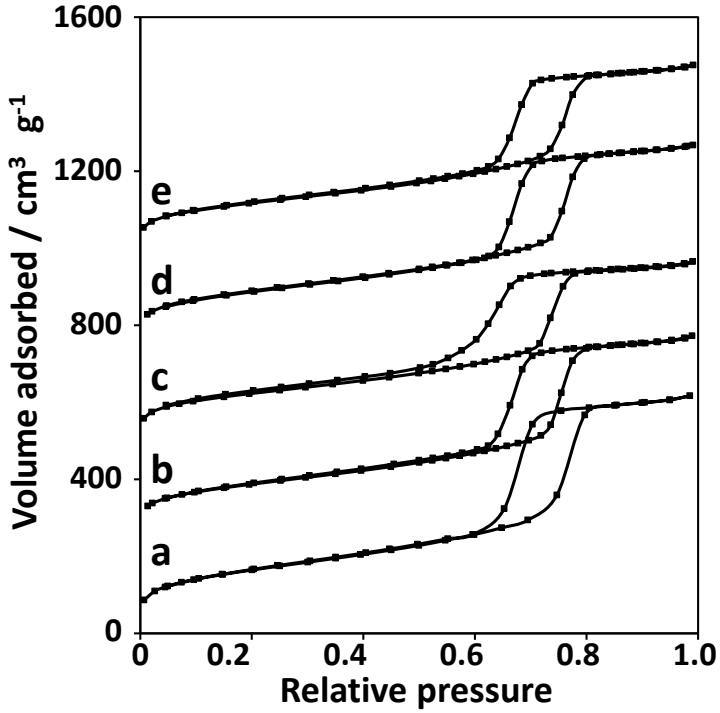

Figure 4-2. N_2 adsorption-desorption isotherms for (a) TDMS, (b) Propyl-TDMS, (c) Dodecyl-TDMS, (d) Benzyl-TDMS, and (e) Tridecafluoro-TDMS. Each isotherm is vertically offset by 250 cm^3 g^{-1} for clarity. Reproduced from [47] with permission of The Royal Society of Chemistry.

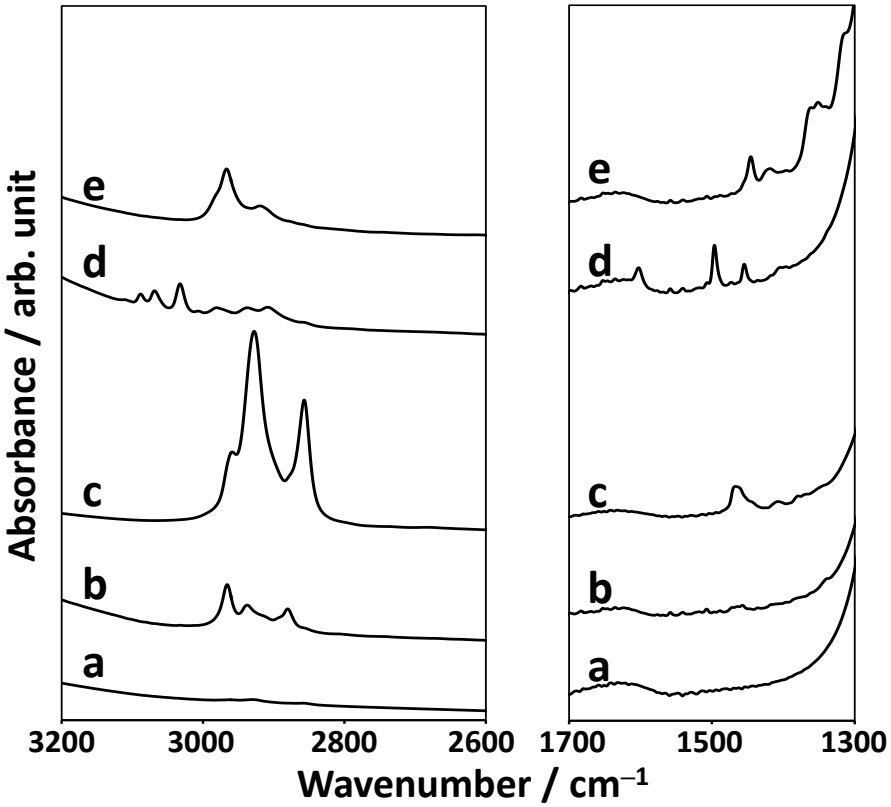

Figure 4-3. FTIR spectra for (a) TDMS, (b) Propyl-TDMS, (c) Dodecyl-TDMS, (d) Benzyl-TDMS, and (e) Tridecafluoro-TDMS. Reproduced from [47] with permission of The Royal Society of Chemistry.

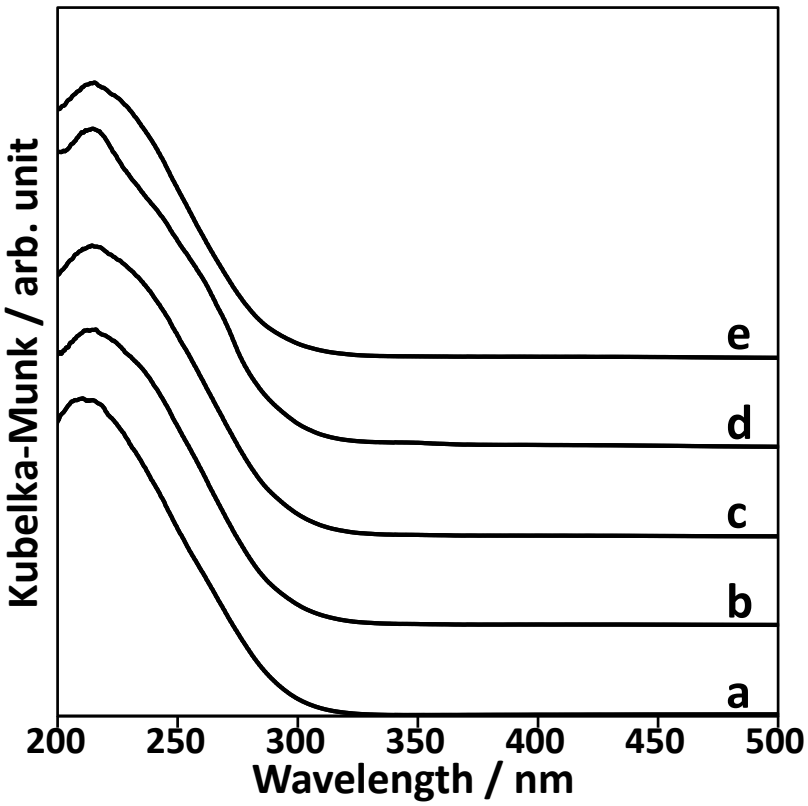

Figure 4-4. UV-Vis DRS spectra for (a) TDMS, (b) Propyl-TDMS, (c) Dodecyl-TDMS, (d) Benzyl-TDMS, and (e) Tridecafluoro-TDMS. Reproduced from [47] with permission of The Royal Society of Chemistry.

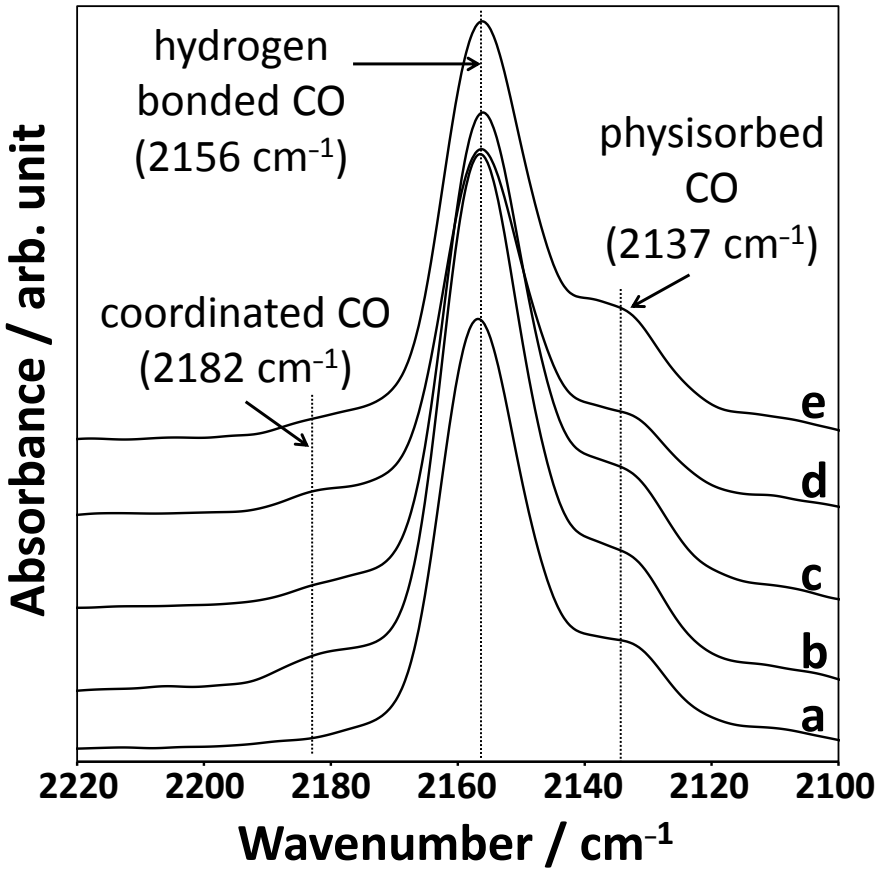

Figure 4-5. Difference FTIR spectra for CO-adsorbed hydrated SBA-15 and TDMS samples. (a) SBA-15, (b) Propyl-TDMS, (c) Dodecyl-TDMS, (d) Benzyl-TDMS, and (e) Tridecafluoro-TDMS. Prior to measurements, all samples were exposed to water vapor (20 Torr) followed by evacuation for 5 min. Reproduced from [47] with permission of The Royal Society of Chemistry.

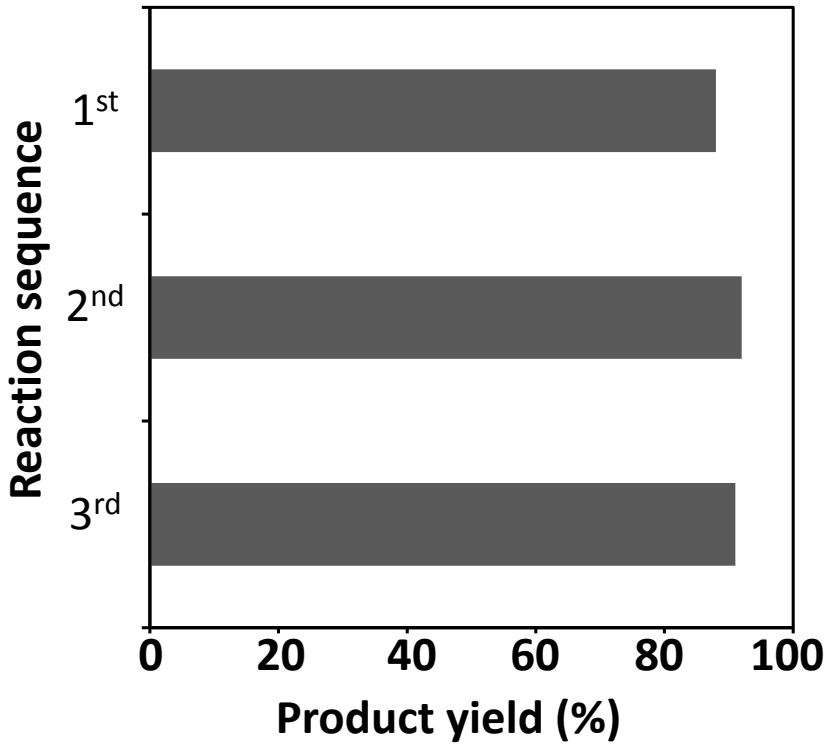

Figure 4-6. Catalytic activities of fresh and reused Tridecafluoro-TDMS for the surfactant-free Mukaiyama-aldol reaction of benzaldehyde with 1-(trimethylsilyloxy)cyclohexene in water. Reproduced from [47] with permission of The Royal Society of Chemistry.

(A)

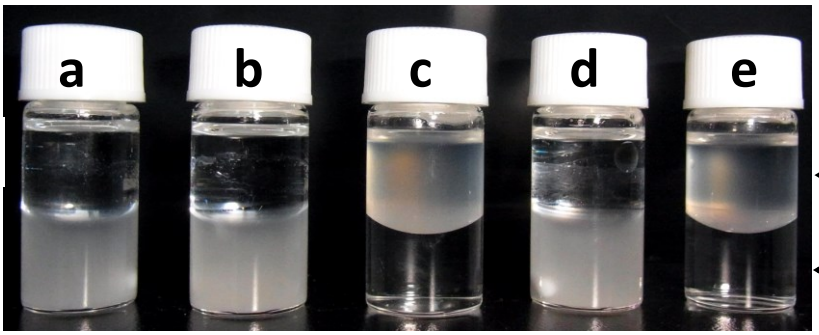

(B)

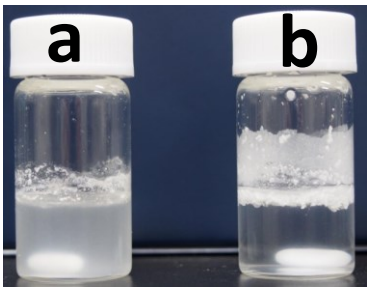

Figure 4-7. (A) Photograph of TDMS samples dispersed in water-benzene (1:1 vol%) solution. (a) TDMS, (b) Propyl-TDMS, (c) Dodecyl-TDMS, (d) Benzyl-TDMS, and (e) Tridecafluoro-TDMS. (B) Photograph of TDMS samples suspended in water-ethanol (4:1 vol%) solution. (a) Dodecyl-TDMS, (b) Tridecafluoro-TDMS. Reproduced from [47] with permission of The Royal Society of Chemistry.

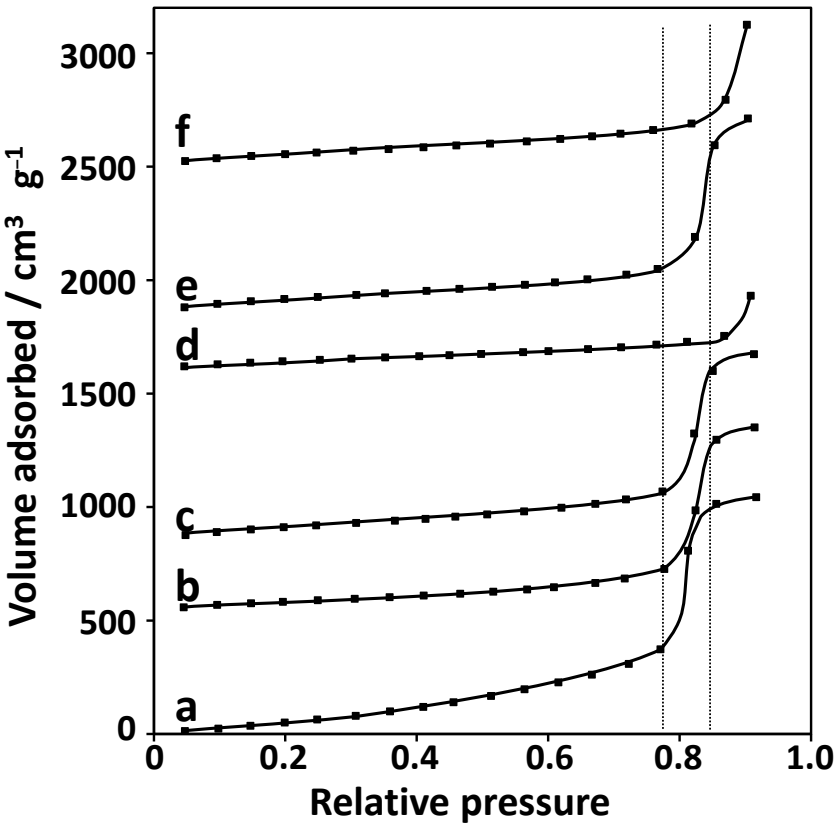

Figure 4-8. H_2O adsorption isotherms for SBA-15 and TDMS samples measured at 298 K. (a) SBA-15, (b) bare TDMS, (c) Propyl-TDMS, (d) Dodecyl-TDMS, (e) Benzyl-TDMS, and (f) Tridecafluoro-TDMS. Reproduced from [47] with permission of The Royal Society of Chemistry.

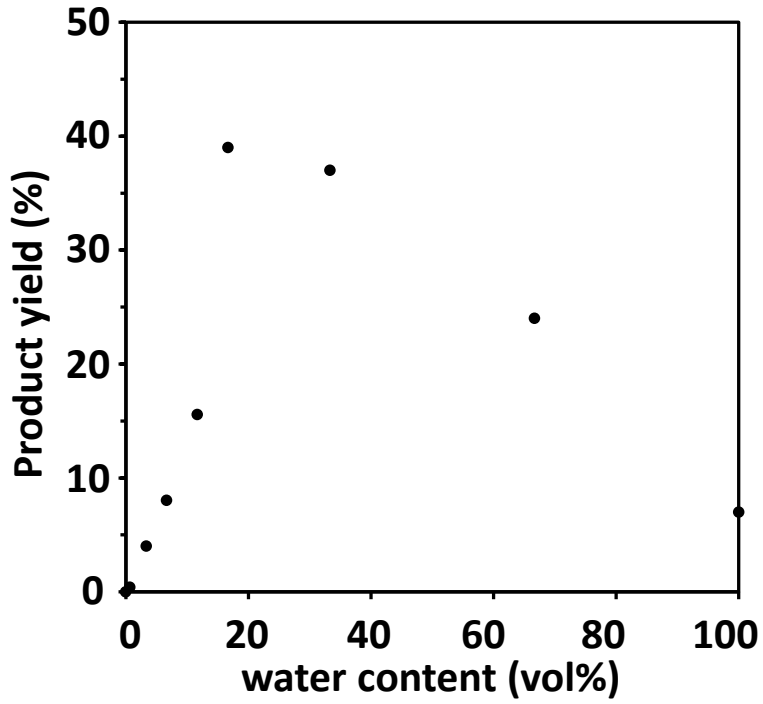

Figure 4-9. Dependence of product yield of bare TDMS for the Mukaiyama-aldol reaction in THF on various water contents. Reproduced from [47] with permission of The Royal Society of Chemistry.

Dehydrated TDMS (0.1 g, prepared by heating at 473 K under vacuum) was added to a mixture of benzaldehyde (0.4 mmol), 1-(trimethylsilyloxy)cyclohexene (0.6 mmol), water (x mL) and THF (3-x mL) under argon. After stirring the mixture at 298 K for 2 h, TDMS was separated by centrifugation. THF (10mL) and 1 M HCl (0.5mL) were added, and then stirred for 1 h at 298 K for desilylation of product. THF was removed under reduced pressure and water (7 mL) was added. The product was extracted with ethyl acetate and organic solvent was removed under reduced pressure. The product yield was analyzed using ^{1}H NMR spectroscopy with dioxane used as an internal standard.

Chapter 5

Summary

Chapter 2

TiO_4 deposited mesoporous silica (TDMS) was investigated as a water-tolerant solid Lewis acid catalyst. TDMS prepared by a simple post-grafting technique using Ti(OPr-*i*)$_4$ has a large BET surface area (ca. 450 m^2 g^{-1}) and ordered mesoporous structure. Ultraviolet-visible diffuse reflectance spectroscopy (UV-Vis DRS), X-ray absorption near edge structure (XANES), and CO adsorption measurements with Fourier transform infrared (FTIR) spectroscopy revealed that isolated TiO_4 tetrahedra on mesoporous silica can interact with CO even in the presence of water. Lewis acid centers on TDMS exhibit higher catalytic performance for the hydride transfer of pyruvaldehyde to lactic acid and the Mukaiyama-aldol condensation of benzaldehyde with 1-trimethylsilyloxy-cyclohexene in water than those of conventional heterogeneous and homogeneous Lewis acids, including scandium(III) triflate ($Sc(OTf)_3$), which also work even in water. The high catalytic performance of TDMS can be attributed to Lewis acid catalysis of isolated TiO_4 tetrahedra in water.

Chapter3

TiO_4 deposited Mesoporous silica (TDMS) was prepared by a co-condensation of Si(OMe)$_4$ and Ti(OPr-*i*)$_4$ in the presence of an amphiphilic block copolymer as a structure directing agent. The resulting TDMS samples with various Ti contents have ordered mesopores and higher surface areas than TDMS prepared by post-grafting method. Ti content in the final material can be controlled by intial concentration of titanium alkoxide. However, due to the difference in hydrolysis rate between silicone and titanium alkoxide, titania nanoparticles were also simultaneously formed for TDMS with high titanium content: band intensity for TiO_6 octahedra, a main component of bulk TiO_2 particle, in Ultraviolet-visible diffuse reflectance spectra (UV-Vis DRS) spectra increases with the increase in titanium content. While all TDMS samples synthesized by co-condensation method can catalyze hydride transfer reaction of pyruvaldehyde into lactic acid water, TDMS with high Ti content show low lactic acid selectivity. This would be due to TiO_2 nanoparticles that contain active site for by-product formation. Post-grafting method is superior method to prepare TDMS catalyst with isolated titanium tetrahedral species.

Chapter 4

A new heterogeneous catalyst, hydrophobic TiO_4-deposited mesoporous silica, has been

designed for the efficient Mukaiyama-aldol condensation, a water-participating Lewis acid-catalyzed reaction between hydrophobic carbonyl compound and silyl enol ether. The introduction of dodecyl- and tridecafluoro-groups onto TDMS gave rise to strong hydrophobicity for the material, which resulted in high catalytic activity for the reaction even in the absence of sodium dodecylsulfate (SDS) as a surfactant. For tridecafluoro-TDMS, the product yield reached 85%, even without SDS, which is comparable to that for bare TDMS and $Sc(OTf)_3$ with SDS. The high catalytic performance of hydrophobic TDMS can be attributed to both inherent Lewis acidity of TiO_4 tetrahedra workable in water and a highly hydrophobic organic layer that facilitates access of the reactant and water molecules to the Lewis acid sites.

List of Publications

1. Hiroshi Shintaku, Kiyotaka Nakajima, Masaaki Kitano, Nobuyuki Ichikuni, Michikazu Hara
   "Lewis Acid Catalysis of TiO_4 Tetrahedra on Mesoporous Silica in Water" (Chapter 2)
   ACS Catalysis, **2014**, *4*, 1198-1204.

2. Hiroshi Shintaku, Kiyotaka Nakajima, Masaaki Kitano, Michikazu Hara
   "Efficient Mukaiyama aldol reaction in water with TiO_4 tetrahedra on a hydrophobic mesoporous silica surface" (Chapter 4)
   Chemical Communications, **2014**, *50*, 13473-13476.

Acknowledgements

This thesis describes the results about three years' studies which have been supported by many people. I wished to express thankful gratitude to a number of people who contributed directly or indirectly to this research.

First and foremost, I wish to express my deepest thanks to my supervisor, Professor Michikazu Hara, for his valuable discussions, suggestions, and guidance of experimental approach throughout this work. His wide knowledge and continuous encouragements have been very strong motivating force. I had a fruitful and challenging time under his prominent guidance.

I am sincere grateful to Dr. Kiyotaka Nakajima for his great contribution to present research. His valuable suggestion, technical guidance and helpful advices influenced on my research and life. I would like to thank Associate professor Keigo Kamata and Associate professor Masaaki Kitano for many scientific discussions and practical advices that expanded my insights into the science. I spend exiting time under their guidance.

I would like to thank Associate Professor Nobuyuki Ichikuni at Chiba University for X-ray absorption spectroscopy measurement and helpful discussions. I am also thankful to Dr. Shigenobu Hayashi at National Institute of Advanced Industrial Science and Technology for his help in the measurement of solid state NMR.

Special acknowledgements is made to Professor Emiel Hensen, Dr. Evgeny Pidko, William N. P. van der Graaff, Christiaan H. L. Templeman and all of inorganic Material Chemistry group members in Eindhoven University of Technology for their hearty support during my four months stay in the Netherlands.

I am grateful to researcher of my laboratory, Madoka Akimoto, Tomoko Fukuoka, Takeo Kato, Takako Kawaguchi, Masayuki Nambo, Eri Ono, Erika Sano, Yukio Takasaki and Naomi Watanabe, for their kind assistance of my research and cordial encouragements.

I am very grateful for the secretary of my group, Tsuguko Tani, for her kind assistance management.

I would like to thank also my colleagues and students in Hara group. Dr. Satoshi Suganuma, Dr. Kiichi Fukuhara, Dr. Yasunori Inoue, and Dr. Tasuku Komanoya gave me a helpful suggestions and

hearty enjoyable time. I thank to the member of Lewis acid catalyst sub-group, Dr. Yusuke Koito, Ryohei Noma, Shingo Shimizu, Ayaka Suzuki and Daiki Takeda for their fruitful discussions and daily supports. I'd like to thank many other colleagues, Tatsuya Saito, Takuma Mori, Yohei Yamazaki, Kazuto Yamamoto, Atsuhito Sugiyama, Ikki Morita, Shinji Kambara, Mai Tokunari, Hiroki Ishikawa, Shuma Kawasaki and Yusuke Fujita for their general help and the good atmosphere in the laboratory.

Finally, I express my deep gratitude to my family for their understanding, encouragement and supports.

Hiroshi Shintaku
February, 2015